CATIONIC LATEXES FOR *o*-IODOSOBENZOATE CATALYZED ORGANOPHOSPHATE HYDROLYSIS

By

HUI YU

Bachelor of Science
Wuhan University
Wuhan, P. R. China
1982

Master of Science
Wuhan University
Wuhan, P. R. China
1985

Submitted to the Faculty of the
Graduate College of the
Oklahoma State University
in partial fulfillment of
the requirements for
the degreee of
DOCTOR OF PHILOSOPHY
May, 1993

CATIONIC LATEXES FOR *o*-IODOSOBENZOATE CATALYZED ORGANOPHOSPHATE HYDROLYSIS

Thesis Approved:

Warren T. Ford
Thesis Advisor

K D Berlin

Nabil El Rassi

Bruce J. Carter

Thomas C. Collins
Dean of the Graduate College

PREFACE

This research is concerned with decontamination of organophosphate chemical warfare (CW) agents and pesticides. Some of these compounds can inactivate the enzyme cholinesterase in nervous system, make victims fail to breathe, and cause death. Decontamination of CW agents and pesticides is very important to human life and environmental protection.

An ideal way to decompose these organophosphate compounds will be to use a solid catalyst for oxidation by air. However, at present there is no general method of oxidation of all compounds. Hydrolysis reactions may be alternatives. Since the hydrolysis reactions of the organophosphate compounds are very slow due to their poor solubility in water, catalysts and phase transfer agents are needed to improve the rate of the reaction.

Catalysts are classified as either homogeneous or heterogeneous. Heterogeneous catalysts are often less selective than homogeneous catalysts, but their advantage is the ease of separation from reaction mixtures and its reuse. Insoluble functionalized polymers and polymer colloids (also called polymer latexes) have been used as supports for catalysts to achieve the advantages of both homogeneous and heterogeneous catalysts. The activity of any supported catalyst usually depends on its surface area. The smaller the particles of the support, the greater the surface area per unit mass, and the higher the activity. Polymer latexes are produced by emulsion polymerization for synthetic rubber and for paints. They are also promising catalyst supports because of their < 1 μm size.

In this research, we used cationic polymer latexes as supports for *o*-iodosobenzoic acid to catalyze the hydrolysis of *p*-nitrophenyl diphenyl phosphate, a model compound for

CW agents. The latexes remarkably improve the rate of the hydrolysis and have the highest activity of any known heterogeneous medium on the basis of weight of the catalyst.

ACKNOWLEDGMENTS

I would like to express deep appreciation to my research advisor, Dr. Warren T. Ford, for his kind guidance, patience, valuable advice, and encouragement throughout my graduate program. I wish to express my appreciation to Dr. K. Darrell Berlin for introducing me to advanced organic chemistry and to the graduate program, and for serving on my advisory committee. Appreciation is also extended to Dr. Ziad El-Rassi and Dr. Bruce J. Ackerson for serving on my advisory committee.

I wish to thank all fellow graduate students and postdocs in our research group for their help and friendship. I also want to thank U. Nobbmann and K. Davis from Dr. Ackerson's group in the Department of Physics for particle characterization.

I owe a very special debt of gratitude to my parents for their endless love, encouragement, and sacrifices during the course of my Ph.D. study.

I especially thank my husband, Mingyang Zhao, my lovely daughter, Beryl Zhao, for their love, affection, and understanding.

Finally, I would like to acknowledge the Department of Chemistry and U.S. Army for their generous financial support in the form of teaching and research assistantships during the course of my graduate study at Oklahoma State University.

TABLE OF CONTENTS

LIST OF TABLES

Chapter I

Chapter II

Chapter III

LIST OF FIGURES

Chapter II

Chapter III

APPENDIX

CHAPTER I

INTRODUCTION

Polymer Colloids as Catalyst Supports

A catalyst is a substance that increases the rate of a reaction by providing a lower activation energy pathway but does not change the position of its thermodynamic equilibrium. It is not consumed and normally is used in small amounts compared with the reactant. Enzymes are well known natural catalysts.

Catalysts are classified either homogeneous or heterogeneous. The advantage of heterogeneous catalysts is that they are immiscible with reactants or products and may be easily separated from products after reactions. The disadvantage is a low efficiency due to less contact with reactants. A method to upgrade heterogeneous catalysts is to use heterogeneous media in which reactants and catalysts in different phases contact each other at the interfaces. Heterogeneous media can be liquid-liquid or solid-liquid. However, either one must have large interfacial area to provide good contact of reactants and catalysts. A good way to achieve large interfacial area is to use colloids. Colloids consist of a dispersed phase distributed uniformly in a finely divided state in a continuous phase. Colloids can be association colloids and polymer colloids.

Association colloids are low molecular weight aggregates such as micelles. The dispersed phase of micelles consists of surfactant aggregates about 5 nm in diameter, in which the oily tails of surfactants form micelle cores, and charged head groups form the shells and stabilize the micelles in the continuous phase. Polymer colloids are also called polymer latexes and are synthesized by emulsion polymerization. The dispersed phase consists of polymer particles with $< 1\mu m$ diameter which are stabilized by either charge or

steric forces. Charged latexes are often used for supporting ionic catalysts. Cationic and anionic polymer latexes have been used for catalyzing organic reactions as phase transfer agents.[1] Functionalized polymers are widely used elsewhere.[2] Most functionalized polymers are synthesized by suspension polymerization. Suspension polymerization produces polymer beads 10-1000 μm in diameter, and it is difficult to control particle size and distribution. Because large particles have small interfacial area and catalysis is limited by mass transfer and intraparticle diffusion, often porous structures are preferred to solve these problems.

Polymer latexes show several advantages as catalyst supports: (1) The latexes are easily made by emulsion polymerization, the size and distribution of latex particles are easily controlled, and the compositions of the latexes are also controllable. Compared with functionalized polymers, (2) the latexes provide larger interfaces for the contact of catalysts and reactants, and (3) their size minimizes mass transfer and diffusional limitations to reaction rates. They are more efficient than association colloids in which reactions occur on the surface of the dispersed phase because (4) the expanded ion exchange latexes function as porous functionalized polymers so that reactions proceed inside latexes as well.

Hydrolysis of Phosphate Esters in Colloidal Media

Some organophosphorus compounds are very toxic and have been used as chemical warfare (CW) agents and pesticides. The decontamination of CW agents and pesticides is practically and theoretically important.[3] An ideal way to decompose these compounds will be to use a solid catalyst for oxidation of the CW agents by air. However, at present there is no general method of oxidation of all organic compounds. Hydrolysis reactions may be alternatives for decontamination. Since these organophosphorus compounds are not soluble in water, the rates of hydrolysis are extremely slow. Micelles and microemulsions improve their solubility. To avoid the hazards of research with very toxic compounds,

often *p*-nitrophenyl diphenyl phosphate (PNPDPP) has been used as a model compound. PNPDPP is a popular substrate because it produces *p*-nitrophenoxide ion which can be easily monitored by UV.

In early organophosphate hydrolysis studies Bunton and his group used many nucleophilic reagents, such as hydroxide and phenoxide,[4-9] peroxide and hydroperoxide,[10] flouride ion,[11] imidazole, benzimidazole,[12] hydroxamates, and oximates.[4] Lately vesicular[13] and microemulsified reagents[14] have been studied. Moss and his group tested hydroxyl-functionalized cationic surfactants and aryloxide ions[15] solubilized in cetyltrimethylammonium bromide (CTAB) micelles as nucleophilic reagents for hydrolyzing PNPDPP. Hydrophobic hydroxamic acids, oximes, amidoximes and imidazoles solubilized in micellar CTAB, either included in functionalized surfactant or supplied as benzimidazole, strongly catalyzed hydrolysis of PNPDPP. Menger found that an aldehyde-hydrate functionalized surfactant cleaved PNPDPP in dodecyltrimethyl-ammonium bromide (DTAB) at pH 9.0 with a catalytic advantage (k_{obsd}/k_o) of 210 and 1800 relative to nonfunctionalized surfactant and pure buffer, respectively. The k_{obsd} is the maximum pseudo first-order rate constant found over all DTAB concentrations, and k_o is the rate constant for substrate cleavage in the nonfunctionalized surfactant or only in buffer. Menger's catalyst turns over.[16] Turnover is derived from the term "turnover number", which is the number of moles of products formed per mole of catalyst per unit of time, and is used to characterize the efficiency of catalysts. In a turnover experiment, the amount of catalyst is less than the amount of substrate. However, for the efficient cleavage of phosphates, many of above reagents suffered from one or more of these disadvantages: the cleavage reaction was too slow, high catalytic reagent concentration or high pH($\geq$10) was needed, or the catalyst did not turn over.

o-Iodosobenzoic acid (IBA) has been used as an oxidant of protein thiol groups in biochemistry.[17] More than a decade ago Moss and his group found that IBA is an efficient nucleophilic catalyst for cleavage of active organophosphates, and its activity was

remarkably enhanced in cationic micellar surfactants.[18] The IBA-catalyzed hydrolysis of PNPDPP is shown in Scheme 1. The kinetic expressions are also shown under the scheme.

Scheme 1

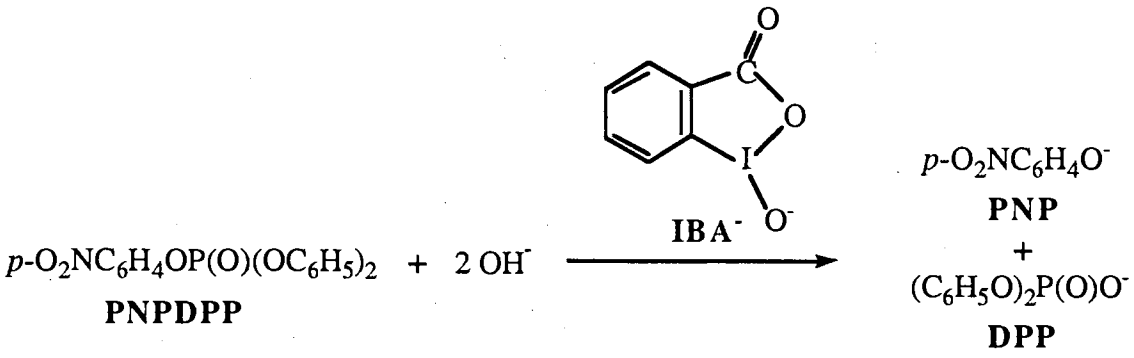

The kinetic expressions are equations (1) - (3):

$$-d[PNPDPP]/dt = (k_o[OH^-] + k_{IBA}[IBA])[PNPDPP] \quad (1)$$

When $[OH^-]$ is constant in buffer

$$k_{obsd} = k_o + k_{IBA}[IBA] \quad (2)$$

$$-d[PNPDPP]/dt = k_{obsd}[PNPDPP] \quad (3)$$

The fastest IBA-catalyzed PNPDPP hydrolysis was in CTACl micelles. The second-order rate constant reached 645 M^{-1} s^{-1}, and the shortest half life was 10.7 seconds.[18] The kinetic advantage (k_{obsd}/k_o) was 97.4. The k_{obsd} is the maximum pseudo first-order rate constant over a range of CTACl concentrations, and k_o is the rate constant for substrate cleavage in the absence of the iodoso catalyst. The conditions and results of several different heterogeneous systems for PNPDPP hydrolysis catalyzed by IBA and its derivatives are summarized in Table 1.

Furthermore, the rates of phosphate hydrolysis catalyzed by IBA in microemulsions were studied.[19-22] Microemulsions as micelles are association colloids, in which the dispersed phase consists of oil molecules, surfactant, and cosurfactant (usually low molecular weight alcohols). Different compositions of microemulsions were used: for example, 18 wt % CTAB, 18% 1-butanol (cosurfactant), 4% hexadecane (oil) and 60% borate buffer,[19,21] or 25 wt % CTACl, 5% Adogen 464, 1.4% hexadecane, and 68.7% 0.03 M pH 9.08 borate buffer.[21] Compared with micellar solutions, the solubility of phosphate esters is much higher in microemulsions. However, the second-order rate constants of IBA are at least 100 times lower in microemulsions than in micelles.

These phenomena can be understood in terms of the mechanism of the hydrolysis of PNPDPP and the differences between the structures of microemulsions and micellar solutions. A nonpolar phosphate is more likely to be present in the oily interior of the microemulsion droplets, but the IBA anions are most likely in the more polar interface and in the aqueous solution. This reduces the opportunity for substrate and catalyst contact so that although microemulsions solubilize more substrate, they have lower activity for the hydrolysis. Efforts to improve the hydrolysis activity in microemulsions by changing surfactants, cosurfactants and compositions of oil, surfactant, cosurfactant, and aqueous phases have shown that when the aqueous phase was more than 80% of the microemulsion, the activity went up more rapidly in microemulsions of CTAB, 1-butanol, hexadecane, and aqueous borate buffer than in compositions with low percent of aqueous phase.[20]

Table I. Activties of IBA and its Derivatives for PNPDPP Hydrolysis in Different Heterogeneous Conditions[a]

catalyst	medium	[PNPDPP] 10^5 (M)	[catalyst] 10^5 (M)	k_{IBA} ($M^{-1}s^{-1}$)	k_{obsd}/k_o	ref.
IBA	CTACl 0.32 mg mL^{-1}	1.0	10.0	645	97.4	25
IBA	25% CTACl, 5% Adogen 464, 1.4% hexadecane microemulsion[b]	-	24.9	7.2	-	21
5-octyloxy IBA	CTACl 0.064 mg mL^{-1}	1.0	7.14	14,400	18,000	25
5-N-(*n*-hexadecyl)-N,N-dimethyl-β-ammonioethoxy IBA	CTACl 0.064 mg mL^{-1}[c]	1.0	4.0	28,500	14,700	26
covalently bound IBA	polystyrene 2 mg mL^{-1}	2.4	240.0	4.6	-	28
covalently bound IBA	polyacrylate 2mg mL^{-1}	2.4	64.0	17	-	28
covalently bound IBA	silica IBA1 5 mg mL^{-1}	5.0	50.0	36	-	29
covalently bound IBA	silica IBA2 5 mg mL^{-1}	5.0	50.0	34	-	29

Table I. (continued)

catalyst	medium	[PNPDPP] 10^5 (M)	[catalyst] 10^5 (M)	k_{IBA} ($M^{-1}s^{-1}$)	k_{obsd}/k_o	ref.
covalently bound IBA	titanium dioxide 3.33 mg mL^{-1}	3.3	43.3	10	-	30
covalently bound IBA	nylon-6 3.33 mg mL^{-1}	3.3	83.3	14	-	30
covalently bound IBA	acrylic anion exchange resin 3.33 mg mL^{-1}	3.3	306.7	22	-	31

[a] All experiments were in 0.02 M phosphate buffer at pH 8.0 unless indicated. [b] In 0.03 M borate buffer at pH 9.08. [c] In 0.01 M tris buffer at pH 8.0.

In order to further upgrade IBA catalytic activity, two factors have been studied. The first factor is the benzo ring electronic effect. Because the electron density of the I-O oxygen can vary with substituents, is it possible that they affect I-O oxygen nucleophilicity? Two IBA derivatives with the electron donating methoxy group and electron withdrawing nitro group at the 5-position were tested for catalytic activity by the Moss group. Surprisingly, these two IBA derivatives did not show a significant difference in their catalytic behavior in 1 mM CTACl and 0.02 M pH 8.0 phosphate buffer.[24] Similar experiments in the microemulsion of CTACl, Adogen, and hexadecane in borate buffer showed that the activity of 5-nitro-IBA was a little higher than that of IBA.[21] The second factor is the solubility of IBA in the micelle or microemulsion phase. Aggregates such as micelles and microemulsions bring catalyst and substrate in a close proximity. The rate of a second-order reaction is proportional to the concentrations of substrate and catalyst in the reactive phases. To test the solubility effects, several IBA derivatives were synthesized by attaching different substituents on the benzo ring. The substituents were lipophilic alkoxy groups such as butoxy (**1b**), octyloxy (**1c**), and dodecyloxy (**1d**) at the 5 position, and methoxy (**2a**), ethoxy (**2b**), propyloxy (**2c**), and butoxy (**2d**) at the 4 position.[23] There were also hydrophilic ones such as carboxyl (**1e**), quaternary salt (**1f**), hydroxyethoxy (**1g**), and *N*-(*n*-hexadecyl)-*N*,*N*-dimethyl-β-ammonioethoxy (**1h**) at the 5 position.[21,22,24-27] Except **1g** and **1h**, the hydrophilic substituted IBAs were less active than IBA.

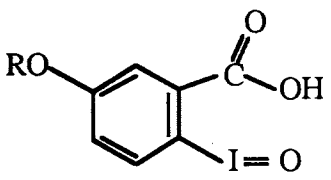

5 substituted IBA

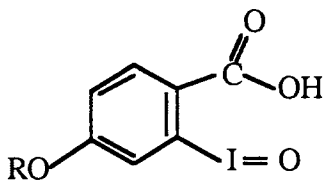

4 substituted IBA

1a, R = CH_3
1b, R = n-C_4H_9
1c, R = n-C_8H_{17}
1d, R = n-$C_{12}H_{25}$
1e, R = COOH
1f, R = $(CH_3)_3N^+CH_2CH_2$
1g, R = $HOCH_2CH_2$
1h, R = n-$C_{16}H_{33}N^+(CH_3)_2CH_2CH_2$

2a, R = CH_3
2b, R = C_2H_5
2c, R = n-C_3H_7
2d, R = n-C_4H_9

However, among the alkoxy groups different chain lengths did not significantly affect the rates. The most active one was **1c** in CTACl micelles. The compound **1h** had the highest activity among derivatives.

The above results showed that the nucleophilicity of IBA was not affected much by a benzo ring electronic effect, but the activity of IBA was enhanced by improving the solubility in the micelle phase with alkoxy substituents. The hydrophilic substituted IBA normally gained less activity than alkoxy analogues.

For the development of solid catalysts, which would be easier to handle and apply for the flow-through treatment of contaminated water and for small "spills" of toxic agents, in 1988 Moss designed cationic iodosobenzoate-functionalized polymers which were synthesized by bonding cationic surfactant-functionalized IBA covalently to polystyrene and to polyacrylate.[28] These two polymers were loaded with 1.2 mequiv/g and 0.32 mequiv/g of iodoso groups, respectively. Their hydrolysis activities are in Table 1. Although the polymer-immobilized catalysts were not as active as CTACl micelle-

solubilized IBA derivatives, they were active against the nerve agent Soman (GD) with half lives of 18.1 and 41.4 minutes for cleavage of 5 μmol of GD by 100 mg of polystyrene and 25 mg of polyacrylate, respectively. However, the polymers are not easy to prepare

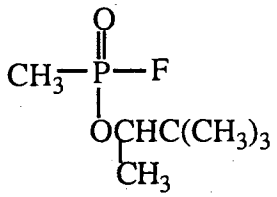

GD

and not "wettable" under hydrolysis conditions. Moss therefore used silica, which is more polar and can be purchased, as a support for two *o*-iodosobenzoate catalysts. These two silica reagents, both loaded with 0.10 mequiv/g of iodoso groups, were twice as active as his best polymer catalyst against both PNPDPP and Soman.[29] Subsequently they attached iodosobenzoates to titanium dioxide, and to nylon-6.[30] These reagents are potential "self-decontaminating" materials for and coatings protective clothing. Titanium dioxide and nylon-6 reagents loaded with 0.13 and 0.25 mequiv/g of iodoso groups gave comparable activities with the polymer catalysts. Nylon-6 catalyst activity was enhanced up to 80 M^{-1} s^{-1} by addition of 1.0×10^{-4} M CTACl. Finally, they tried to mimic IBA/CTACl micellar catalyst by loading IBA to acrylic anion-exchange resin which functioned in nonmicellar aqueous suspension.[31] The activity of the ion exchange resin modified IBA was further improved by addition of 5.0×10^{-4} M CTACl for PNPDPP hydrolysis.

IBA, its derivatives, and IBA modified polymers and inorganic solids are active catalysts for organophosphate hydrolyses. The only disadvantage for practical use of IBA and its derivatives is their instability.[32] *o*-Iodoxybenzoic acid (IBX) was found more

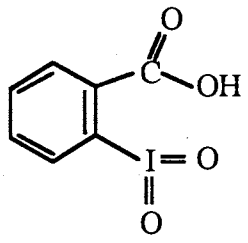

IBX

stable and more easily synthesized. The iodoxybenzoates with 5-dodecyloxy, octyloxy, butoxy, methoxy and *p*-nitro substituents were also synthesized. Their activities are 82-106% times those of their iodoso analogues for PNPDPP hydrolysis in microemulsions.[22,25,33]

Mechanisms of IBA Catalysis of Phosphate and Acetate Hydrolysis

Baker suggested that *o*-IBA exists as the 1-hydroxy-1,2-benziodoxolin-3-one (1-hydroxy-1,2-benziodoxol-3(3*H*)-one) valence tautomeric form **3b**.[34] Shefter's

Scheme 2

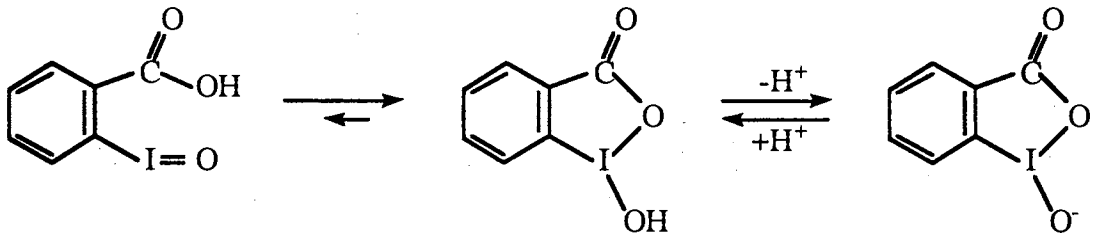

3a **3b** **3c**

X-ray results [35,36] showed that its sodium salt exists in the cyclic form **3c** (Scheme 2). Moss inferred that its conjugate base could be a potential O-nucleophile near neutral pH due to its 7.02 pK_a.[19] Since *m*-iodosobenzoic acid is inactive for catalyzing PNPDPP hydrolysis, the conjugate base (**3c**) is responsible for catalytic activity of *o*-IBA.[18]

As shown in Scheme 3, the mechanism of IBA catalysis involves nucleophilic IBA attack of the ester at phosphorus with the lose of *p*-nitrophenoxide. The catalyst IBA is then regenerated from the IBA-ester intermediate by hydroxide ion attack. Moss and his group proved by NMR analysis that the acetylated iodosobenzoate was an intermediate in the reaction of **3b** with *p*-nitrophenyl acetate (PNPA) in DMSO-d_6. There are three possible sites for hydroxide ion to attack the intermediate and regenerate the IBA: (a) at carbonyl carbon, (b) at iodine, and (c) at phosphorus. The reaction of the acetylated iodosobenzoate with sodium methoxide in DMSO-d_6 produced the methyl ether of iodosobenzoate. This

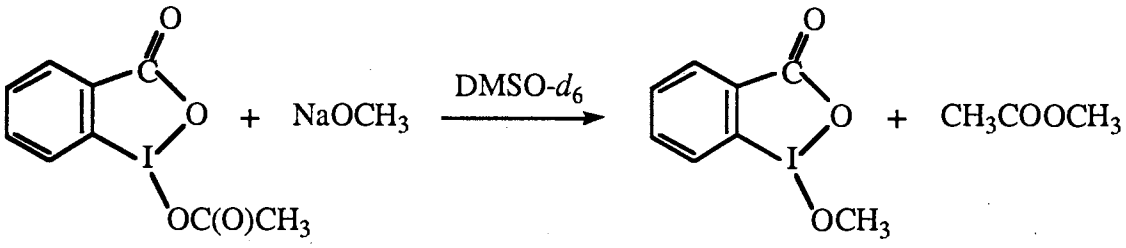

excluded reaction pathway (c) of Scheme 3 by which the products should be IBA^- and methyl acetate. However, this ether could be obtained by either pathway (a) or pathway (b). Further experiments were done by exchanging IBA with $H_2{}^{18}O$. The IBA after exchange showed most of the ^{18}O atoms at the iodoso position.[37] This indicated that the pathway (b) was dominant, and nucleophiles attacked iodine with the release of acetate or phosphate anions. They explained that the hypervalent iodine atom plays an important role:

Scheme 3

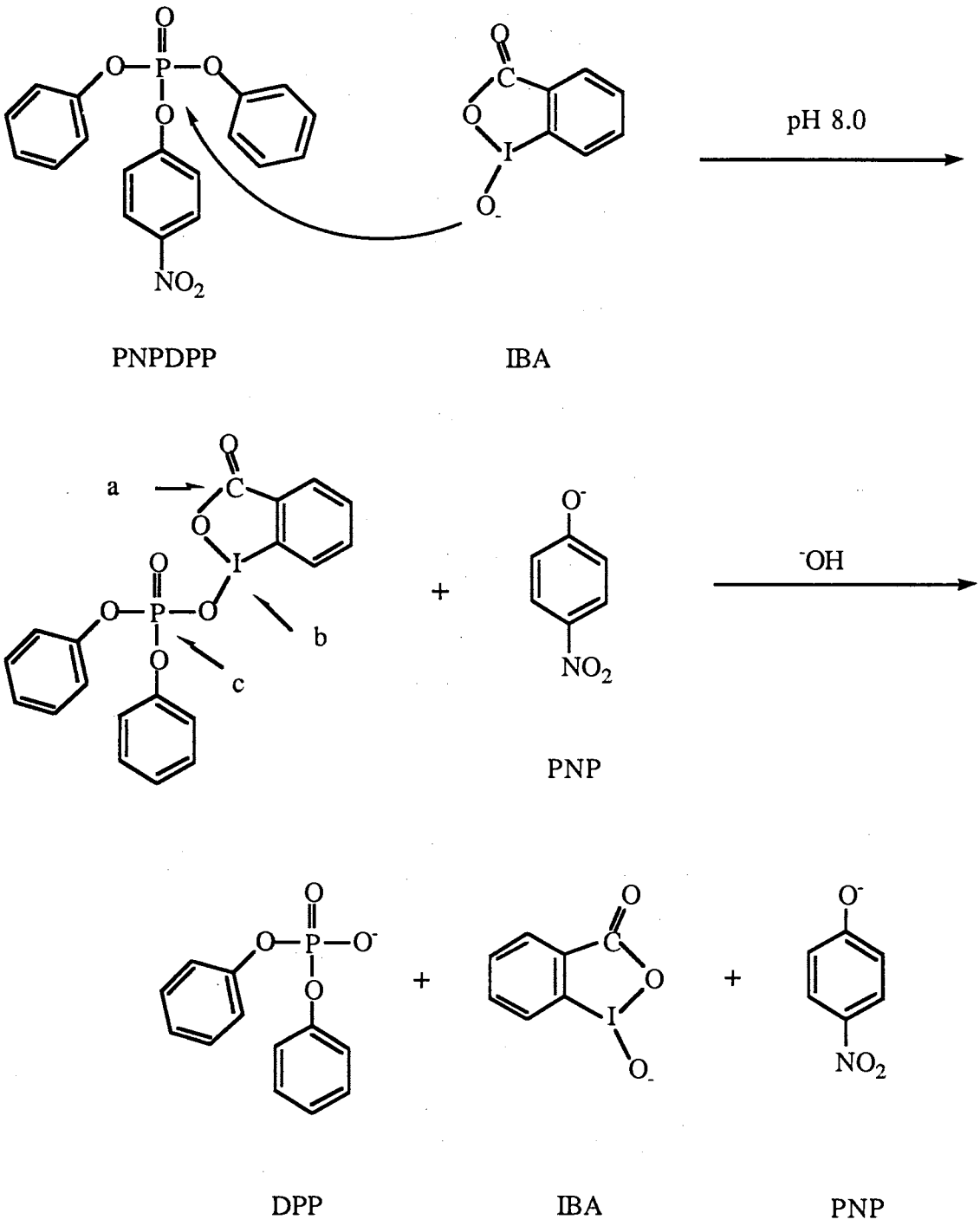

Its special bonding creates a highly polarized I^+-O^- bond in **3c** (Scheme 2), so that the negative oxygen is a potent nucleophile. Since substitution of electron donor and acceptor groups at the para position of the benzo ring had little effect on catalytic activities, the reactivity of I-O^- group is not affected by the electron density of the ring. However, the lipophilicity of ring substituents did affect the activity of IBA catalysis in micelle and microemulsion media due to the higher solubility of IBA derivatives in micelle and microemulsion phases.[20,24]

In Scheme 3, if the first step is rate limiting, the overall reaction will show pseudo first-order kinetics in excess [OH^-] or in buffer, and the catalyst will be an efficient turnover catalyst. If the second step is rate limiting, turnover of the phosphate-catalyst complex is not efficient, and "burst kinetics"[38] will be observed. In "burst kinetics" an amount of PNP equal to the amount of catalyst will be formed fast, and the rest of the PNP will be produced more slowly. Moss reported that deacylation of acetylated iodosobenzoate in CTACl micelles is about 20 times faster than cleavage of *p*-nitrophenyl acetate (PNPA) by *o*-IBA under comparable conditions.[37] This indicates that *o*-IBA is an efficient nucleophilic catalyst. Although IBX exists in a cyclic form too, there is no evidence regarding the mechanism for IBA catalysis of PNPA hydrolysis. It has been assumed that IBX may resemble the IBA for PNPA hydrolysis.

Function of Colloids for the IBA-Catalyzed PNPDPP Hydrolysis

Previous investigations of various heterogeneous systems for the hydrolysis of PNPDPP established the basis for the success of CTACl micelles with IBA catalyst. With the IBA catalyst, the substrate hydrolyzes very slowly without colloids. What is the function of the colloids? Using micelles to explain, CTACl possesses cationic head groups and forms cationic micelles. CTACl micelles are capable of solubilizing the substrate in the hydrophobic core and binding IBA anions to their surface where hydrophilic head groups

form the shell. As shown in Scheme 4, the binding constant of the substrate to the dispersed phase is K_S, and that of the catalyst is K_C. The reaction proceeds in both the dispersed phase and the continuous phase, with rate constants k_c and k_w, respectively. The overallrate depends on the concentrations in the two phases and rate constants in the two phases as shown in equation 4. Because the concentrations of the substrate and catalyst are

Scheme 4

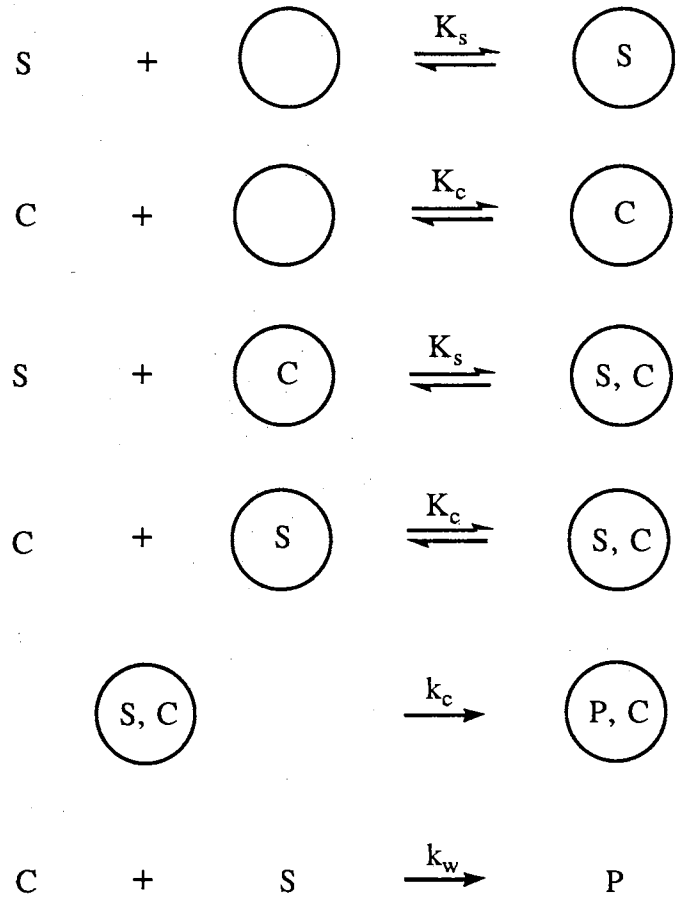

$$\text{rate} = k_C [S]_c [C]_c + k_W [S]_W [C]_W \qquad (4)$$

much higher in the dispersed phase than in the continuous phase, the reaction rate, relative to the rate in the absence of micelles, can be accelerated by a higher chance of collision of

the reactants and catalyst. The function of cationic micelles is to bring the substrate and catalyst into close proximity and enhance the rate of the reaction.

Other heterogeneous systems, such as polymer particles, have functions similar to those of micelles. A major difference is that in the cases of polymer particles, such as ion exchange resins and latexes, the polymer phase is stable during the reaction time. In the cases of micelles and microemulsions the colloidal phase is often called a "pseudophase" because the dispersed phase is formed by molecular association of aggregates in which association and dissociation occur faster than the chemical reactions.

Based on this mechanism, we designed polymer latexes as supports for the IBA-catalyzed hydrolysis. The latexes are polystyrenes modified with quaternary ammonium ions. They were synthesized by emulsion polymerization of styrene and vinylbenzyl chloride, and subsequent quaternization with trimethylamine. As in micelles, the hydrophobic cores of the latexes solubilize the substrate, and quaternary ammonium ions attract the IBA and hydroxide ions.

References

(1) Ford, W. T.; Badley, R. D.; Chandran, R. S.; Babu, S. H.; Hassanein, M.; Srinivasan, S.; Turk, H.; Yu, H.; Zhu, W. *Am. Chem. Soc. Symp. Ser.* **1992**, *492*, 423.

(2) (a) Sherrington, D. C.; Hodge, P. Synthesis and Separations using Functional Polymers; John Wiley & Sons, Ltd. 1988.
(b) Hodge, P.; Sherrington, D. C. Polymer-Supported Reactions in Organic Synthesis; John Wiley & Sons, Ltd. 1980.

(3) Yang, Y.-C.; Baker, J. A.; Ward, J. R. *Chem. Rev.* **1992**, *92*, 1792.

(4) Bunton, C. A.; Robinson, L.; Stam, M. *J. Am. Chem. Soc.* **1970**, *92*, 7393.

(5) Bunton, C. A.; Ionescu, L. G. *J. Am. Chem. Soc.* **1973**, *95*, 2912.

(6) Bunton, C. A.; Sepulveda, L. *Isr. J. Chem.* **1979**, *18*, 298.

(7) Bunton, C. A.; Cerichelli, G.; Ihara, Y.; Sepulveda, L. *J. Am. Chem. Soc.* **1979**, *101*, 2429.

(8) Bunton, C. A.; Gan, L-H.; Savelli, G. *J. Phys. Chem.* **1983**, *87*, 5491.

(9) Biresaw, G.; Bunton, C. A.; Quan, C.; Yang, Z.-Y. *J. Am. Chem. Soc.* **1984**, *106*, 7178.

(10) Bunton, C. A.; Mhala, M. M.; Moffatt, J. R.; Monarres, D.; Savelli, G. *J. Org. Chem.* **1984**, *49*, 426.

(11) Bunton, C. A.; Frankson, J.; Romsted, L. S. *J. Phys. Chem.* **1980**, *84*, 2607.

(12) Bunton, C. A.; Hong, Y. S.; Romsted, L. S.; Quan, C. *J. Am. Chem. Soc.* **1981**, *103*, 5784.

(13) Okahata, Y.; Ihara, H.; Kunitake, T. *Bull. Chem. Soc. Jpn.* **1981**, *54*, 2072.

(14) Bunton, C. A.; de Buzzaccarini, F.; Hamed, F. H. *J. Org. Chem.* **1983**, *48*, 2457.

(15) Moss, R. A.; Ihara, Y. *J. Org. Chem.* **1983**, *48*, 588.

(16) Menger, F. M.; Whitesell, L. G. *J. Am. Chem. Soc.* **1985**, *107*, 707.

(17) Mahoney, W. L.; Hermodson, M. A. *Biochemistry* **1979**, *18*, 3810.

(18) Moss, R. A.; Alwis, K. W.; Bizzigotti, G. O. *J. Am. Chem. Soc.* **1983**, *105*, 681.

(19) Mackay, R. A.; Longo, F. R.; Knier, B. L.; Durst, H. D. *J. Phys. Chem.* **1987**, *91*, 861.

(20) Knier, B. L.; Durst, H. D.; Burnside, B. A.; Mackay, R. A.; Longo, F. R. *J. Solution Chem.* **1988**, *17*, 77.

(21) Burnside, B. A.; Knier, B. L.; Mackay, R. A.; Durst, H. D.; Longo, F. R. *J. Phys. Chem.* **1988**, *92*, 4505.

(22) Katritzky, A. R.; Duell, B. L.; Durst, H. D.; Knier, B. L. *J. Org. Chem.* **1988**, *53*, 3972.

(23) Panetta, C. A.; Garlick, S. M.; Durst, H. D.; Longo, F. R.; Ward, J. R. *J. Org. Chem.* **1990**, *55*, 5202.

(24) Moss, R. A.; Chatterjee, S.; Wilk, B. *J. Org. Chem.*, **1986**, *51*, 4303.

(25) Moss, R. A.; Alwis, K. W.; Shin, J.-S. *J. Am. Chem, Soc.* **1984**, *106*, 2651.

(26) Moss, R. A.; Kim, K. Y.; Swarup, S. *J. Am. Chem. Soc.* **1986**, *108*, 788.

(27) Moss, R. A.; Ganguli, S.; *Tetrahedron. Lett.* **1989**, *30*, 2071.

(28) Moss, R. A.; Bolikal, D.; Durst, H. D.; Hovanec, J. W. *Tetrahedron. Lett.* **1988**, *29*, 2433.

(29) Moss, R. A.; Chung, Y.-C.; Durst, H. D.; Hovanec, J. W. *J. Chem. Soc. Perkin Trans. I* **1989**, 1350.

(30) Moss, R. A.; Chung, Y.-C. *J. Org. Chem.* **1990**, *55*, 2064.

(31) Moss, R. A.; Chung, Y.-C. *Langmuir* **1990**, *6*, 1614.

(32) Banks, D. F. *Chem. Rev.* **1966**, *66*, 243.

(33) Katritzky, A. R.; Duell, B. L.; Durst, H. D.; Knier, B. *Tetrahedron Lett.* **1987**, *28*, 3899.

(34) Baker, G. P.; Mann, F. G.; Sheppard, N.; Tetlow, A. *J. Chem. Soc.* **1965**, 3721.

(35) Shefter, E.; Wolf, W. *J. Pharm. Sci.* **1964**, *203*, 104.

(36) Shefter, E.; Wolf, W. *Nature (London)* **1964**, *203*, 512.

(37) Moss, R. A.; Scrimin, P.; Rosen, R. T. *Tetrahedron Lett.* **1987**, *28*, 251.

(38) Bender, M. L.; Kezdy, F. J.; Wedler, F. C. *J. Chem. Educ.* **1967**, *44*, 85.

CHAPTER II

SYNTHESIS AND CHARACTERIZATION OF CATIONIC LATEXES AND POLYELECTROLYTES

Introduction

Based on the mechanism of cationic micellar catalysis of organophosphate ester hydrolysis, we designed cationic polystyrene latexes modified by quaternary ammonium ions. Polystyrene is hydrophobic for solubilizing the substrate, and quaternary ammonium ions are positive sites for binding hydroxide ions and catalyst anions. Latexes that have high ion content, small size, and monodispersity are helpful for the catalysis because: (1) The higher the ion content of latexes, the more binding sites available, and the more efficient the latexes are for catalysis. (2) Smaller latex size with larger surface minimizes mass transfer and diffusional limitation to reaction rates. (3) Monodispersity of latexes makes it easier to study the effects of latex structure on catalysis.

Latexes with 0.05-0.7 μm diameter can be synthesized by emulsion polymerization, and 10-1000 μm diameter particles can be obtained by suspension polymerization. These are heterogeneous and free radical polymerization processes. The difference is that suspension polymerization uses polymeric stabilizers to stabilize the interface of 10-1000 μm monomer droplets and water, and emulsion polymerization uses emulsifiers (surfactants) to stabilize the interface of < 0.7 μm polymer particles and water.

Conventional emulsion polymerization results in polymer latexes with emulsifier molecules absorbed on the latex surface. Since the surfactant may affect catalysis, it must be removed, but cleaning surfactants from latexes is a quite difficult task. To solve this problem, emulsifier-free emulsion polymerization was invented. In this kind of emulsion

polymerization, ionic monomers can be used to enhance the particle stability, regulate the size of the particles, and control the types of surface groups on latexes.[1-4] In the past, ionic comonomers have been used in small amounts to stabilize the latex surface without modifying latex bulk properties. Kim developed a two stage "shot growth" or in situ seeding technique for higher surface charge latexes from styrene and sodium styrenesulfonate.[5, 6] In this technique no more than 1 wt % (based on styrene) of sodium styrenesulfonate was used in the first shot of monomers to control the particle size and monodispersity. A larger amount of sodium styrenesulfonate in the second shot of monomer was used to increase the surface charge densities of latexes. The advantages of the technique are: (1) It can control particle size and surface charge independently without losing monodispersity. (2) It results in a higher number of sulfonate groups on the surface of the latex than the theoretical value for a monolayer.

Results

We extended the shot growth technique to the system of styrene/vinylbenzyl chloride (VBC) incorporating vinylbenzyltrimethylammonium chloride as the charged monomer. The water soluble initiator, 2,2'-azobis-(N,N'-dimethyleneisobutyramidine) dihydrochloride (VA-044), was used to produce free radicals. Changing the amount of vinylbenzyl chloride monomer in both shots, seven latexes were synthesized with vinylbenzyl chloride contents of 0-75 wt % (based on total charged monomers in each sample preparation). Through modification by quaternizing with trimethylamine, a series of latexes with a wide range of quaternary group contents was obtained. This functional group conversion creates high ion content latexes as in normal ion exchange resin synthesis and avoids the use of a large amount of ionic monomer in polymerization which would sacrifice the monodisperse property of the latexes.

The sizes of the latexes were measured in dry form by transmission electron microscopy (TEM) and in water by dynamic light scattering (DLS). Quaternized particles

Scheme 1

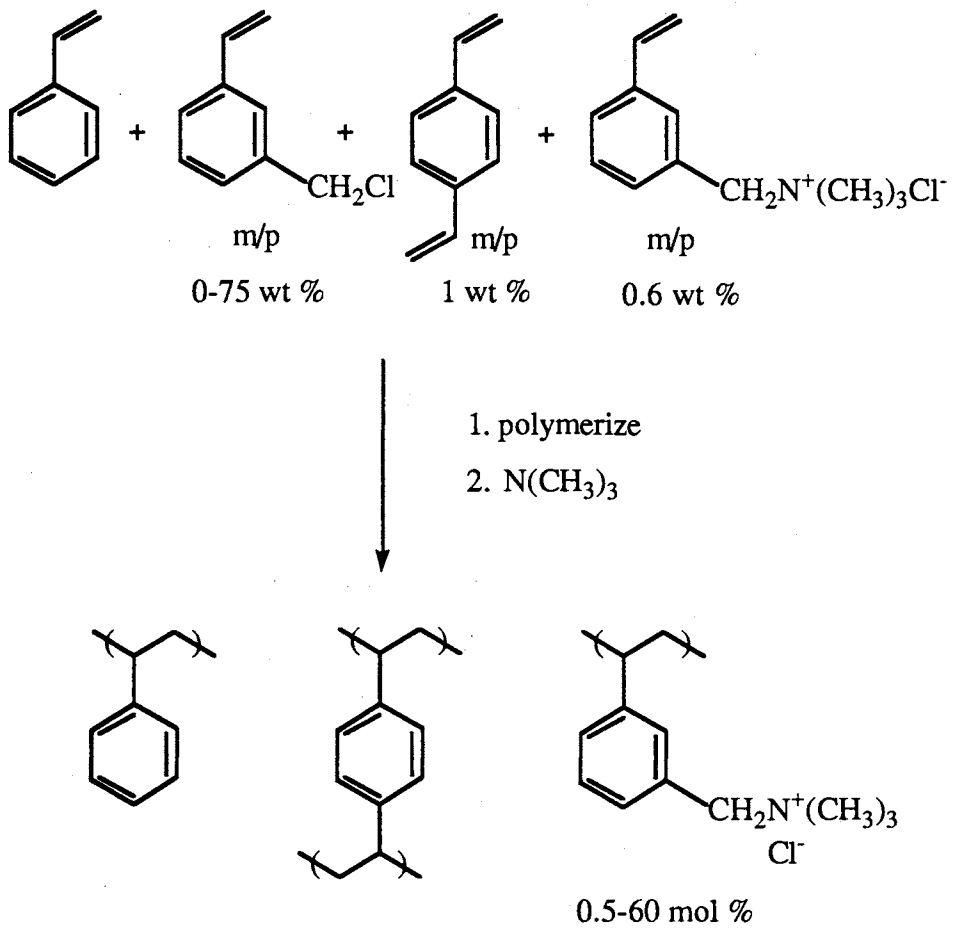

swell in water as ion exchange resins. The swelling is proportional to their ion content. The higher ion content latexes are swollen 2 to 13 times in water.

For the purpose of studying the effect of latex structure on the kinetic activity of catalysis for phosphate hydrolysis, three polyelectrolytes $75N^+$, $50N^+$, and $25N^+$ with the same compositions as corresponding latexes except lacking cross-links were synthesized

by solution copolymerization of styrene and vinylbenzyl chloride and quaternization with trimethylamine. The 75N^+PE and 50N^+PE are soluble in water, but the 25N^+PE is not soluble due to its low ion content.

Particle Synthesis. In the shot growth emulsion polymerization of styrene with sodium styrenesulfonate monodisperse latexes were obtained using no more than 1 wt % of the ionic monomer. In this work varied amounts of the ionic monomer vinylbenzyl-trimethylammonium chloride were investigated for the first shot. A typical composition of the first shot was 0.072 g of the charged monomer, 12.0 g of styrene, 0.15 g of divinylbenzene (DVB), 0.12 g of VA-044 initiator, and 108 mL of water. The sizes of the particles decrease with increase of amount of the charged monomer. The sizes of the latexes were calculated as weight average diameter (D_w) and number average diameter (D_n) of 50 particles measured directly from TEM negatives. The amount of 0.6 wt % the charged monomer (based on nonionic monomers) was chosen to get about 150 nm diameter size of particles as shown by sample LA1-5 in Table I. The TEM of LA1-5 is shown in Figure 1. We also investigated how the amounts of cosurfactant cetyltrimethylammonium bromide (CTAB) affect the size and the monodispersity of the latexes with 0.6 wt % ionic monomer in the first shot. These samples are named LA2-1 and LA2-2. Adding CTAB decreased the size of the latexes and produced polydisperse latexes. After the investigation of homopolystyrene, poly(styrene-co-VBC) was also investigated for the first shot. The copolymer with 0.6 wt % of ionic monomer was synthesized and named LA3-1. The weight average diameter of LA3-1 is 158.9 nm, which is close to the 152.5 nm diameter of homopolymer latex LA1-5 prepared with the same amount of ionic monomer. SG1-2 is a sample that was done with both shots, and VBC monomer was only added in the second shot. The composition of the second shot is given in a footnote of Table I. The amount of ionic monomer of SG1-2 is 0.6 wt % in the first shot, and the weight average diameter is 162.7 nm, close to those of the LA3-1 and LA1-5

latex samples. The TEM photographs of the rest of the samples are in Figures 2-5. The noncoagulated particles were randomly chosen for size measurement in TEM negatives. In Figures 2 and 3, the small white spots were not chosen as particles because their textures were much different from particles. These spots might be caused by TEM sample preparation.

Table I. The Compositions and Diameters of Latexes[a]

sample	D_w (nm)	D_n (nm)	D_w/D_n
LA1-5	152.5	150.0	1.02
LA2-1[a]	73.3	68.8	1.07
LA2-2[b]	105.2	101.0	1.04
LA3-1[c]	158.9	156.6	1.01
SG1-2[d]	162.7	160.8	1.01

[a] Added CTAB 0.20 g. [b] Added CTAB 0.10 g. [c] Added VBC 2.4 g and styrene 9.6 g. [d] The second shot composition: N^+ monomer 1.05 g, VBC 3.0 g, DVB 0.04 g, VA-044 0.04 g, and water 20 mL.

These results show that (1) adding VBC monomer in ether shot did not affect much the size of the latexes compared with the homopolystyrene latex with the same amount of ionic monomer in the first shot, and (2) the shot growth technique is valid for our copolymer system.

Using the shot growth technique seven cross-linked poly(styrene-co-VBC) latexes with different compositions were synthesized using 0.6 wt % of vinylbenzyltrimethyl-ammonium chloride based on nonionic monomers in the first shot to control particle size and monodispersity. The samples are named after the wt % of VBC monomer in each

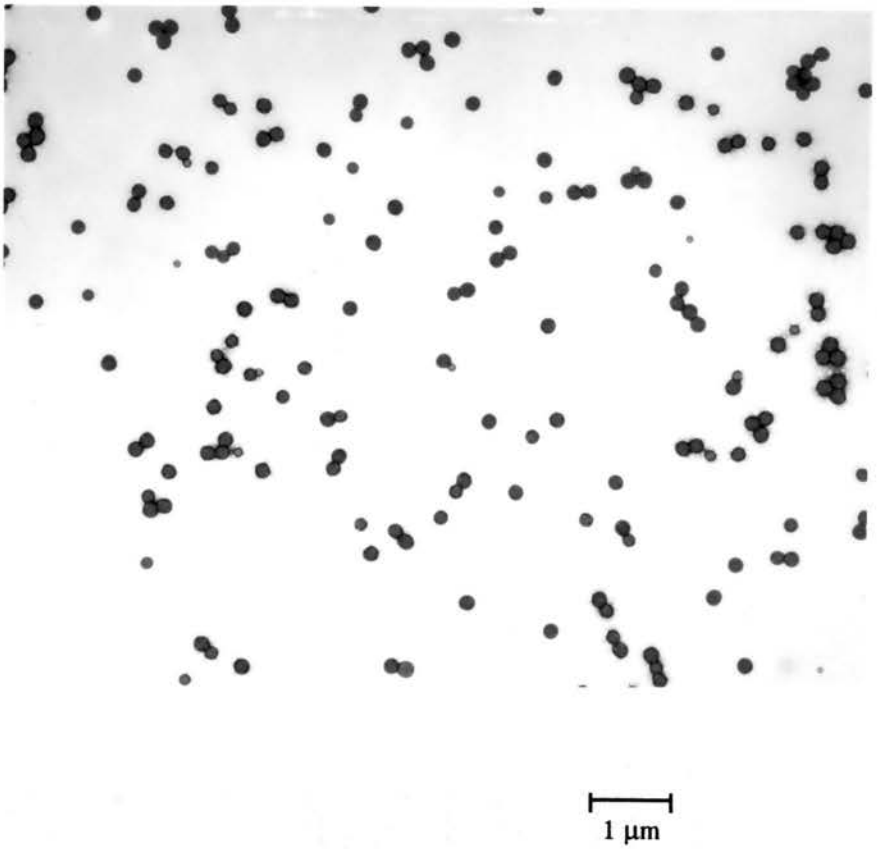

Figure 1. TEM of LA1-5 Latex.

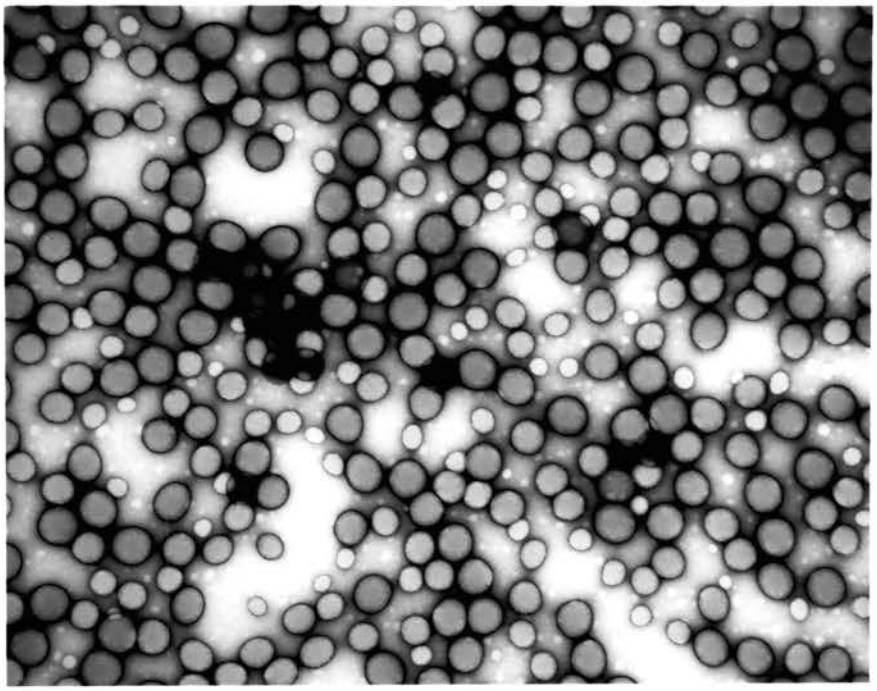

Figure 2. TEM of LA2-1 Latex.

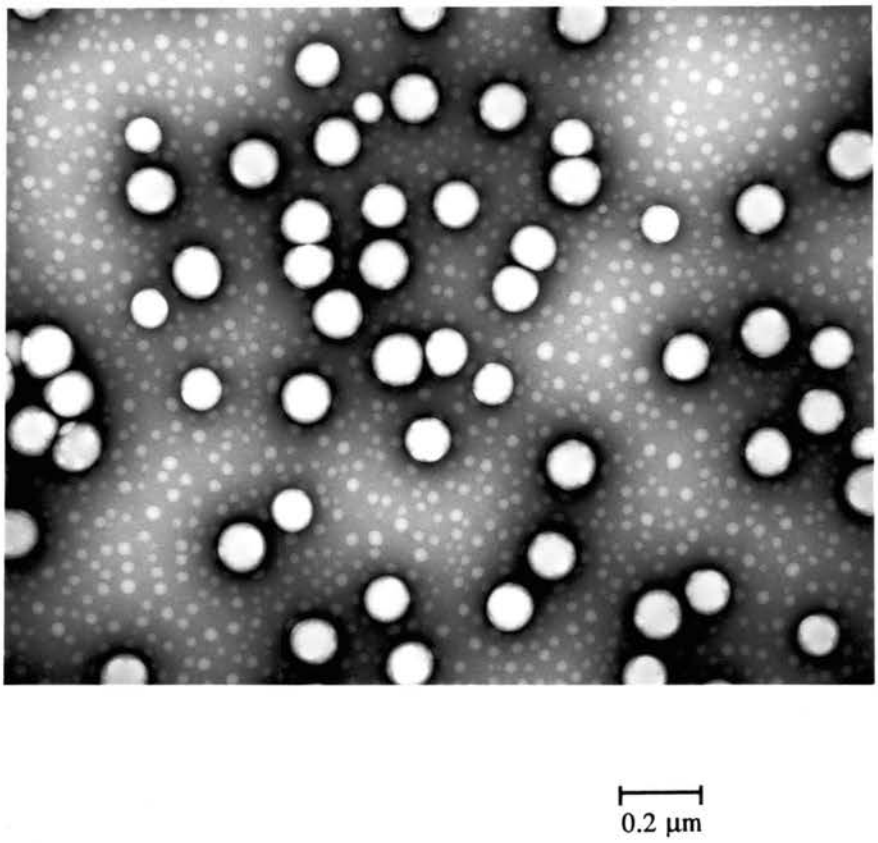

Figure 3. TEM of LA2-2 Latex.

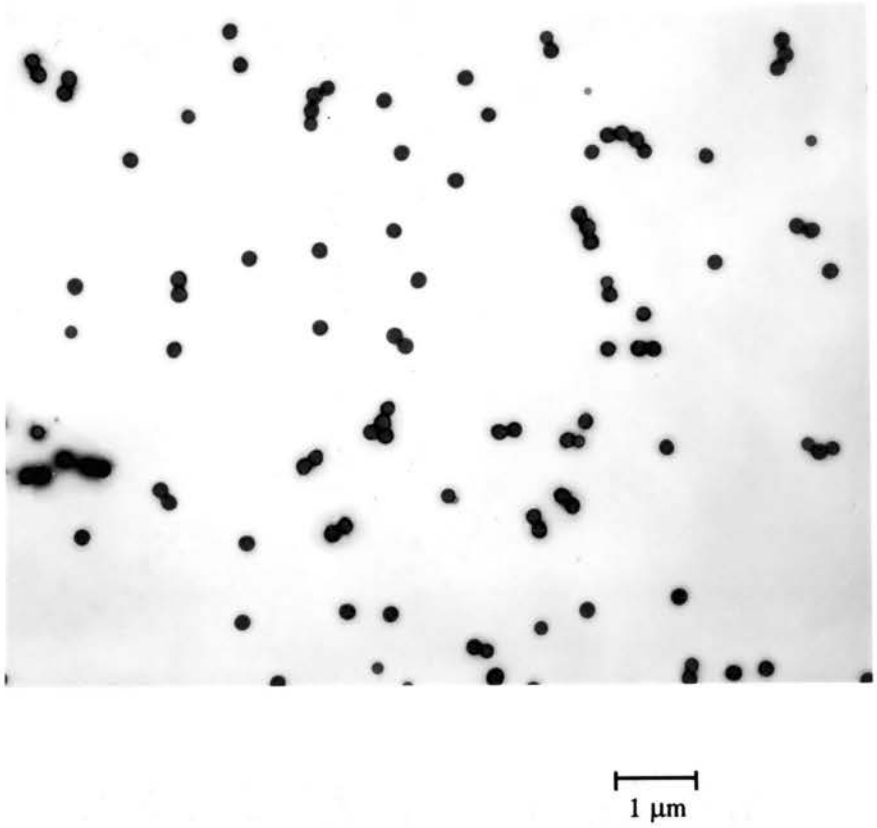

Figure 4. TEM of LA3-1 Latex.

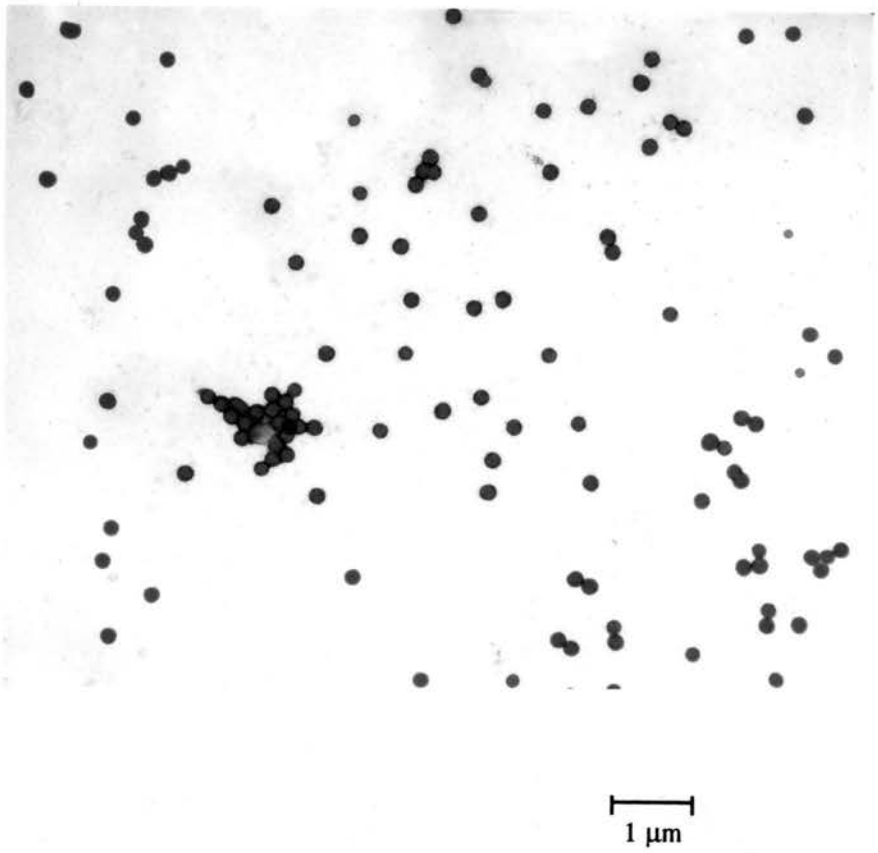

Figure 5. TEM of SG1-2 Latex.

sample preparation: 75 VBC means 75 wt % VBC in the copolymer latex. The latexes were quaternized with trimethylamine to obtain the $1N^+$, $2N^+$, $5N^+$, $10N^+$, $25N^+$, $50N^+$, and $75N^+$ latexes. The symbol N^+ stands for quaternary ammonium ion. The latexes were ultrafiltered with water until the conductance of filtrates reached a low constant value. The amount of quaternary ammonium ions in units of milliequivalents per gram of latex was determined by titration of chloride counterions using an ion selective electrode. The amount of quaternary ammonium ions in mmol % was also calculated from the titration data, and will be used for kinetic activity analysis. The results are all listed in Table II.

Table II. Compositions of Latexes

sample	N^+, mmol g^{-1}	N^+, mol %
$1N^+$	0.06	0.63
$2N^+$	0.05	0.55
$5N^+$	0.12	1.27
$10N^+$	0.56	6.2
$25N^+$	1.37	16.9
$50N^+$	2.42	34.1
$75N^+$	3.50	60.4

Titrations. Volhard titration[7] is a classic method for determining chloride content in liquid samples. This method uses excess silver nitrate to precipitate the chloride ions in samples under acidic conditions, and then NH_4SCN is used to back titrate the excess silver cations with $NH_4Fe(SO_4)_2$ as indicator. The end point is determined by observing the first color change to permanent red-orange. However, the amounts of Cl^- in the latex samples determined by the Volhard method were much lower than we expected for the quaternization reactions. The observation of the titration end point is very difficult due to the light scattering of the particles. Moreover, the end points for latex samples did not reach permanent red-orange color; they faded again and again shortly after color showed up

in the titration solutions. A chloride ion selective electrode was introduced for determination of quaternary content in latex samples to solve the problem. The samples were directly titrated using standard $AgNO_3$ solution. The advantages of the ion-selective electrode method are: (1) End points are easily determined. (2) Experimental preparation is simpler than in the Volhard method. However, latexes might affect the accuracy of the measurements due to contamination on the surface of the electrode. To investigate the accuracy of direct titration of latex samples by electrode, three kinds of samples were tested: latexes, filtrates and supernatants of latexes. The latter two samples were prepared by replacing chloride ions of latexes with concentrated KNO_3, and separating latex particles by ultrafiltration and centrifugation techniques, respectively. The results are listed in Table IV. In direct titration, the amount of chloride ions measured in the $50N^+(12)$ latex is much lower by the Volhard method than by the electrode method. The amounts of chloride ions in the $50N^+(12)$ filtrate and supernatant matched very well by both titration methods and also were consistent with that of the latex sample by electrode direct titration. The amounts of chloride ions in the $50N^+$ and $50N^+(11)$ latexes by electrode titration were very close to the results by elemental analysis for nitrogen, which verified the accuracy of the electrode method. Since the time spent for each titration was less than 10 minutes in normal cases, latexes did not contaminate the surface of electrode, which was rinsed properly with water right after titrations. This was proved by directly checking the surface of the electrode and retesting electrode sensitivity with standard NaCl solutions.

Table III. Analyses of Chloride Ion Contents in Latexes

isolation	analytical method	N^+, mmol g^{-1} sample			
		$50N^+$[a]	$50N^+(11)$[a]	$50N^+(12)$[a]	$75N^+$
none	Volhard	0.90	1.24	1.44	-
	electrode	1.95[b]	2.37/2.47[b]	2.43	3.50
ultrafiltration	Volhard	1.94	2.42	2.24	3.22[c]
	electrode	1.94	2.40	2.43	3.31[c]
centrifugation	Volhard	-	-	2.41	-
	electrode	-	-	2.40	-
	elemental	1.88	2.63	-	-

[a] $50N^+$ was quaternized in a flask at atmospheric pressure. $50N^+(11)$ and $50N^+(12)$ are different ultrafiltration portions of $50N^+(1)$ latex sample which was quaternized in a pressure-resistant can. [b] Titrations were done at about pH 7. All other titrations were done at about pH 2. [c] Samples were not washed well due to difficulty in ultrafiltation.

Particle Sizes. Particle sizes were measured with TEM and DLS. The dry particle sizes were measured by TEM and calculated as weight average diameter and number average diameter of 50 particles directly from the TEM negatives. The photographs of seven copolymer latexes ($1N^+$ latex was 1VBC since this sample was not quaternized after copolymerization) are in Figures 6-12. The results show that seven latexes with different compositions have very close size, about 150 nm diameter. The sizes are also consistent with the preliminary experiments in Table I. The polydispersity indexes, calculated as ratio of weight average diameter to number average diameter of particles, are 1.01.

Table IV. Sizes of Monodisperse VBC Latexes

	TEM		
sample	D_w (nm)	D_n (nm)	D[a]
$1N^+$	151.0	149.4	1.01
2VBC	147.6	146.3	1.01
5VBC	153.9	152.7	1.01
10VBC	156.5	155.2	1.01
25VBC	163.5	161.8	1.01
50VBC	147.1	146.5	1.00
75VBC	154.3	153.4	1.01

[a] Polydispersity index $D = D_w/D_n$.

After quaternization with trimethylamine, the sizes of the latexes were remeasured by TEM. The photographs of the $10N^+$, $25N^+$, $50N^+$ and $75N^+$ latexes are in Figures 13-16 and the results are listed in Table IV. The size of the $10N^+$ latex did not change. The sizes of the higher ion content latexes increased, and the higher the ion content, the bigger

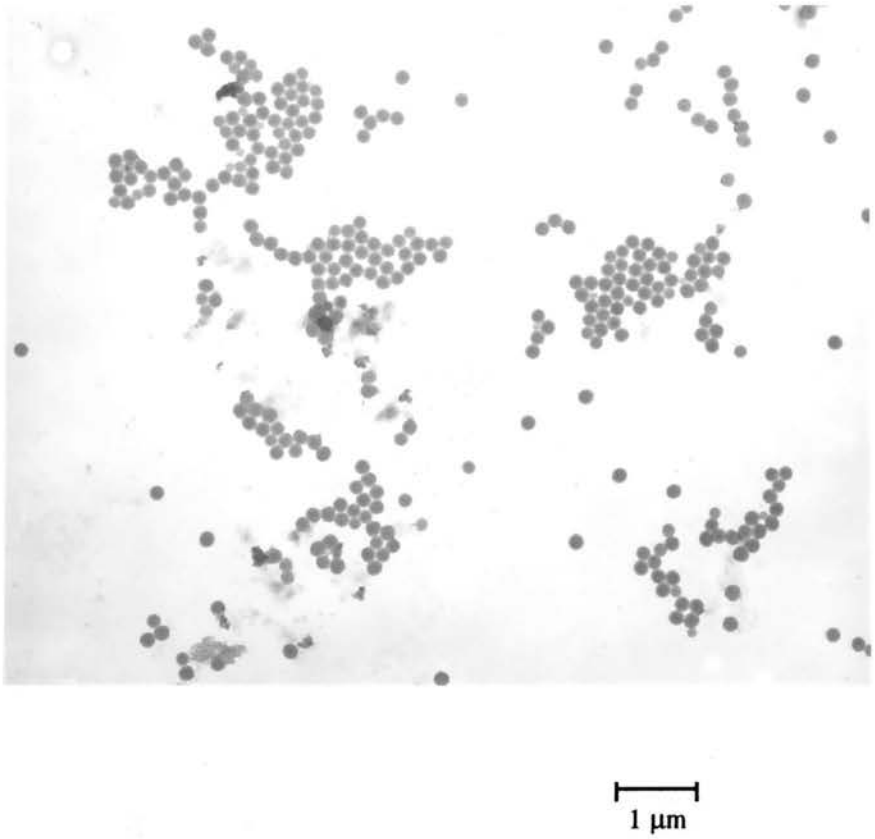

Figure 6. TEM of $1N^+$ Latex.

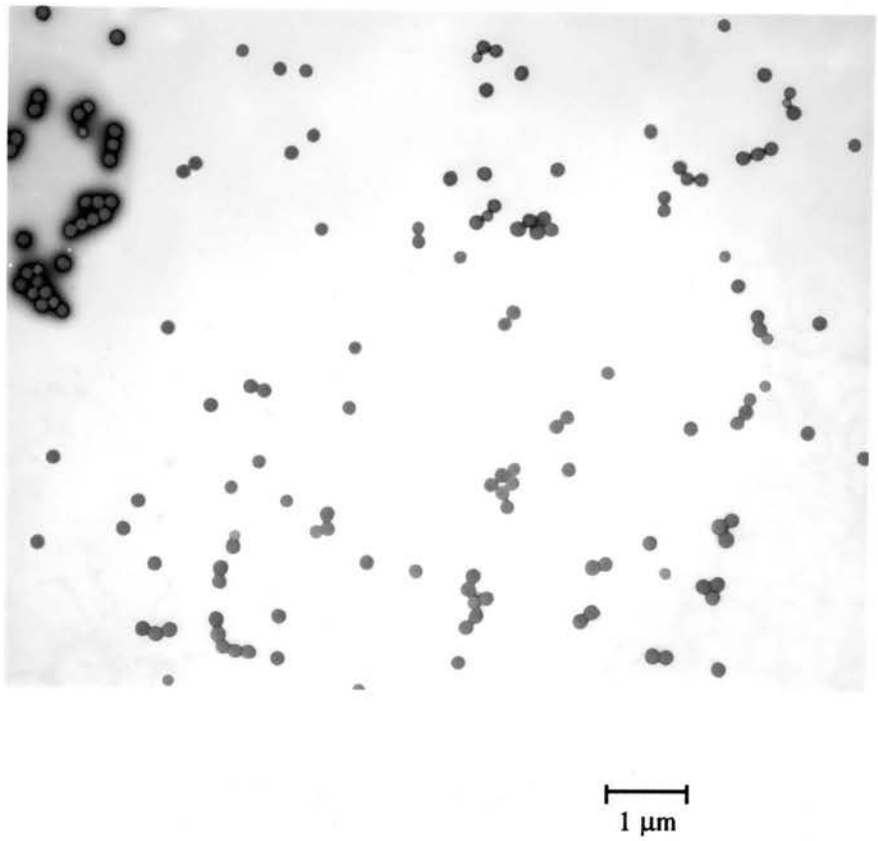

Figure 7. TEM of 2VBC Latex.

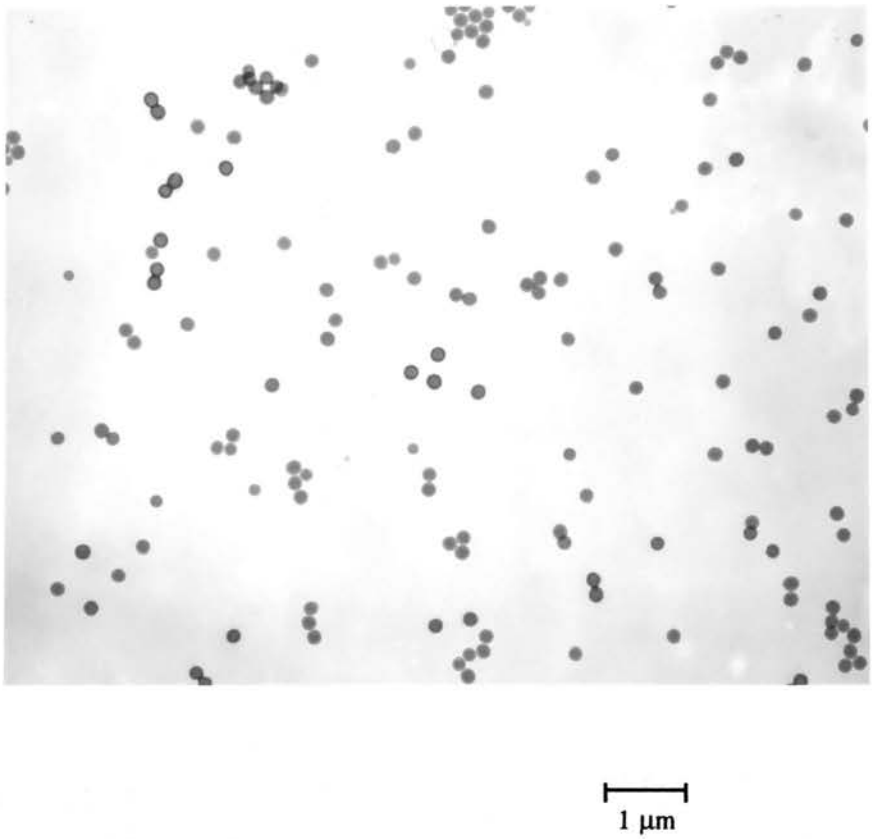

Figure 8. TEM of 5VBC Latex.

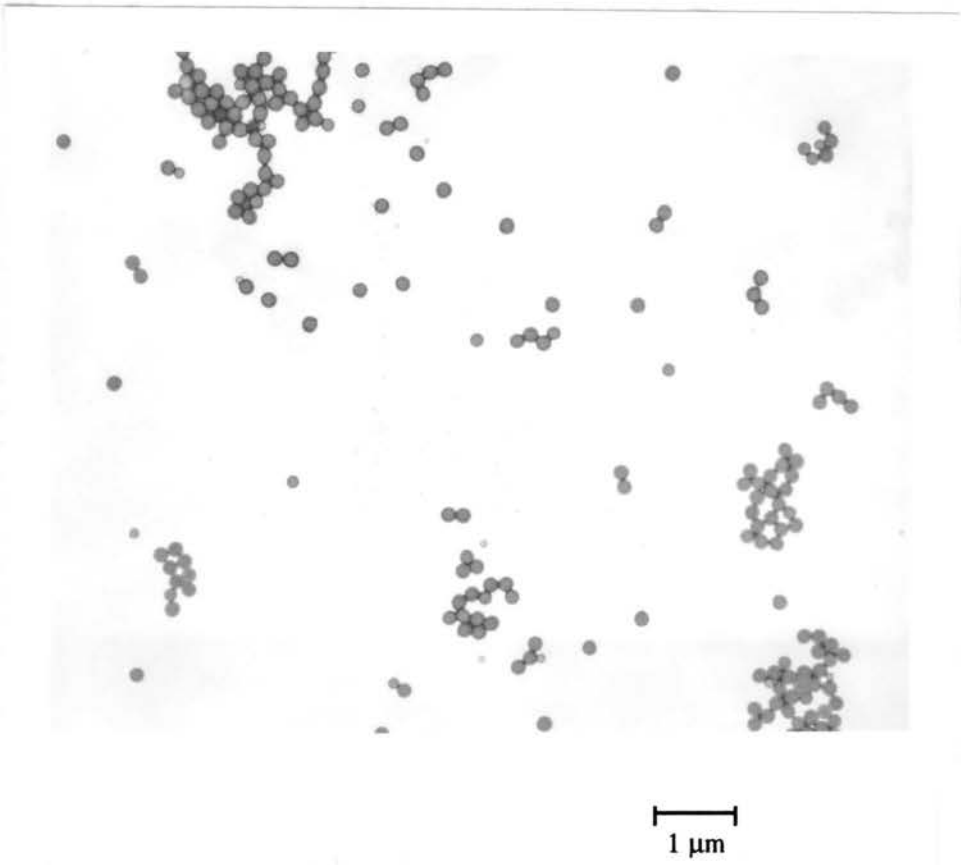

Figure 9. TEM of 10VBC Latex.

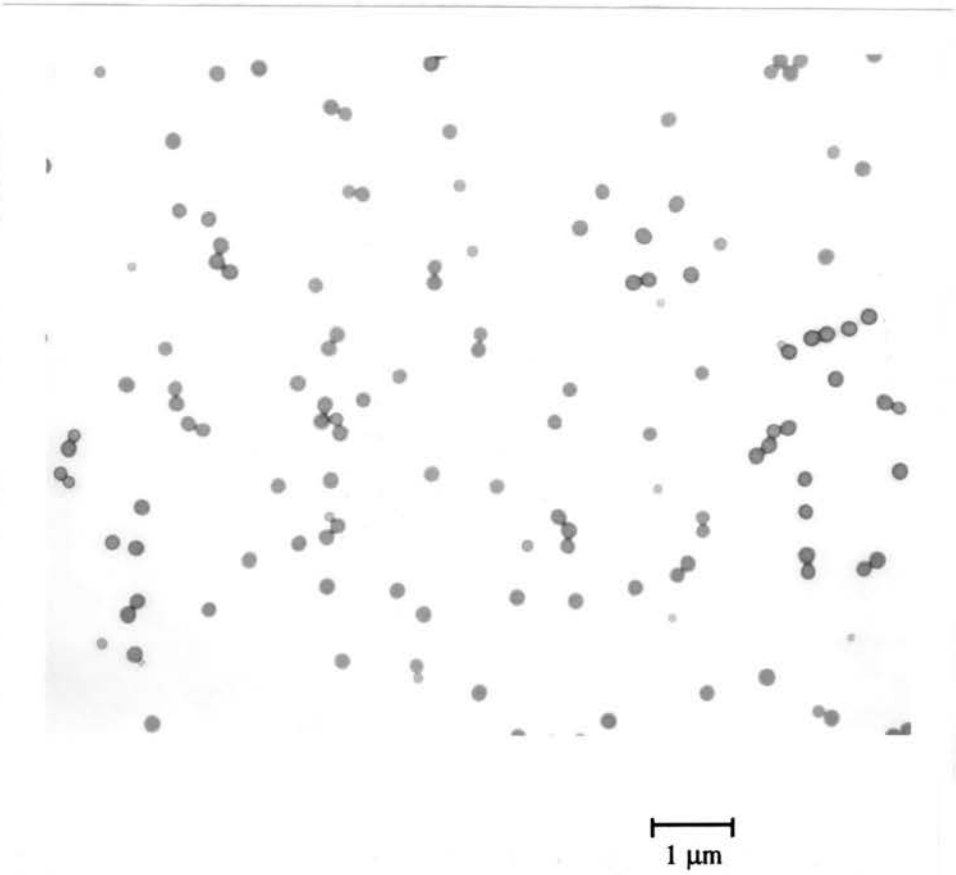

Figure 10. TEM of 25VBC Latex.

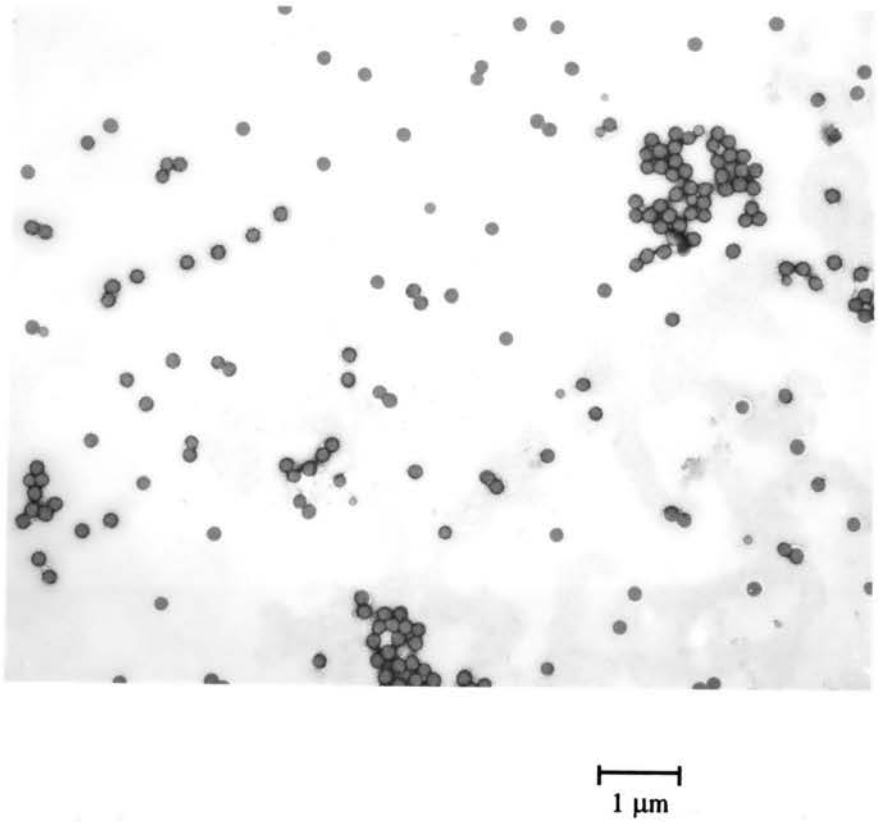

Figure 11. TEM of 50VBC Latex.

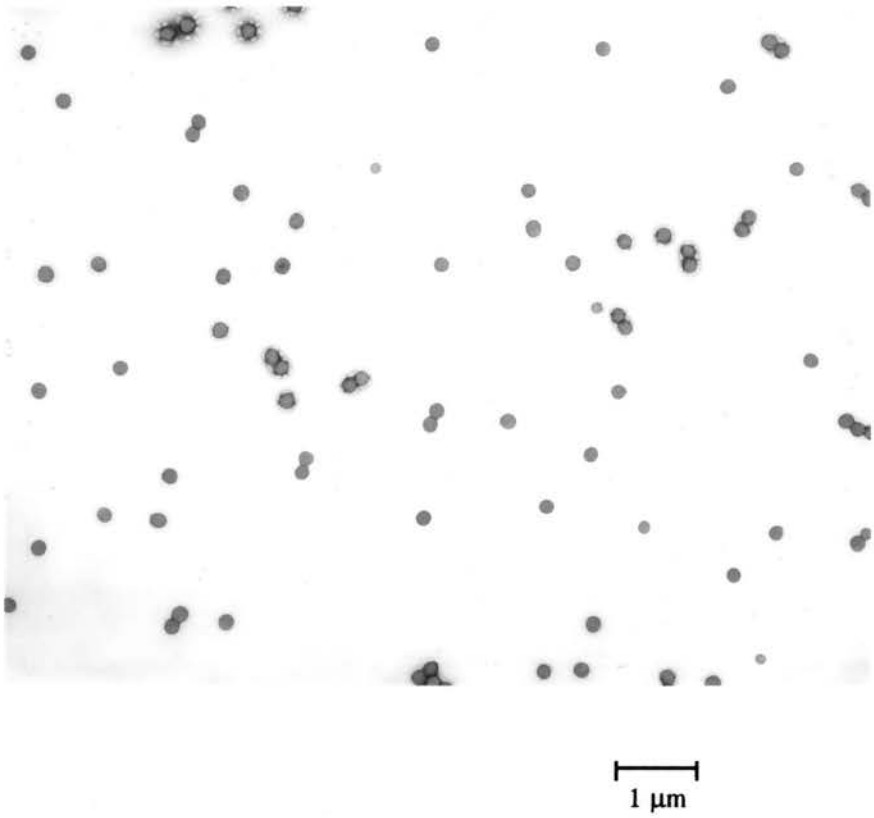

Figure 12. TEM of 75VBC Latex.

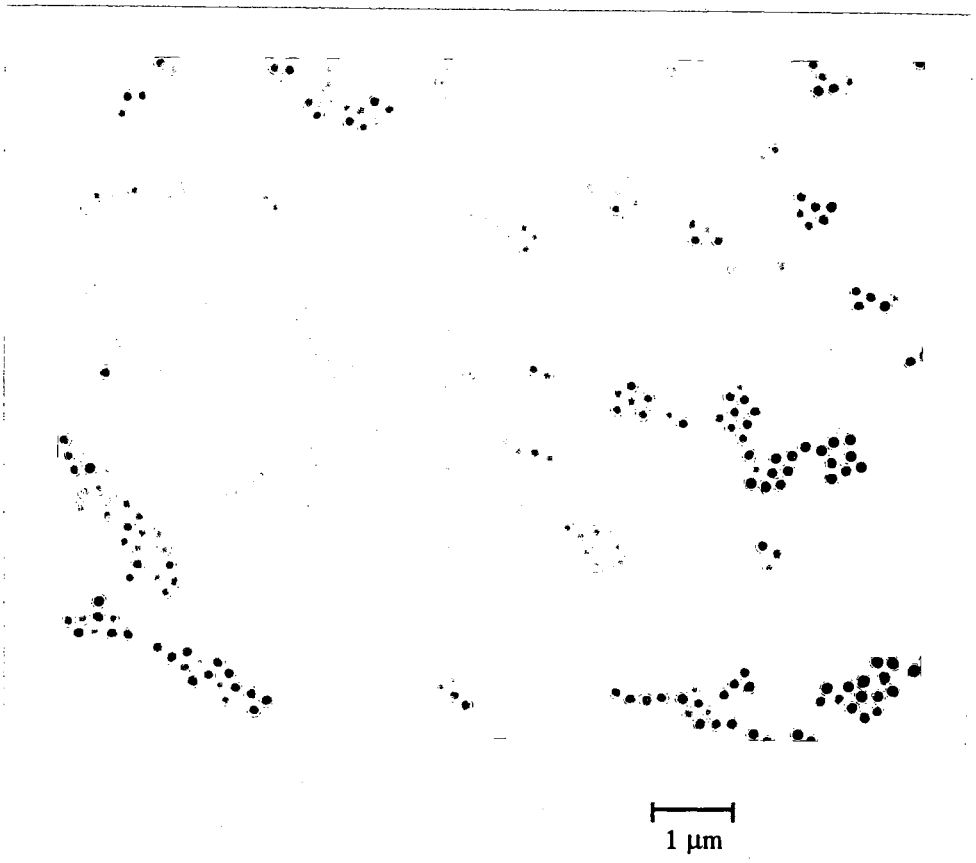

Figure 13. TEM of 10N+ Latex.

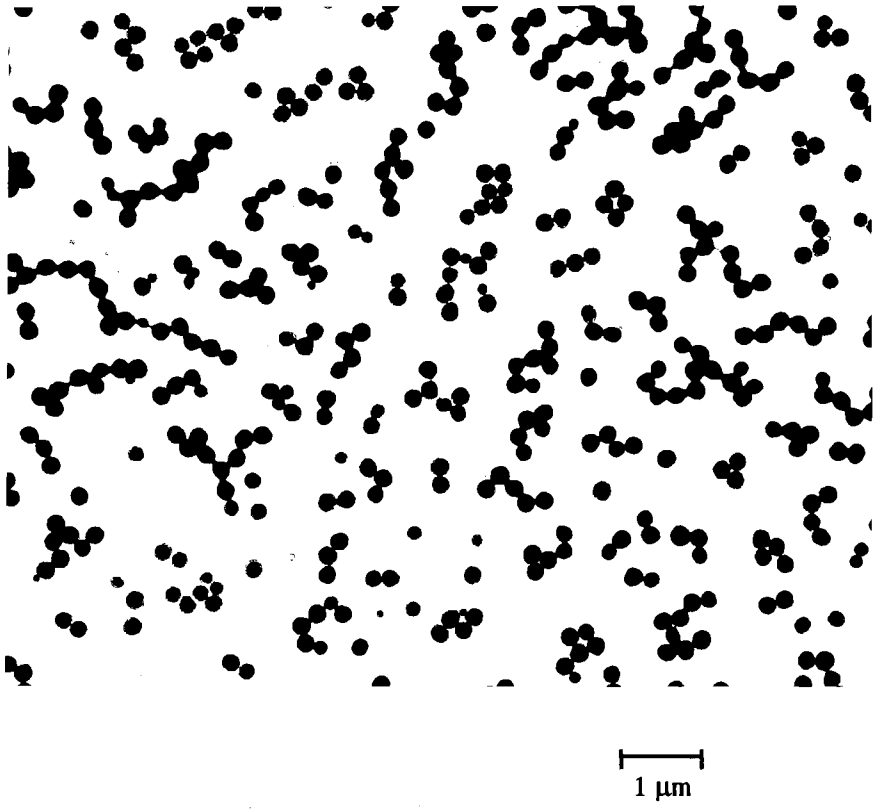

Figure 14. TEM of 25N+ Latex.

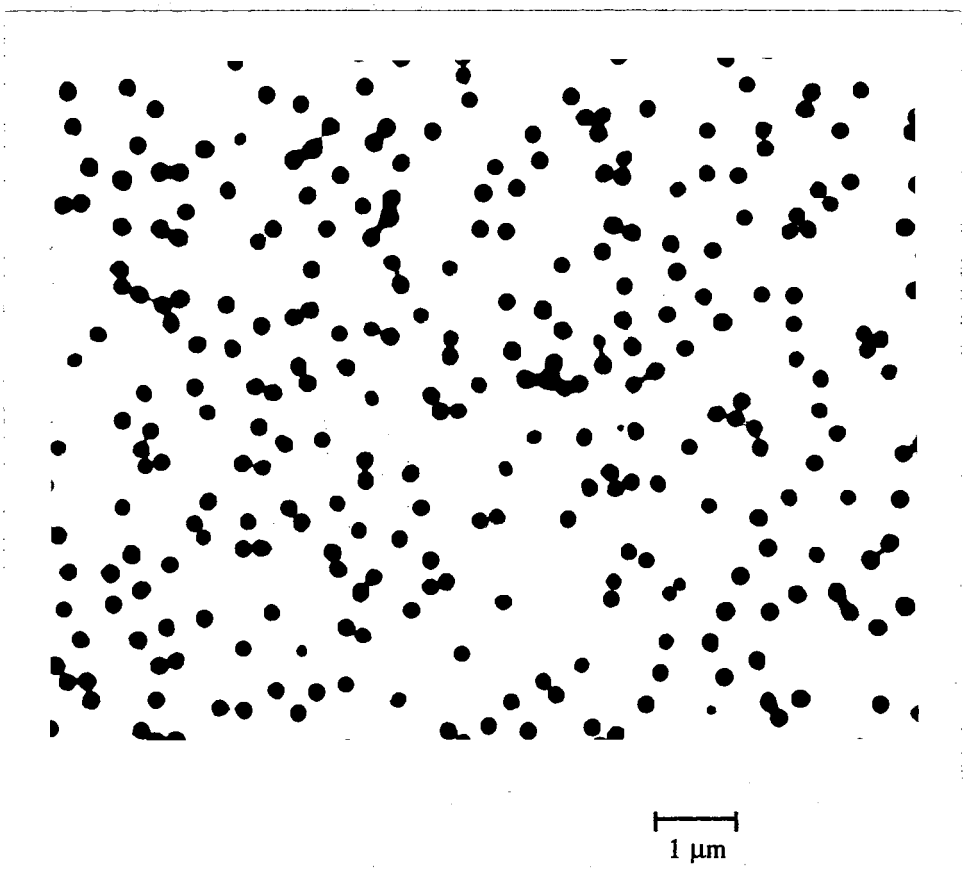

Figure 15. TEM of 50N+ Latex.

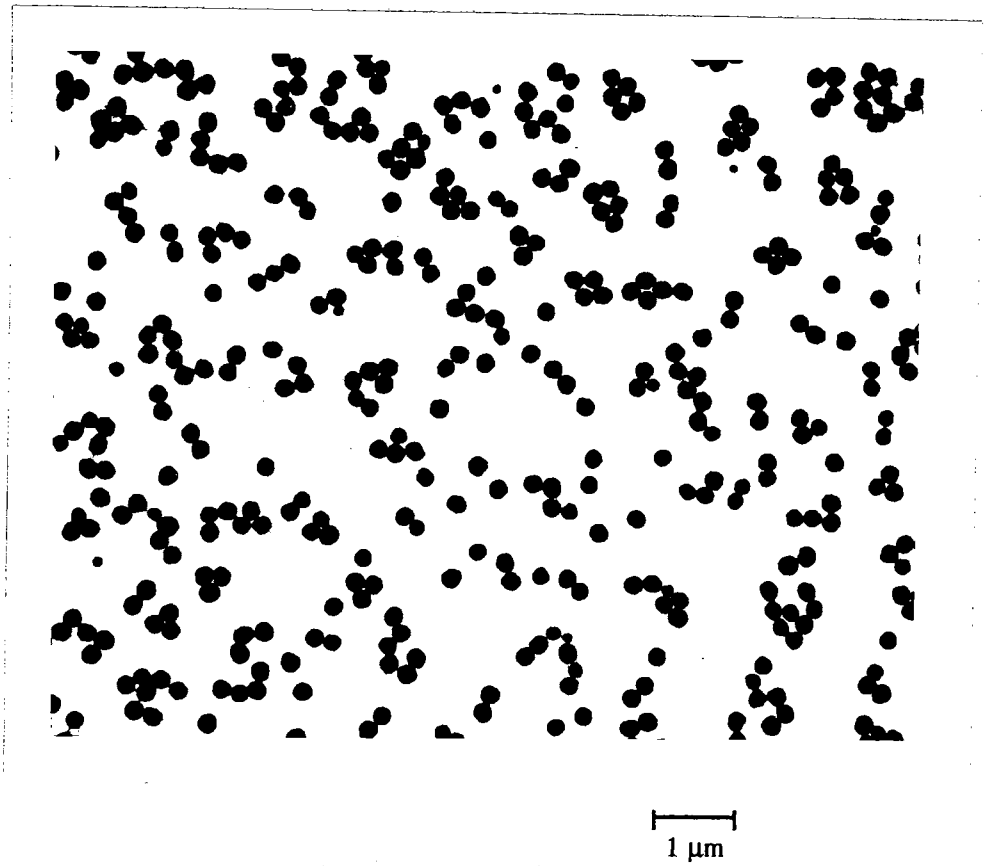

Figure 16. TEM of 75N+ Latex.

the increase. The wet particle sizes of quaternized particles, hydrodynamic diameters (D_h), were measured in water and are also listed in Table IV. The ratio of wet particle volume over dry particle volume for each latex sample was calculated as the ratio of the cube of the particle diameter in water by DLS to the cube of the particle diameter D'_w by TEM. The D'_w is corrected particle diameter, and for the three highest ion content latexes it is different from D_w because the shape of the highly quaternized latexes is deformed in TEM sample preparation.[8] The corrected diameters were based on the copolymer latex diameters by TEM and the change of weight and density of the latexes after quaternization. The calculation is demonstrated in the experimental section.

The three lowest ion content latexes did not swell much, but the more highly ionic latexes were swollen 2 to 13 times in water.

Table V. Sizes of Monodisperse N^+ Latexes

	TEM			DLS		
sample	D_w (nm)	D_n (nm)	D'_w (nm)	D[a]	D_h (nm)[b]	V_{wet}/V_{dry}[c]
$1N^+$	151.0	149.4	151.0	1.01	165.6	1.31
$2N^+$	147.6	146.4	147.6	1.01	159.2	1.23
$5N^+$	154.5	153.9	154.5	1.00	171.6	1.36
$10N^+$	155.5	154.5	155.5	1.01	182.8	1.61
$25N^+$	176.3	174.7	168.4	1.01	217.4	2.15
$50N^+$	170.4	168.4	155.9	1.01	274	5.42
$75N^+$	182.7	181.0	168.2	1.01	379	13.15

[a] Polydispersity index $D = D_w/D_n$. [b] Measured in water. [c] $V_{wet}/V_{dry} = D_h^3/D'^3_w$.

Particle Size by DLS and SLS in Electrolyte. Dynamic light scattering and static light scattering results are usually reported as radii, as in Figures 17-20. For

convenience, we use radius to discuss particle sizes in aqueous dispersions by DLS and SLS. Hydrodynamic radii (R_h) of the $75N^+$ and $50N^+$ latexes were measured by DLS in different concentrations of NaCl in 10 fold intervals. The R_h values of the $75N^+$ latex decrease from 190 nm in 1 x 10^{-6} M added NaCl to 127 nm in 1.0 M NaCl. A similar result was observed with the $50N^+$ sample which has R_h 143 nm in 1.0 x 10^{-6} M NaCl and about 120 nm in 1.0 M NaCl. The radii of gyration (R_g) of the two latexes were obtained by static light scattering (SLS) under the same conditions as R_h. The R_g values almost remain constant over the entire range of NaCl concentrations. Graphs of the R_h and R_g values of the $75N^+$ and $50N^+$ latexes vs. the concentration of NaCl are shown in Figures 17 and 18. The ratios of R_g to R_h of the $75N^+$ and $50N^+$ latexes vs. concentration of NaCl are plotted in Figures 19 and 20 respectively. The straight lines of $R_g/R_h = 0.775$ in Figures 19 and 20 are the theoretical value for hard sphere particles. The ratio of R_g to R_h of the $75N^+$ and $50N^+$ latexes is much less than the hard sphere value at low NaCl concentration and close to the hard sphere value when NaCl concentration reaches 1.0 M.

Synthesis of Polyelectrolytes. Three poly(styrene-co-VBC) samples with the same compositions as the 75VBC, 50VBC, and 25VBC latexes, but lacking DVB, were synthesized by solution polymerization with 2,2'-azobisisobutyronitrile (AIBN) as an initiator. The copolymers were quaternized with trimethylamine to obtain polyelectrolytes which have the same compositions as the $75N^+$, $50N^+$, and $25N^+$ latexes. The polyelectrolytes were named $75N^+$PE, $50N^+$PE, and $25N^+$PE. The $75N^+$PE and $50N^+$PE are soluble in water and methanol, and the $25N^+$PE is soluble in methanol but not in water because it has fewer ionic side chain groups. The $75N^+$PE and $50N^+$PE were characterized and used for catalysis kinetics. The molecular weights of the 75VBC and 50VBC copolymers were determined by gel permeation chromatography (GPC), relative to polystyrene standards, to be M_n = 7100 and 6700, the polydispersity indexes were 1.96

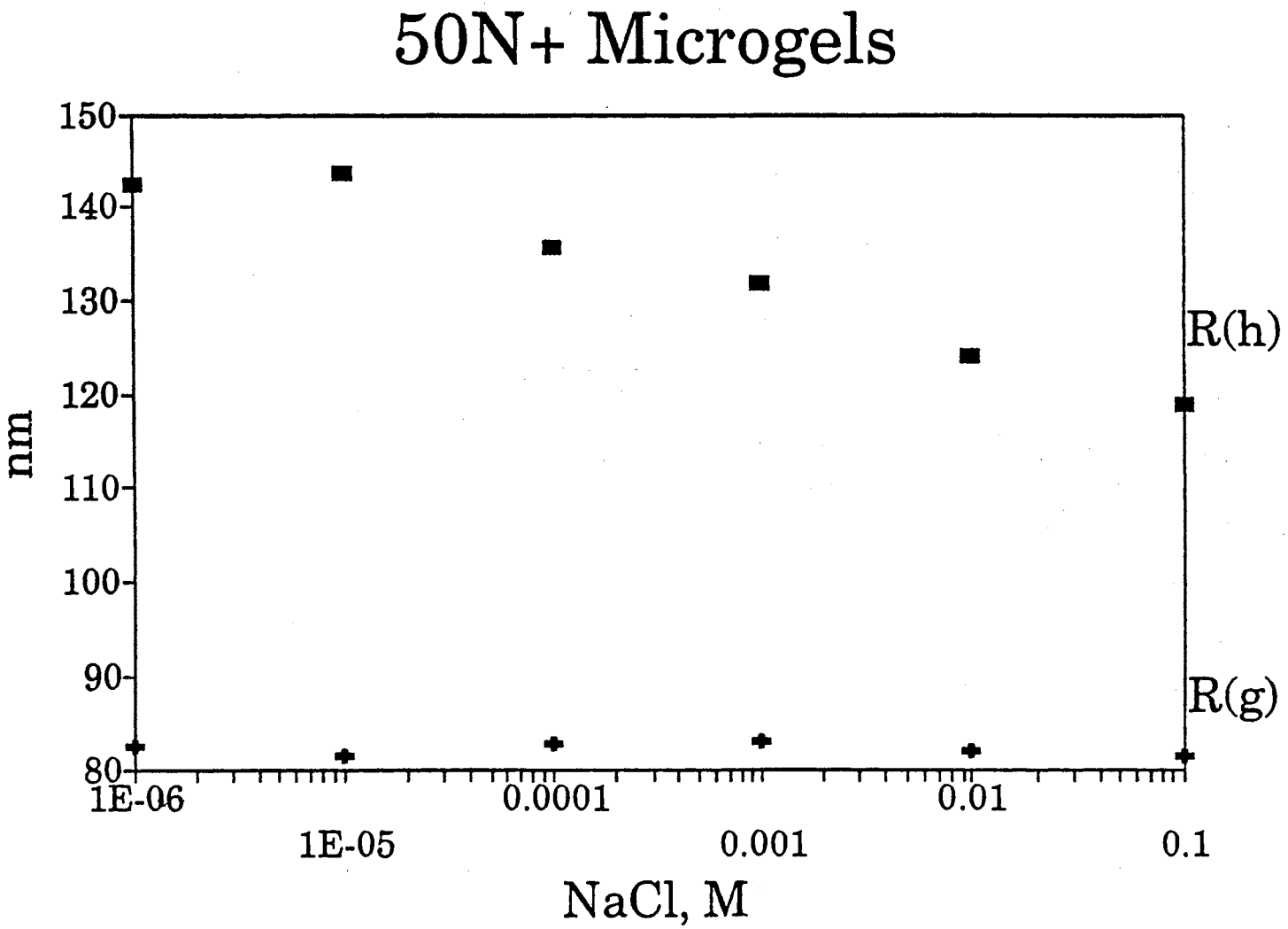

Figure 17. Hydrodynamic radii (R_h) and radii of gyration (R_g) of 50N+ latex in NaCl by DLS and SLS.

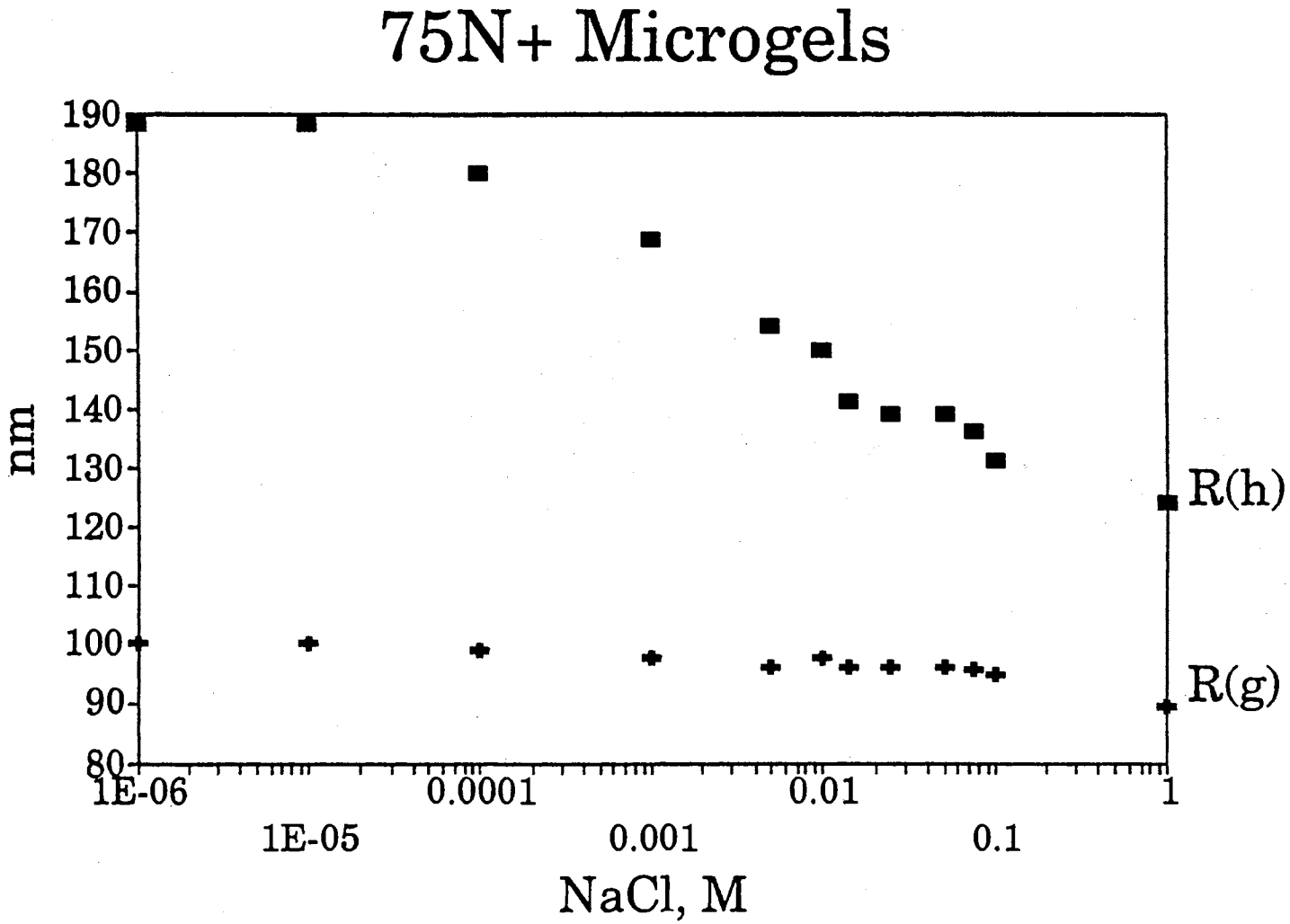

Figure 18. Hydrodynamic radii (R_h) and radii of gyration (R_g) of $75N^+$ latex in NaCl by DLS and SLS.

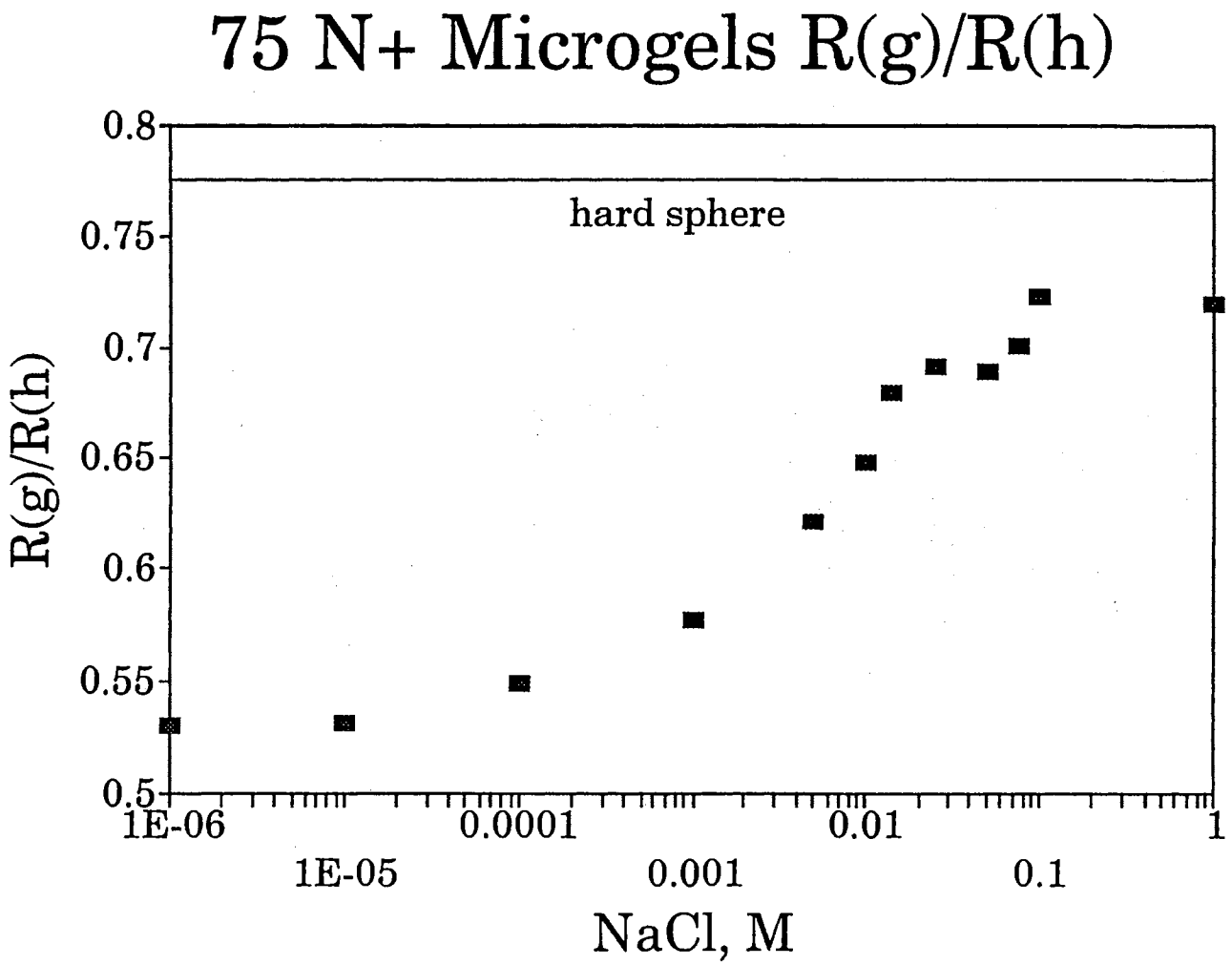

Figure 19. The ratio of R_g to R_h of 75N+ latex as a function of NaCl concentration.

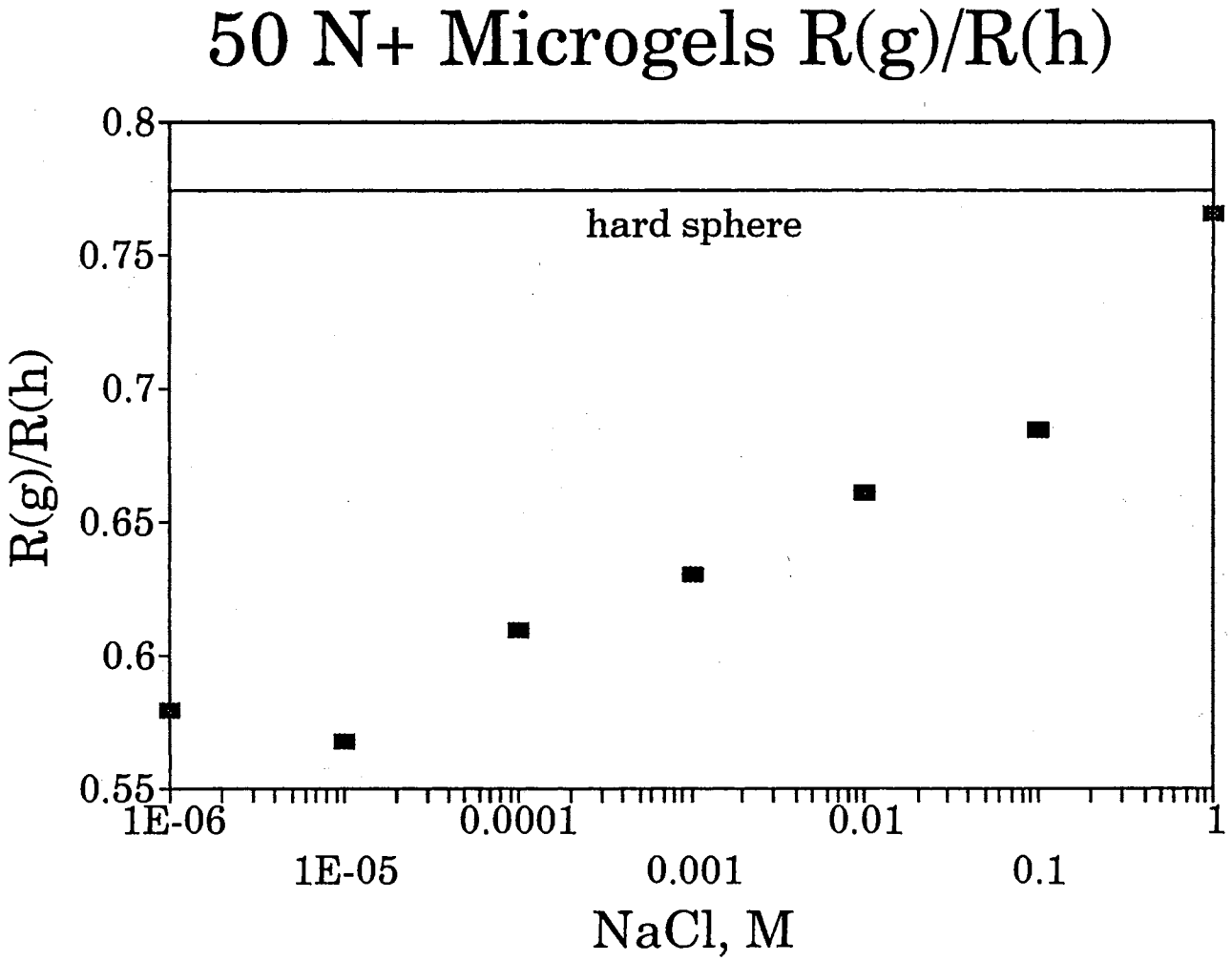

Figure 20. The ratio of R_g to R_h of $50N^+$ latex as a function of NaCl concentration.

and 2.15, respectively, and the quaternary group contents by Cl^- electrode titration were 3.59 and 2.68 milliequivalents per gram of polymer.

Discussion

Latex Synthesis. In conventional emulsion polymerization, oil soluble or water soluble initiators can be used to create free radicals. However, in the absence of emulsifier, water soluble initiators play an important role in imparting stability and monodispersity of latexes in the shot growth method.[5,6] From Kim's investigation of copolymerization of styrene and sodium styrenesulfonate, oil soluble initiators produced stable latexes, but they were not monodisperse even in the presence of ionic comonomers. Monodisperse and stable latexes were produced by water soluble initiators. Our previous investigation of AIBN for copolymerization of styrene, VBC, and vinylbenzylcetyldimethylammonium chloride verified Kim's results.[9] The water soluble initiator 2,2'-azobis(N,N'-dimethyleneisobutyramidine) dihydrochloride was chosen for this investigation so that the ionic groups from the initiator have the same sign of charge and the same counterions as the final quaternary ammonium ion latexes.

In the shot growth polymerization of styrene and sodium styrenesulfonate, no more than 1 wt % of ionic monomer was used in the first shot for controlling latex monodispersity.[5] In our study, different amounts of ionic monomer in the first shot polymerization of styrene were preliminarily investigated as LA1-1 to LA1-5. Since surfactants decrease the surface tension of monomer droplets and particles in water during emulsion polymerization, the amount of surfactant will affect the sizes of particles formed. The more the surfactant, the smaller the particles. The sizes of latexes LA1-1 to LA1-5 decreased with increasing the amount of the ionic monomer from 200 nm to 110 nm. The size of the LA1-5 latex with 0.6 wt % of charged monomer is about 150 nm. The amount of 0.6 wt % ionic monomer in the first shot was chosen to give more stable seed particles

compared with those of lower ionic monomer content, and to give particles of about 150 nm diameter as catalyst supports.

Kim's results showed that up to about a 0.5 ratio of sodium styrenesulfonate to styrene could be used in the second stage without loss of latex monodispersity. Since more binding sites were needed for our catalyst supports, vinylbenzyl chloride was copolymerized with styrene and more quaternary groups were created by reaction of chloromethyl groups with trimethylamine. In the further investigation adding VBC monomer in either shot did not affect the particle size compared with the homopolystyrene latex with the same amount of ionic monomer in the first shot. The seed particles also were monodisperse.

The shot growth technique is different from seed growth polymerization. Seed polymerization uses completely formed polymer seed particles, and a large amount of monomers in the second polymerization step to increase particle sizes. However, in the shot growth polymerization the first shot controls particle sizes, and the second shot varies ion content of latexes by using small amount of monomers. The second shot is added before the first shot is completely polymerized.

In order to get a high vinylbenzyl chloride/styrene ratio in the latex, vinylbenzyl chloride monomer has to be added in both stages in this work. Varying the amount of vinylbenzyl chloride monomer in both shots, the latexes were designed to contain 0 to 75 wt % (based on total monomers in each sample preparation) of VBC monomer. After quaternization, a series of latexes with a wide range of quaternary group contents was obtained. This method indirectly creates high ion content latexes as in normal ion exchange resins and avoids the use of high ionic monomer content in polymerization, which would produce polydisperse latexes and polyelectrolyte.

Particle Sizes under Different Conditions. The sizes of latex particles are different by TEM and DLS. TEM measures dry particle sizes and DLS measures wet

particle sizes. The four latexes with lower ion content have only slightly greater size by DLS than by TEM, but the three more ionic latexes show tremendous difference between wet and dry sizes. This difference is due to hydration of fixed ionic groups on the latexes in aqueous conditions as in normal ion exchange resins.

Swelling of ion exchange resins depends on their degree of cross-linking, amount of ionic groups, and the affinity of the fixed ionic groups and their counterions for water. It is explained by three kinds of expansion forces: (1) Fixed ionic groups and their counterions tend to form solvation shells. (2) Electrostatic repulsion increases the distance between fixed ion groups when they dissociate in water. (3) Concentrated ions in the particles cause an osmotic pressure difference between the interior of particles and the external solution. This is also applicable to ion exchange latexes. Because the latexes are all about 1 wt % cross-linked, it is the amount of ionic groups in the latexes that makes them swell differently in water. The higher the ion content, the more the latexes swell. Structures of the ionic groups were not varied in this work, but would also affect swelling according to their degree of hydration.

The hydrodynamic radii of the $75N^+$ and $50N^+$ latexes decrease with increase of electrolyte concentration. This is caused by the mass action effect of electrolyte: Concentrated NaCl screens the charges on the particles and decreases the degree of dissociation of the fixed ionic groups. Therefore interchain electrostatic repulsion in particles is reduced. However, the radii of gyration R_g of the latexes are not changed when electrolyte concentration changes. What is the difference between these two radii? The hydrodynamic radius of a hard spherical particle is calculated by the Stokes-Einstein equation:

$$R_h = kT/6\pi\eta D \qquad (1)$$

Here k is the Boltzmann constant, T is absolute temperature, η is the viscosity of the medium, and D is the diffusion coefficient of the particle. Dynamic light scattering

measures the diffusion coefficient of the particles, and R_h is calculated using equation (1) and measured D, assuming no particle interaction. R_h includes the ionic double layer around the particle which moves with the particle.

The radius of gyration is defined by the following equation:

$$R_g = [(\Sigma M_i R_i^2)/\Sigma M_i]^{1/2} \qquad (2)$$

R_g is the root mean square distance between a chain segment and the center of mass of the particle. Here M_i is the molecular weight of a repeat unit of the polymer and R_i is its distance from the center of mass. R_g is obtained by static light scattering (SLS) as a function of scattering angle. It can be imagined that the radius of gyration is a measure of the size of the particle core, which does not change with electrolyte concentration in the surrounding water. The change of the hydrodynamic particle size in electrolyte affects the structure of latexes and therefore affects the kinetics in particles. This will be discussed later in Chapter III.

Polyelectrolyte Synthesis. To study the effects of latex structure on the catalysis, three highly charged polyelectrolytes with the same compositions as corresponding latexes were synthesized by solution polymerization with oil soluble initiator AIBN. Previously, we tried to synthesize these polyelectrolytes by emulsion polymerization. The polymers obtained were not soluble in organic solvents or water and were assumed to be cross-linked. Chonde[10] reported that a copolymer of styrene and VBC (0.3 mole ratio) contained 0.85 wt % polyelectrolyte based on total produced polymer after sulfonation of the chloromethyl groups, that adding 2% and 8.6% of DVB for cross-linking decreased the amounts of polyelectrolyte to 0.28 and 0.14 wt %, respectively, and that a homopolymer of VBC contained even more polyelectrolyte. Another paper[11] indicated that copolymers of styrene and VBC could be autocrosslinked by a Friedel-Crafts reaction under Lewis acid. Some others reported[12,13] that linear copolymers of styrene and

vinylbenzyl chloride could be obtained by solution polymerization in organic solvents. If water is critical for cross-linking to occur, there are two possible mechanisms: (1) Chloromethyl groups hydrolyze and condense with one another to form ether groups. (2) Chloromethyl groups hydrolyze, form benzyl cations, and undergo Friedel-Crafts reaction with styrene rings. If (1) is the case, the amount of cross-linked polymer will increase with the amount of vinylbenzyl chloride in the copolymer. If (2) is the case, the amount of cross-linked polymer will decrease with the amount of vinylbenzyl chloride at higher VBC content because benzyl cations will tend to react with styrene rather than VBC due to steric factor. There is no further evidence to prove which mechanism is more reasonable in this work.

Conclusions

The shot growth method has been successfully extended to copolymer latexes of styrene, divinylbenzene, vinylbenzyl chloride, and vinylbenzyltrimethylammonium chloride. A series of latexes with a range of 0.5- 60 mol % ionic repeat units was synthesized by the shot growth technique and further modification by trimethylamine quaternization. The copolymer latexes have almost the same dry sizes by TEM, about 150 nm diameter, and they are monodisperse. Instead of controlling charge density in the second shot, this work used sequential modification as in ion exchange resins to reach higher charge content in the latexes and avoid a high ratio of ionic monomer to nonionic monomers in the second stage which would sacrifice the monodispersity of the latexes.

Dynamic light scattering showed that latexes with low ion content were not swollen much in water, and higher ion content latexes were swollen 2 to 13 times in water compared with their dry form. The hydrodynamic radii of the $75N^+$ and $50N^+$ latexes decreased with increase of electrolyte concentration. The radii of gyration, which are measures of the sizes of the latex cores, were not changed by electrolyte.

For the purpose of studying the effects of the latex structure on kinetics, three copolymers of styrene and vinylbenzyl chloride were synthesized by solution polymerization in chlorobenzene and modified by trimethylamine to give polyelectrolytes having the same compositions as the three highest ion content latexes except lacking cross-linking.

Experimental Section

Materials. Styrene and divinylbezene (DVB, 55% of active DVB) from Aldrich, and vinylbenzyl chloride (VBC, *m/p* 70/30 based on NMR spectra) from Scientific Polymer Products were distilled under vacuum and stored at 5 ^{o}C in a refrigerator. Trimethylamine gas was from Matheson. Trimethylamine 25 wt % aqueous solution from Aldrich was used as received. Trimethylamine 25 wt % in methanol from Eastman Kodak was decolorized through an active carbon column. The initiator 2,2'-azobis(N,N'-dimethylene isobutyramidine) dihydrochloride (VA-044) was a sample from Wako Chemicals USA Inc. Deionized water with resistivity 1.4 x 10^6 ohm cm was used in all experiments.

Instruments. FTIR spectra were recorded on a Nicolet Impact 400 instrument. ^{1}H NMR spectra at 300 MHz and ^{13}C NMR spectra at 75 MHz were obtained with a Varian XL-300 instrument. Gas chromatographic analyses were performed with a Hewlett-Packard model 5840A instrument equipped with a thermal conductivity detector, temperature programming and a 6 ft x 1/8 inch o.d. Tenax® column (Supelco Inc.). The conductivities of aqueous solutions were measured with a YSI Model 31 conductivity meter equipped with a cell having 1.00 cm^{-1} constant.

Synthesis of *m,p*-Vinylbenzyltrimethylammonium Chloride.[14,15] A 250 mL three neck round bottom flask was equipped with a trimethylamine inlet, and a

condenser with acetone and dry ice. The outlet of the condenser led through a safety flask to a beaker of aqueous HCl solution. The flask was charged with 70 mL (74.9 g) of VBC and 50 mL of dry ethanol, and then was cooled in an ice bath. Trimethylamine gas was passed through a NaOH trap and an empty trap for safety purpose and bubbled slowly into the mixture with magnetic stirring at 0 °C for 3 h, and the mixture of solid and liquid stood at room temperature overnight. The mixture was extracted with ethyl ether and acetone respectively, and the extracting solutions were injected into GC. There was no VBC peak. The solid product was dissolved by adding more ethanol, precipitated into acetone, washed several times with acetone, and washed last with ethyl ether. The residual solvent was removed under vacuum. White needle-like crystals, 58.9 g (57% yield), were obtained. ^{1}H NMR ($CDCl_3$) δ 3.42 [t, 9 H, $N(CH_3)_3$], 5.08 [d, 2 H, $ArCH_2N$], 5.35 and 5.82 [2t, 2 H, $CH{=}CH_2$], 6.7 [q, 1 H, $CH{=}CH_2$], 7.4-7.7 [m, 4 H, C_6H_4]. ^{13}C NMR ($CDCl_3$) ppm 52.7 [CH_3], 68.6 [CH_2], 116.0, 117.2, 126.8, 129, 129.4, 130.8, 132.4, 133.3, 135.8, 138.5, and 140.0 [13, $CH{=}CH_2$ and C_6H_4]. There are many aromatic ring carbon signals due to meta and para isomers. The NMR and FTIR spectra are in Appendices. The product is highly hygroscopic.

GC Analysis of Styrene. Distilled styrene (100 mg), hexadecane (100 mg) and ether (3 mL) were mixed by shaking, and 2 μL of ether solution was injected into the GC. The chromatograph was temperature programmed (T_1 = 175 °C, T_2 = 275 °C, rate = 15 deg/min). The corresponding ratio shown in Table V was calculated by the following formula:

$$R = (A_{st}/A_s) \times (W_s/W_{st}) \qquad (3)$$

A_{st}: area of styrene A_s: area of standard

W_{st}: weight of styrene W_s: weight of standard

Table VI. Corresponding Ratio of Styrene and Hexadecane by GC

sample	A_{st}/A_s	W_s/W_{st}	R
1	1.034	0.991	1.025
2	1.033	0.991	1.024
3	1.037	1.007	1.044
4	1.025	1.007	1.032
AV			1.031

Conversion of the First Shot Polymerization. For the first shot of shot growth polymerization, samples (0.75 mL) were withdrawn by syringe at the beginning and at 1, 1.5, and 2 hours, respectively. The sample was mixed with 4 mL of ethyl ether and 50 mg of hexadecane, and 2 μL of the ether solution was injected into GC. The analysis was obtained by using the preceeding calibration. The results calculated by the following equations are shown in Table VII.

$$(A_{st}/A_s) \times (W_s/W_{st}) = R = (A'_{st}/A'_s) \times (W'_s/W'_{st}) \quad (4)$$

$$W'_{st} = (A'_{st}/A'_s) \times W'_s/R \quad (5)$$

Here A'_{st}, W'_s, and A'_s were measured data , and W'_{st} was calculated from equation (5).

Table VII. Conversion of Polymerization

sample	time (h)	A'_{st}/A'_s	W'_s	W'_{st}	% conv.
1-1	0.0	2.409	0.0438	0.102	0.0
1-2	0.0	2.383	0.0438	0.101	0.0
AV.	0.0			0.102	0.0
2	1.0	1.266	0.050	0.061	39.7
3	1.5	0.181	0.047	0.008	91.9
4	2.0	0.072	0.046	0.003	96.9
5	2.5	0.087	0.041	0.003	96.6
6	3.0	0.081	0.046	0.004	96.6

75VBC Latex. A 250 mL three-neck round-bottom flask was equipped with an overhead stirrer with a teflon blade, a condenser, an argon inlet, and an addition funnel that was also equipped with an overhead flexible shaft stirrer (Ace Glass Co. 8081) with a teflon blade and an argon inlet. The flask was charged with 108 mL of water and 0.072 g of *m,p*-vinylbenzyl-trimethylammonium chloride, and purged with argon for 20 min under stirring. The hygroscopic N^+ monomer was weighed by adding N^+ monomer into a weighed vial containing water on an analytical balance (A better way to get an accurate amount of the N^+ monomer is to make an aqueous solution of N^+ monomer, determine its concentration by titration for chloride ion, and measure certain volume of the solution for each polymerization). A mixture of 3.0 g styrene, 9.0 g of VBC, and 0.15 g of DVB was added, the system was heated for 20 min in a 60 ^oC oil bath, 0.12 g of VA-044 was added, and the mixture was stirred at 60 ^oC for 1.5 h.

The addition funnel was charged with 20 mL of water and 0.1 g of *m,p*-vinylbenzyltrimethylammonium chloride, and was purged with argon for 20 minutes under stirring. A mixture of 3.0 g of VBC, 0.05 g of DVB, and 1.0 g of styrene was added. After 5 min 0.04 g of VA-044 initiator was added. The mixture in the funnel was transferred to the flask under stirring 1.5 h after addition of initiator of the first shot. The mixture was stirred at 60 °C for another 3 h. The latex was filtered through a cotton plug.

The other latexes with compositions listed in Table VIII were made by the same procedure. There was a little coagulum (< 0.5 g) on the stir blade and the bottom of the flask in each sample.

Table VIII. Latex Compositions

	composition, wt (g)[a]			
	first shot		second shot	
sample	styrene	VBC	styrene	VBC
1VBC	12.00	0	4.00	0
2VBC	12.00	0	3.80	0.20
5VBC	12.00	0	3.30	0.70
10VBC	12.00	0	2.50	1.50
25VBC	11.00	1.00	1.00	3.00
50VBC	7.00	5.00	1.00	3.00
75VBC	3.00	9.00	1.00	3.00

[a] All samples contained 0.15 g of DVB, 0.072 g of N^+ monomer, and 108 mL of water in the first shot, and 0.05 g of DVB, 0.10 g of N^+ monomer, and 20 mL of water in the second shot.

75N+ Latex. A mixture of 70 mL of 75VBC latex (8.3 g solid, 29.3 mmol of VBC units) and 21 mL of 25 wt % aqueous trimethylamine solution (5.25 g, 89 mmol) was poured into a 150 mL beaker, and the beaker was sealed into a stainless steel reactor. The reactor was kept for 48 h half immersed in a 60 °C oil bath, and the mixture was kept stirring by adjusting the reactor position to synchronize the magnetic stirring bars in the reactor and in the oil bath. The excess trimethylamine was evaporated by bubbling nitrogen through the mixture. The latex was washed by ultrafiltration through a 0.1 μm cellulose acetate/nitrate membrane (Millipore®) under 60 psi of nitrogen with water for several days until the conductance of the filtrate decreased from 5 x 10^3 μmhos to a constant value of around 20 μmhos for the last three 30 mL portions of filtrate. The ultrafiltration was done in a stainless steel cylinder (from Gelman Scientific Company) kept shaking with a wrist action shaker from Burrell Corporation.

The results from quaternization of all six VBC latexes are in Table IX.

Table IX. Latex Quaternization

reactant	VBC (mmol)	25% $(CH_3)_3N$ (mL)	product	% yield	% solid (w/v)
75VBC	29.3	21	75N+	93.0	4.32
50VBC	19.6	14	50N+	87.7	5.98
25VBC	9.81	7	25N+	90.7	5.19
10VBC	3.92	7	10N+	89.2	5.02
5VBC	1.96	7	5N+	36.4	6.13
2VBC	0.78	7	2N+	39.7	7.30

Latex Solid Content. After purification, 3 mL latex was pipetted to an aluminum dish and dried in an oven at 100 °C more than 24 h. The sample was cooled in a desiccator and weighed on an analytical balance. The sample was heated and cooled several times until constant weight (±0.2 mg) was reached.

Ultrafiltration for Analysis. The ultrafiltration cylinder was filled with 4 mL of latex, and 10 mL of 5 M $NaNO_3$ was added to replace chloride ion. The mixture was stirred for 30 min and then ultrafiltered. The latex sample was washed and ultrafiltered four times with about 5 mL of $NaNO_3$ solution. The filtrate was collected directly in a 50 mL volumetric flask. Finally the solution was diluted to the mark with water.

Centrifugation for Analysis. Each 25 mL centrifuge tube was filled with 4 mL of latex sample and 20 mL of 5 M $NaNO_3$ used for replacing chloride anion. The mixture was shaken by a Vortex Mixer for 30 s, and centrifuged. The latex was washed and centrifuged four times with about 5 mL of $NaNO_3$ solution. The supernatants were collected directly in a 50 mL volumetric flask. Finally the solution was diluted to the mark with water.

Volhard Titration. This method uses excess standard $AgNO_3$ solution to react with chloride anions in aqueous solution. The excess amount of $AgNO_3$ is back titrated with NH_4SCN standard solution. For determining latex quaternary sites, 1 mL of latex sample or 12.5 mL of filtrate or supernatant equivalent to 1 mL of latex was pipetted in a 125 mL Erlenmeyer flask, 1 mL of 1 N HNO_3 was added, and 10 mL of 0.050 M $AgNO_3$ was mixed with the sample under stirring. About 7 mL of toluene was added slowly to protect the solution from air. The sample was back titrated with 0.0488 M NH_4SCN solution and reached an orange-red color end point.

Chloride Selective Electrode Titration. The quaternary sites were determined by titrating the chloride counterions with a chloride ion selective electrode (Orion Research Inc.). The sensitivity of the electrode was occasionally checked with six concentrations of NaCl standard solutions ranging from 1.0 M to 1.0×10^{-5} M in 10-fold intervals. A standard 0.050 M NaCl solution was also titrated for calibration every day.

Latex sample, 1 mL, or 12.5 mL of filtrate or supernatant, was pipetted into a 50 mL beaker, 0.6 mL of 5 M $NaNO_3$ was added as ionic strength adjustor, and 15 mL of water was added to cover the electrode. The mixture was adjusted to about pH 2 with 1N HNO_3 solution. The latex was titrated with 0.050 M $AgNO_3$ standard solution with recording of millivolts of the electrode potential. The titration curves were sharp and symmetrical, and the end points were determined by the normal method for potentiometric titration.

Measurement of Latex Particle Sizes by TEM.[16] Transmission electron micrographs were obtained with a JEOL 100-CXII instrument at a magnification of 10,000. The filament current and accelerating voltage were 100 μamp and 80 kV. The samples were prepared by placing a drop of a latex that had been diluted to <1% solids on a Formvar®-coated Cu grid, removing the excess latex by touching a piece of filter paper to the top, and drying in air. Subsequently a drop of 1% solution of uranyl acetate was placed on the grid, excess solution was removed again with filter paper, and the grid was dried in air. Diameters of 50 non-aggregated particles were measured directly from the micrograph negatives using an optical microscope equipped with a calibrated stage and a 10-fold objective lens. The number average radii, weight average radii and polydispersity indexes were calculated from the following equations and are reported in Table I and III.

$$D_n = (\Sigma D_i^3/\Sigma n)^{1/3} \tag{6}$$

$$D_w = (\Sigma D_i^6/\Sigma D_i^3)^{1/3} \tag{7}$$

$$D = D_w/D_n = R_w/R_n \tag{8}$$

The correction of D_w for the three highly quaternized latexes was done by the following equations:

$$\Delta W = (\text{mmol } N^+(CH_3)_3/\text{g polymer}) \times 59 \text{ mg } N^+(CH_3)_3/\text{mmol } N^+(CH_3)_3 \quad (9)$$

$$W_c = 1.000 \text{ g} - \Delta W \text{ (g)} \quad (10)$$

$$V_c = W_c/d_c \quad (11)$$

$$V_q = 1/d_q \quad (12)$$

$$D_q/D_c = (V_q/V_c)^{1/3} \quad (13)$$

Here ΔW is the weight increase due to quaternization, W_c is the weight of the copolymer latex per gram of the quaternized latex, V_c ,V_q , d_c , and d_q are the volume and density of the copolymer latex and quaternized latex, respectively. D_q/D_c is the ratio of quaternized latex diameter to copolymer latex diameter.

The corrected particle diameter was calculated from the copolymer latex diameter and corresponding D_q/D_c:

$$D'_w = D_w \times D_q/D_c \quad (14)$$

A calculation example is given for $75N^+$ latex below:

$\Delta W = 3.5$ mmol $N^+(CH_3)_3$/g polymer x 59 mg $N^+(CH_3)_3$/mmol $N^+(CH_3)_3$

$= 206.5$ mg $N^+(CH_3)_3$/g polymer

$W_c = 1.000 \text{ g} - 0.2065 \text{ g} = 0.7935$ mg

$V_c = 0.7935 \text{ g} \times 1 \text{ mL}/ 1.169 \text{ g} = 0.679$ mL

$V_q = 1 \text{ g} \times 1 \text{ mL}/ 1.142 \text{ g} = 0.876$ mL

$D_q/D_c = (0.876/0.679)^{1/3} = 1.09$

$D'_w = 154.3 \times 1.09 = 168.2$

Table X. Correction of TEM Size for the highly quaternized latexes

latex	D_w (nm)	N+ mmol/g	dc (g/cm^3)	dq (g/cm^3)	D_q/D_c	D'_w (nm)
75N$^+$	154.3	3.50	1.169	1.142	1.09	168.2
50N$^+$	147.1	2.42	1.130	1.110	1.06	155.9
25N$^+$	163.5	1.37	1.083	1.070	1.03	168.4

Measurement of Latex Particle Sizes by DLS and SLS. A drop (15-50 μL) of latex was diluted in 25-50 mL of water or aqueous NaCl of known concentration. Light scattering experiments were performed using as ALV-5000 multiple, logarithmic, digital correlator. DLS measurements were done at 90° and SLS measurements were taken from 20° to 140° in 5° increments. The measurements were done by U. Nobbmann and K. Davis from the Physics Department.

Poly(styrene-co-VBC). A 100 mL three-neck flask was charged with 55 mL of chlorobenzene, purged with argon for 20 min, and heated in a 75 °C oil bath for 20 min. VBC (12.12 g), styrene (3.16 g) and AIBN (0.24 g, 0.3% w/v) in 5 mL of chlorobenzene were added to the flask. The mixture was stirred for 24 h at 70 °C. After cooling, the mixture was added dropwise to about 250 mL methanol with stirring. The precipitated poly(styrene-co-VBC) was filtered and washed with methanol. The copolymer was reprecipitated from dichloromethane into methanol, isolated, and dried under vacuum at room temperature.

Molecular Weight of Copolymers. Molecular weights of polymers were determined by gel permeation chromatography (GPC) using three 300 mm x 7.5 mm PL gel columns of 10^3, 10^4, and 10^5 Å pore size, and 10 μm particle size (Polymer Lab. Ltd.), equipped with a Waters 590 pump, and UV detector and Interactive Microware PC-based data system. THF was the solvent with flow rate 1.0 mL/min at room temperature.

The molecular weight of the copolymer was calculated by cubic fit values. The calibration was done with polystyrene standards of molecular weight (0.8-600) x 10^3.

Quaternization of Soluble Copolymers The copolymer, 3 g, was dissolved in 15 mL of 1,4-dioxane in a beaker. Excess 25% trimethylamine in methanol was added to the beaker. The beaker was sealed in a stainless steel reactor. The mixture was kept at room temperature for 5 h and heated to 40 °C for 43 h, and the solvent was evaporated by rotary evaporator. The polyelectrolyte was dried under vacuum at 40 °C. The amount of quaternary ammonium ion units was determined by chloride ion selective electrode titration.

References

(1) Juang, M. S.; Krieger, I. M. *J. Polym. Sci. Polym. Chem. Ed.* **1976**, *14*, 2089.

(2) Greene, B. N.; Sheetz, D. P.; Fisher, T. D. *J. Colloid Interface Sci.* **1970**, *32*, 97.

(3) Schild, R. L.; El-Aasser, M. S.; Poehlein, G. W.; Vanderhoff, J. W. *Emulsion, Latices, and Dispersion,* Becher, P., ed. Marcel Dekker: New York, **1978**, p 99.

(4) Woods, M. E.; Dodge, J. S.; Krieger, I. M.; Pierce, *J. Paint Technol.* **1968,** *40*, 541.

(5) Kim, J. H.; Chainey, M.; Poehlein, G. W.; Vanderhoff, J. W. *J. Polym. Sci. Part A: Polym. Chem.* **1989**, *27*, 3187.

(6) Kim, J. H.; Chainey, M.; Poehlein, G. W.; Vanderhoff, J. W. *J. Polym. Sci. Part A: Polym. Chem.* **1992**, *30*, 171.

(7) Stevens, J. M.; Young, J. D. "*Solid Phase Peptide Synthesis*" Pierce Chem. Co., Rockford, Illinois, **1984**, p 115.

(8) Ford, W. T.; Yu, H.; Lee, J. J.; El-Hamshary, H. submitted to *Langmuir.*

(9) Hassanein, M., 1988, unpublished results, found that in shot growth polymerization of styrene, VBC, and (vinylbenzyl)cetyldimethylammonium chloride, water soluble initiator VA-044 produced monodisperse particles, but oil soluble initiator AIBN produced polydisperse particles.

(10) Chonde, Y.; Liu, L-J.; Krieger, I. M. *J. Appl. Polym. Sci.* **1980**, *25(10)*, 2407.

(11) Negre, M.; Bartholin, M.; Guyot, A. *Angew. Makromol. Chem.* **1979**, *80*, 19.

(12) Arshady, R.; Reddy, B. S. R.; George, M. H. *Polymer* **1984**, *25*, 1161.

(13) Arshady, R.; Reddy, B. S. R.; George, M. H. *Polymer* **1984**, *25*, 717.

(14) Hennion, G. F.; Digiovanna, C. V. *J. Org. Chem.* **1965**, *30*, 3696.

(15) Hamid, S. M.; Sherrington, D. C. *Brit. Polym. J.* **1984**, *16*, 39.

(16) Turk, H. Ph.D. Dissertation, Oklahoma State University, 1989.

CHAPTER III

KINETIC ACTIVITIES OF PNPDPP AND PNPEPP CATALYZED BY IBA IN LATEXES

Introduction

Some organophosphorous compounds are very toxic and are used as chemical warfare (CW) agents and pesticides. The decontamination of CW agents and pesticides is practically and theoretically important. For more than three decades, there has been research on decomposing these organophosphorous compounds. Since these compounds are not soluble in water, the rates of hydrolysis are extremely slow. Thus heterogeneous media and efficient nucleophilic catalysts for the hydrolysis have been studied. Because the compounds are harmful, their use is forbidden in common research laboratories. Substitute compounds such as *p*-nitrophenyl diphenyl phosphate (PNPDPP) are used as model compounds for toxic agents. Hydrolysis of PNPDPP produces *p*-nitrophenoxide anion which can be easily monitored by UV.

About ten years ago, Moss, Alwis, and Bizzigotti at Rutgers University, found that the conjugate base of *o*-iodosobenzoic acid (IBA) is an efficient nucleophilic catalyst for organophosphate hydrolysis. Cationic cetyltrimethylammonium chloride (CTACl) micelles as heterogeneous media improved the activity remarkably.[1-3] After this contribution, other heterogeneous systems were also used for the IBA-catalyzed hydrolysis, such as microemulsions[4-7] and lyotropic liquid crystals.[8] There were also some IBA derivatives synthesized and tested as catalysts.[9-12] Some IBA derivatives are more stable and active than the parent compound. Furthermore, silica gel, titanium dioxide, and ion exchange resins[13-15] modified by IBA and its derivatives were tried for organophosphate hydrolysis.

Among the heterogeneous systems, cationic CTACl micelles showed the highest activity with a second-order rate constant k_{IBA} of 645 $M^{-1}s^{-1}$ at 25 °C for the IBA-catalyzed PNPDPP hydrolysis.[2]

Micelle catalyzed hydrolysis is due mainly to higher concentrations of substrate and catalyst in the micelles than in water. We have designed polymer latexes composed of polystyrene modified by quaternary ammonium ions for the IBA-catalyzed PNPDPP hydrolysis. The hydrophobic latexes improve the solubility of organophosphate compounds, and hydrophilic head groups can attract hydroxide ions and catalyst anions. In the latex phase, the concentrations of substrate, catalyst, and hydroxide ions are much higher than in aqueous solution. The purpose of this design is to find more active and practical useful catalytic conditions. Latex activity twice as high as that of CTACl micelles for PNPDPP hydrolysis was obtained, k_{IBA} 1.35 x 10^3 $M^{-1}s^{-1}$, and reported in our previous paper.[16]

Results

Latexes and Polyelectrolytes Used in Hydrolysis. The latexes used for the hydrolysis study were synthesized by emulsion copolymerization of styrene, vinylbenzyl chloride (VBC), and divinylbenzene (DVB) incorporating vinylbenzyl(trimethyl)ammonium chloride by the shot growth technique[17] as shown in Scheme 1. The charged monomer vinylbenzyl(trimethyl)ammonium chloride functioned as emulsifier, and no more than 1 wt % was used in the first shot to control the size and monodispersity of the latexes. The amounts of VBC in polymerization were 2, 5, 25, 50, and 75 wt % for five latexes respectively. After quaternization with trimethylamine, the latexes contained different amounts of quaternary ammonium ions. Polyelectrolytes with the same compositions as the two higher ion content latexes were used for study of the effect of the polymer structure on the kinetics. They were synthesized by solution

Scheme 1

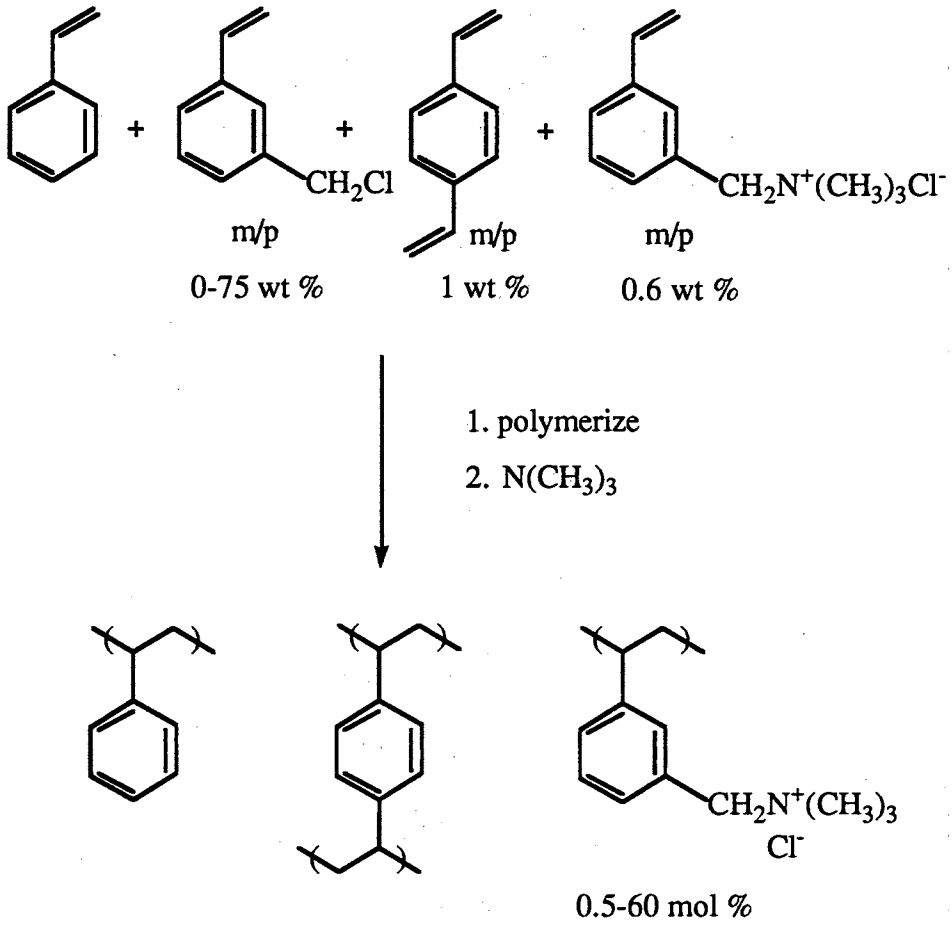

polymerization and quaternization.[17] The latexes were characterized by TEM and Cl^- selective electrode titration, and the data are in Table I. The quaternary ammonium chloride contents of the polyelectrolytes were also determined using the Cl^- selective electrode. The molecular weights of the copolymer precursor of the polyelectrolytes were determined by GPC with THF. The polyelectrolyte 44P+ was used for study of the effect of binding site

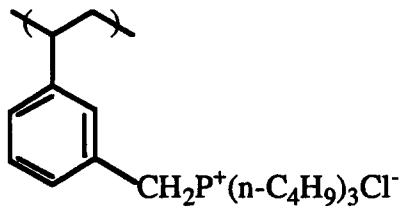

m/p

44P⁺PE

nature on the kinetics. It was obtained from Dr. Tomoi of Yokohama National University. The data of the polyelectrolytes are in Table II.

Table I. Characterization of the Latexes

sample	N^+, mol %	N^+, mmol g^{-1}	TEM R_w (nm)	TEM R_n (nm)	D[a]
$2N^+$	0.55	0.05	73.8	73.2	1.01
$5N^+$	1.67	0.12	77.3	77.0	1.00
$25N^+$	16.9	1.37	88.2	87.4	1.01
$50N^+$	34.1	2.42	85.2	84.2	1.01
$75N^+$	60.4	3.50	91.4	90.5	1.01

[a] Polydispersity index $D = R_w/R_n$.

Table II. Characterization of the Polyelectrolytes

sample	mmol g^{-1}	M_n[a]	D[b]
$50N^+$PE	2.69	7100	1.96
$75N^+$PE	3.46	6700	2.15
44P⁺PE	2.06	16000	-

[a] The molecular weights before quaternization. [b] Polydispersity index $D = M_w/M_n$.

Kinetic Conditions. The kinetic experiments proceeded in UV cells under stirring, and the data were collected during the hydrolysis by UV monitoring of *p*-

nitrophenoxide anion at 402 nm. Solid contents of 0.020, 0.102, and 0.408 mg/mL of the 50N$^+$ latex showed turbidity 0.090, 0.707, and 1.392 at 402 nm respectively due to particle light scattering. The same latex dispersion was filled in the reference cell for each run so that the interference by particle light scattering could be avoided. Solid contents of 0.8 and 0.6 mg/mL were also studied to get a wider range of effects of the particle solid content on the activity. The plots of UV absorbance versus time of hydrolyses in 0.8 mg/mL latex showed noise due to very small amount of light reaching the detector, but the accuracy of k_{obsd} was still good because the data still followed pseudo first-order kinetics by the plot of $\ln(A_\infty - A_t)$ versus time. In the kinetic study, the concentration of the latexes and polyelectrolytes was 0.01-0.8 mg/mL.

The substrates PNPDPP and *p*-nitrophenyl ethylphenylphosphinate (PNPEPP) are not soluble in water. Micelles and organic solvents have been used to improve the solubility. In this work, the PNPDPP was prepared as a solution in acetonitrile and tested in the lowest solid content, 0.01 mg/mL, of the 50N$^+$ latex. When the concentration of PNPDPP was more than 1.5×10^{-5} M, apparent absorbance due to light scattering by precipitated PNPDPP occurred initially and then diminished when the hydrolysis reaction went on. Eventually the kinetic curves went back to normal. To avoid such problems and to insure solubility 1.0×10^{-5} M of the substrate was chosen for the whole kinetic study.

A buffer is needed for convenient kinetic study of this complex second-order reaction. This buffer must not cause coagulation of the latexes, because the coagulation will increase the particle size, increase light scattering, and cause errors in the UV measurement of *p*-nitrophenoxide anion absorbance. The stability of a latex is influenced by several factors: (1) the higher valent an electrolyte of charge opposite to that of the latex, the more likely the electrolyte causes coagulation of the latex; (2) the higher the charge on the latex, the more stable the latex; (3) the more concentrated the electrolyte in the latex dispersions, the more likely is coagulation.

Phosphate and borate buffers, which were used in most other groups for organophosphate hydrolysis in micelles, were tested for the latexes. Sodium phosphate buffer, which exists mainly as HPO_4^{2-} at pH 8.0, caused precipitation of the latexes even at 0.005 M concentration. Using borate buffer at pH 8.0 the activity of the hydrolysis was not measurable. This might be caused by reaction of borate with catalyst IBA.[18,19]

N-Tris(hydroxymethyl)methyl-3-aminopropanesulfonic acid (TAPS) was used as buffer for most of the kinetic studies because its univalent anion did not coagulate the latexes during the time of kinetic experiments. The lowest solid content, 0.01 mg/mL, of the $50N^+$ latex was investigated in 0.10, 0.050, and 0.0050 M TAPS at pH 8.0, and the 0.01 mg/mL latex was stable only when TAPS concentration was 0.0050 M. The higher solid contents of the $50N^+$ latex sample were stable in 0.050 M and even in 0.10 M TAPS. For the sake of consistency in kinetic studies, the buffer concentration 0.0050 M was chosen as a standard condition.

The IBA catalyst and PNPDPP substrate were used in this work to directly compare the activities of the latexes with other systems. PNPEPP was used only for substrate comparison. The substrate concentration was 1.0×10^{-5} M. The temperature was controlled by a circulating water bath at 25.0 ± 0.1 °C. Two examples of absorbance curves versus time for the hydrolysis are given in Figure 1. Such data fit first-order kinetics for more than five half lives.

Determination of k_0 in NaOH. The second-order rate constant k_0 in NaOH was determined by measuring the first-order constant k_{obsd} at four different NaOH concentrations without the latexes and the IBA. The first-order rate constants are in Table III. The k_0 from the slope of the plot of k_{obsd} versus NaOH concentration (Figure 2) is 0.398 $M^{-1}s^{-1}$, and the correlation coefficient is 0.9977.

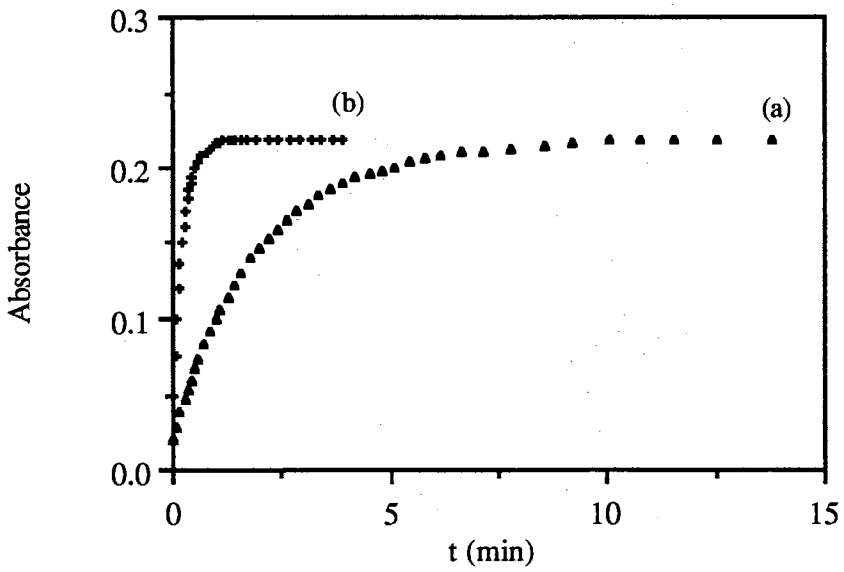

Figure 1. Absorbance of PNP vs. time in 0.2 mg/mL 50N$^+$ latex with (a) 0.4 x 10^{-5} M and (b) 5.0 x 10^{-5} M IBA.

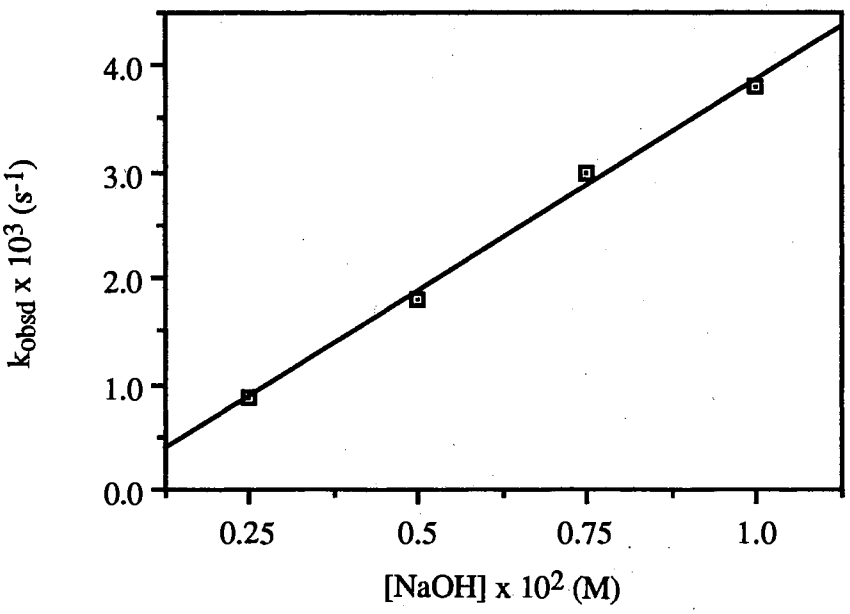

Figure 2. Dependence of k_{obsd} on NaOH concentration.

Table III. k_{obsd} vs. [NaOH][a]

[NaOH] x 10^2 (M)	k_{obsd} x 10^3 (s^{-1})
0.25	0.88
0.50	1.79
0.75	2.98
1.00	3.80

[a] [PNPDPP] = 1.0 x 10^{-5} M, 25.0 °C.

Dependence of k_{obsd} and k_{IBA} on Solid Content of the Latexes. The $50N^+$ and $75N^+$ latexes were used for studying the effect of the latex solid content on the activity of the IBA-catalyzed PNPDPP hydrolysis. The pseudo first-order rate constant was calculated from the plot of $\ln(A_\infty - A_t)$ versus time. The plots for the hydrolyses in 0.2 mg/mL $50N^+$ latex with 0.4 x 10^{-5} M and 5.0 x 10^{-5} M IBA (in Figure 3 (a) and (b) respectively) show that the linearity is good to more than five half lives. The rate constant k_{obsd} of the hydrolysis increases with increase of the latex solid content up to about 0.2 mg/mL and then decreases with further increase of the solid content. The data of k_{obsd} versus the solid contents of the $50N^+$ and $75N^+$ latexes are in Tables IV and V, and the plot of k_{obsd} versus solid content of the $50N^+$ latex at 4.0 x 10^{-5} M IBA is in Figure 4. The second-order rate constants k_{IBA} were obtained from the graphs of k_{obsd} versus at least four IBA concentrations for each latex solid content as shown in Figure 5. The correlation coefficients R of all such graphs are larger than 0.995. Hydrolyses with particles but no IBA were done as control experiments. There was no reaction with no IBA in pH 8.0 TAPS buffer as shown in Figure 5. The change of the k_{IBA} shows the same tendency as k_{obsd} when the solid content of the latexes increases. The data of k_{IBA} versus the latex solid content are in Tables VI and VII, and the plots of k_{IBA} versus latex solid contents are in Figures 6 and 7.

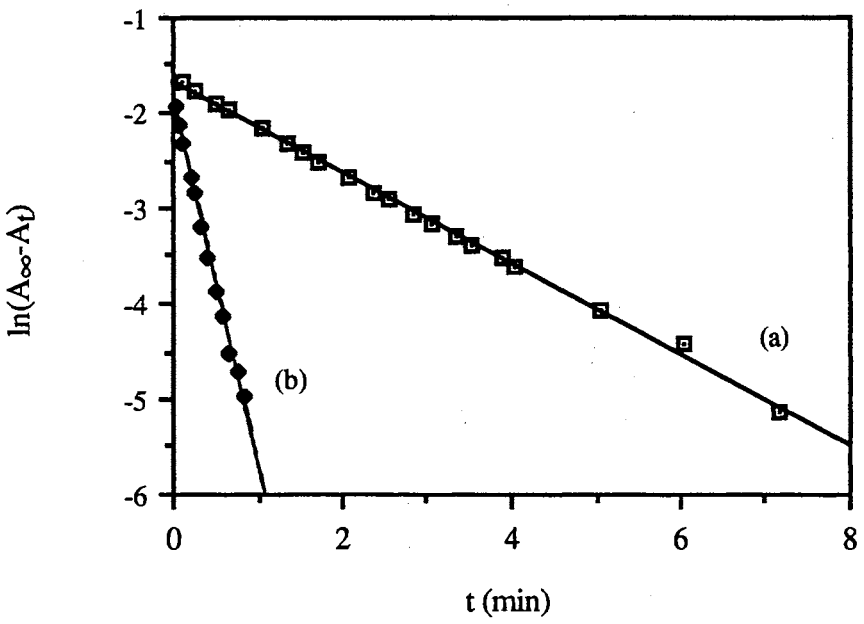

Figure 3. $\ln(A_\infty - A_t)$ vs. time in 0.2 mg/mL 50N$^+$ latex with (a) 0.4 x 10^{-5} M and (b) 5.0 x 10^{-5} M IBA over five half lives.

Table IV. Dependence of k_{obsd} on [IBA] and Amount of the 50N+ Latex[a]

[IBA] x 10^5 (M)	k_{obsd} x 10^3 (s^{-1}) solid content (mg mL^{-1})									
	0.010	0.020	0.031	0.061	0.102	0.154	0.204	0.408	0.612	0.816
0.00	0.06	0.09	0.15	0.20	0.32	0.38	0.36	0.36	0.48	0.25
0.40	–	–	–	2.19	–	–	8.07	–	–	–
0.60	–	–	–	4.46	–	–	11.00	–	–	–
1.00	0.56	0.78	1.26	7.26	8.80	20.10	17.50	17.20	7.80	9.50
2.00	0.94	1.89	2.92	12.03	17.30	35.10	27.50	34.60	19.80	20.90
3.00	1.02	2.50	3.47	15.60	22.40	46.80	42.90	45.10	30.20	25.20
4.00	1.59	3.29	6.02	17.90	28.30	63.70	53.80	54.40	41.20	29.70
5.00	–	–	–	–	–	–	64.60	–	–	–

[a] [PNPDPP] = 1.0 x 10^{-5} M, [TAPS] = 0.0050 M, pH 8.0, 25.0 °C.

Table V. Dependence of k_{obsd} on [IBA] and Amount of the 75N+ Latex[a]

[IBA] x 10^5 (M)	k_{obsd} x 10^3 (s^{-1}) solid content (mg mL^{-1})								
	0.01	0.050	0.103	0.205	0.309	0.410	0.513	0.615	0.819
0.00	0.06	0.02	0.18	0.20	0.24	0.23	0.25	0.24	0.28
1.00	0.29	2.87	5.15	6.40	7.09	7.06	6.20	6.40	6.00
2.00	0.56	4.27	7.81	11.60	14.30	12.90	11.80	10.80	11.30
3.00	0.69	6.20	13.20	18.00	19.90	20.10	15.90	16.90	17.10
4.00	0.90	8.15	15.60	23.10	28.50	24.80	20.70	22.10	21.00

[a] [PNPDPP] = 1.0 x 10^{-5} M, [TAPS] = 0.0050 M, pH 8.0, 25.0 °C.

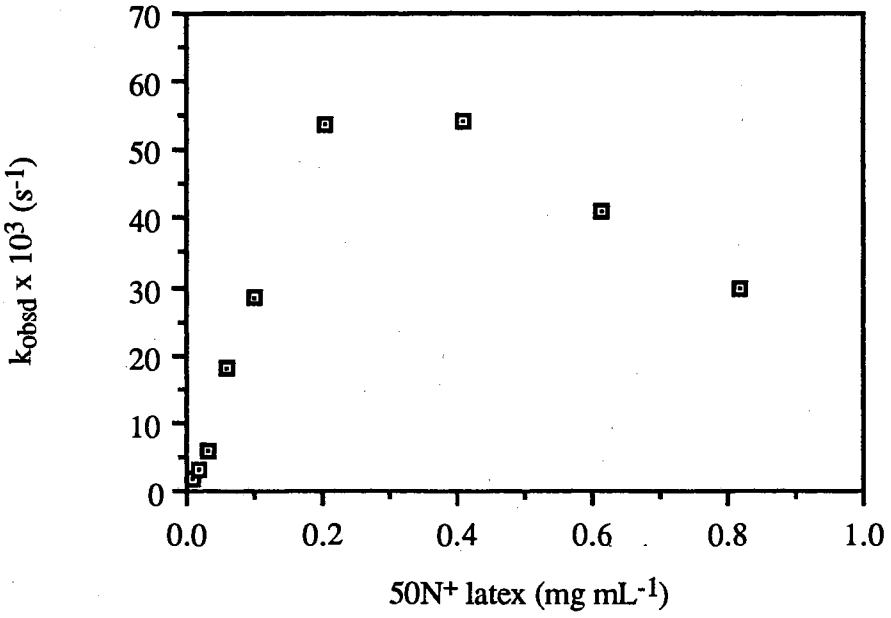

Figure 4. Dependence of k_{obsd} on solid content of the 50N+ latex with 4.0 x 10^{-5} M IBA.

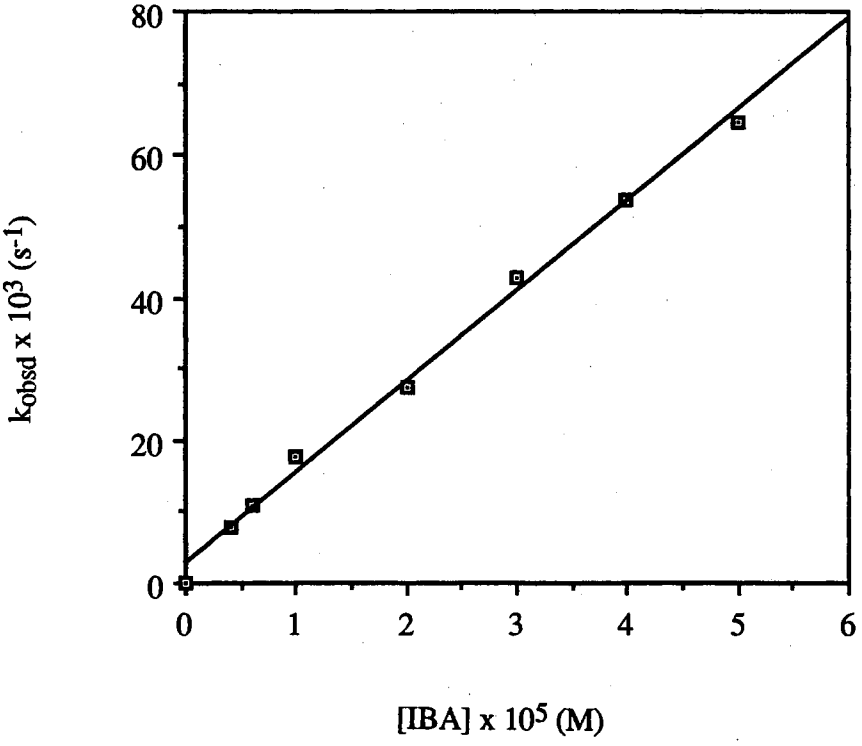

Figure 5. Dependence of k_{obsd} on IBA concentration in 0.2 mg/mL 50N+ latex.

Table VI. Dependence of k_{IBA} on Amount of the 50N+ Latex

sample	k_{IBA} ($M^{-1}s^{-1}$)[a] solid content (mg mL^{-1})									
	0.01	0.020	0.031	0.061	0.102	0.154	0.204	0.408	0.612	0.816
50N+	35	78	140	451	696	1353	1323	1359	1038	786

[a] The k_{IBA} values were calculated from at least five IBA concentrations for each amount of solid. [IBA] = 0-5.0 x 10^{-5} M, [PNPDPP] = 1.0 x 10^{-5} M, [TAPS] = 0.0050 M, pH 8.0, 25.0 °C.

Table VII. Dependence of k_{IBA} on Amounts of the 75N+ Latex and 75N+PE

sample	k_{IBA} ($M^{-1}s^{-1}$)[a] solid content (mg mL^{-1})								
	0.01	0.05	0.10	0.20	0.3	0.4	0.5	0.6	0.8
75N+	21	182	389	578	683	622	506	542	526
75N+PE	10	55	92	128	176	185	195	158	152

[a] The k_{IBA} values were calculated from five IBA concentrations for each amount of solid. [IBA] = 0-4.0 x 10^{-5} M, [PNPDPP] = 1.0 x 10^{-5} M, [TAPS] = 0.0050 M, pH 8.0, 25.0 °C.

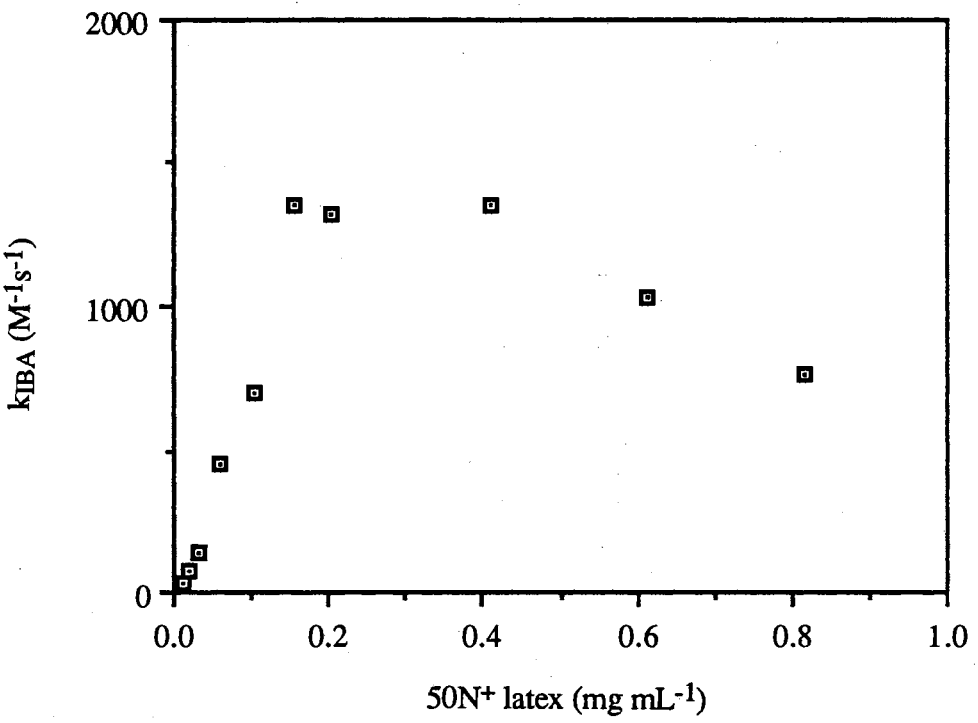

Figure 6. Dependence of k_{IBA} on solid content of the 50N+ latex.

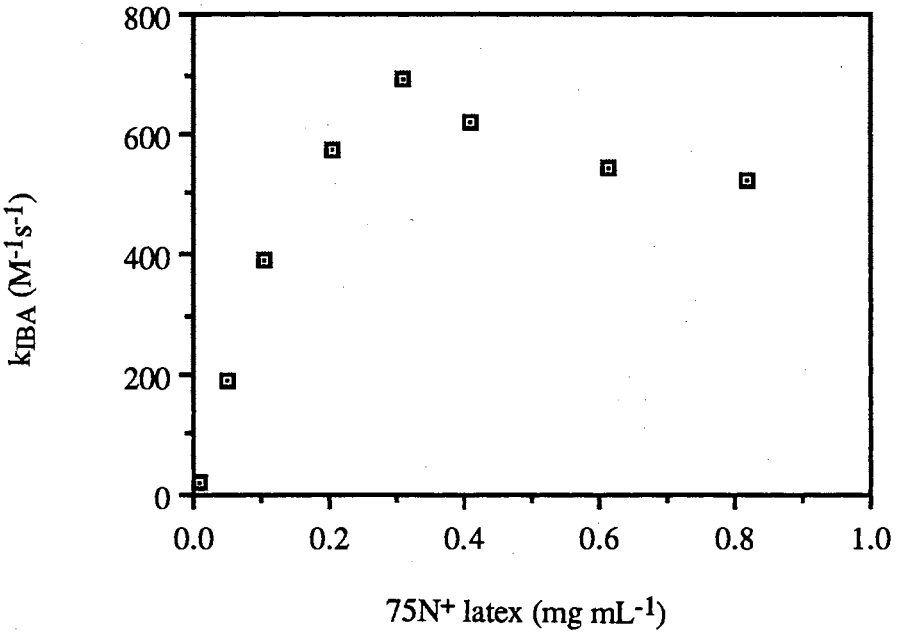

Figure 7. Dependence of k_{IBA} on solid content of the $75N^+$ latex.

Dependence of k_{IBA} on the Compositions of Latexes. Following the study of the solid content, the $2N^+$, $5N^+$, and $25N^+$ latexes, based on the data of the $50N^+$ and $75N^+$ latexes, were used for studying the effects of the latex composition on the activity of the IBA-catalyzed PNPDPP hydrolysis. The condition of 0.4 mg/mL solid content was chosen for the comparison. Five values of k_{obsd} from different IBA concentrations for each of the three latexes are in Table VIII, and the k_{IBA} values for the three latexes are at the bottom of the table. The dependence of the k_{IBA} on the latex composition is in Figure 8. The latex with the highest k_{IBA} is $25N^+$.

Table VIII. Dependence of Activity on [IBA] in Three Latexes[a]

	$k_{obsd} \times 10^2$ (s^{-1})		
[IBA] x 10^5 (M)	$2N^+$	$5N^+$	$25N^+$
0.00	0.034	0.027	0.048
1.00	0.24	0.27	1.43
2.00	0.38	0.46	2.46
3.00	0.73	0.63	4.11
4.00	0.71	0.73	7.32
k_{IBA} ($M^{-1}s^{-1}$)	183	167	1722

[a] Solid content of latexes was 0.4 mg/mL.

Particle Sizes in the Buffer Solution. We reported the particle sizes in deionized water and in solutions of different NaCl concentrations.[17] The particle sizes in TAPS buffer were also measured here. The weight average radii (R'_w) of the latexes were used for particle swelling ratios. The R'_w values for the $2N^+$ and $5N^+$ latexes were the same as those of the corresponding copolymer latexes. For the three highest ion content latexes the corrected radii were used.[17,20] The radii of the latex particles and the swelling ratios of the latexes in the buffer are listed in Table IX.

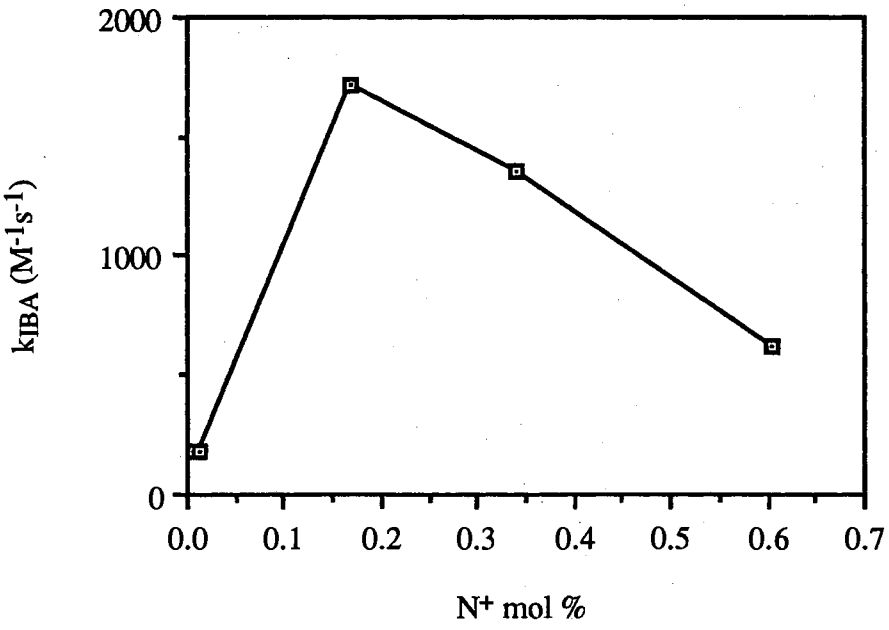

Figure 8. Dependence of k_{IBA} on composition of the latexes.

Table IX. Sizes of the Ion Exchange Latexes

sample	TEM	DLS[a]		
	R'_w (nm)	R_h (nm) in water	R_{hB} (nm) in buffer[b]	V_{wet}/V_{dry}[c]
$2N^+$	73.8	79.6	79.4	1.25
$5N^+$	77.3	85.8	85.6	1.35
$25N^+$	84.2	109	109	2.17
$50N^+$	78.0	137	125	4.12
$75N^+$	84.1	190	168	7.97

[a] Hydrodynamic radii calculated from diffusion coefficients determined by dynamic light scattering. [b] TAPS was 0.0050 M at pH 8.0. [c] $V_{wet}/V_{dry} = R_{hB}^3/R'^3_w$.

The sizes of the latex particles are smaller in the buffer solution than in water. Comparing the swelling ratios with those in water for the highest two latexes, the $75N^+$ latex swells about 13 times in water but 8 times in the buffer, and the $50N^+$ latex swells 5.4 times in water but about 4 times in the buffer.

Dependence of k_{IBA} on Ion Contents of the Latexes. As the results of Figure 8 show, the activity does not consistently increase with increasing of the percent of ionic repeat units of the latexes. Besides the percent of ionic repeat units, the swelling ratio also plays an important role in the catalysis: the greater the percent of ionic groups, the greater the swelling in aqueous dispersions. The particle volumes and the concentrations of ionic groups in the swollen particles in buffer were calculated and are listed in Table X. The plot of the activity versus the ion content of the latexes in aqueous dispersion is in Figure 9.

Table X. Dependence of k_{IBA} on Latex Composition

character	sample 2N+	5N+	25N+	50N+	75N+
N+, mol %	0.55	1.67	16.9	34.1	60.4
N+, mmol, mL^{-1}[a]	0.05	0.10	0.63	0.54	0.37
k_{IBA} ($M^{-1}s^{-1}$)[b]	183	167	1722	1323	622

[a] Of particle phase. [b] The solid content of latex was 0.4 mg/mL.

Kinetic Comparison of the Polyelectrolytes with Latexes. In order to understand the latex structure effect on the kinetic activity, the polyelectrolyte 75N+PE was used for comparison. The activity was tested as a function of the concentration of the polyelectrolyte. The results in Figure 10 are qualitatively the same as with the latexes. Comparing the maximum value of the activity in the 75N+PE with that in the 75N+ latex, the k_{IBA} at 0.4 mg/mL 75N+ latex is 3.4 times that in 75N+PE. The polyelectrolyte 50N+PE was studied only at 0.4 mg/mL, and the k_{IBA} with the 50N+ latex is 1.6 times that with the 50N+PE. The latexes are more active than the polyelectrolytes for the IBA-catalyzed PNPDPP hydrolysis. The data of k_{obsd} versus IBA concentration for the 75N+PE are in Table XI, and those of k_{IBA} versus the 75N+PE concentration are in Table VII. The data of k_{obsd} versus IBA concentration in 0.4 mg/mL 50N+PE are in Table XII, and the k_{IBA} is at the bottom of the table.

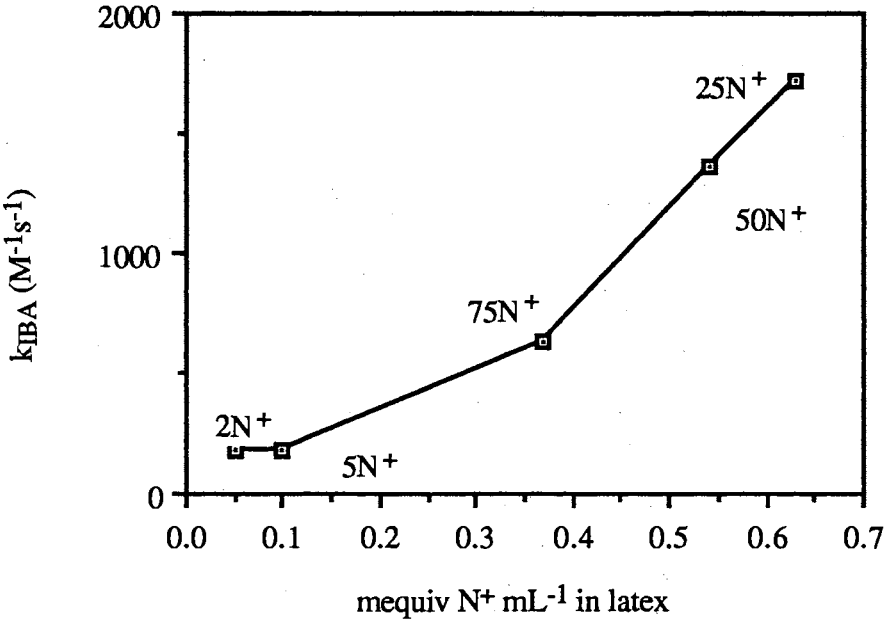

Figure 9. Dependence of k_{IBA} on N^+ concentration in the latexes.

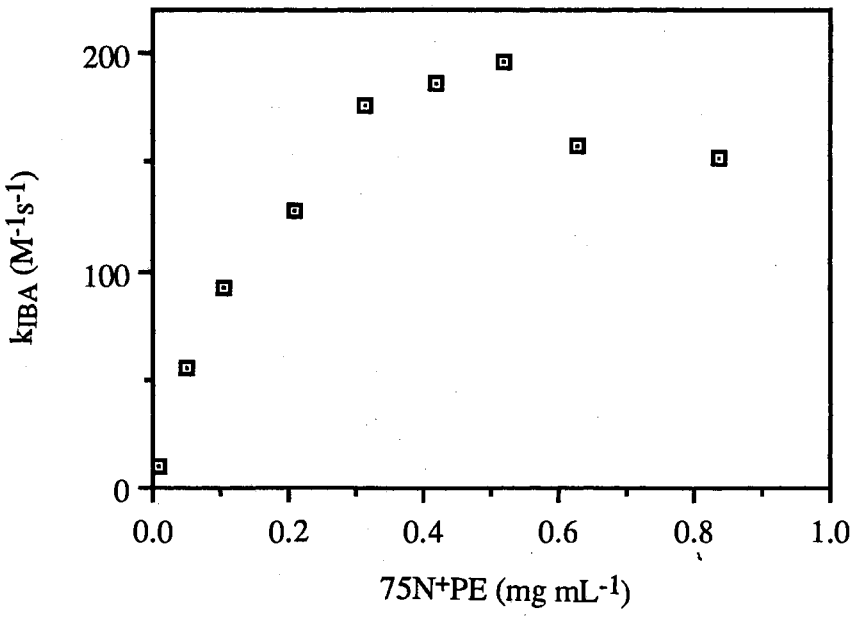

Figure 10. Dependence of k_{IBA} on solid content of the 75N+PE.

Table XI. Dependence of k_{obsd} on [IBA] and Amount of the 75N+PE[a]

[IBA] x 10^5 (M)	k_{obsd} x 10^3 (s^{-1}) solid content (mg mL^{-1})								
	0.01	0.052	0.104	0.209	0.312	0.418	0.520	0.626	0.836
0.00	0.09	0.04	0.06	0.07	0.11	0.09	0.11	0.16	0.25
1.00	0.20	0.50	1.10	1.70	1.84	1.90	2.08	1.70	1.90
2.00	0.29	1.20	2.10	2.90	3.67	3.70	3.85	3.40	3.30
3.00	0.37	1.70	2.80	4.00	5.43	5.40	5.90	4.80	5.00
4.00	0.51	2.20	3.80	5.30	7.09	7.60	7.96	6.50	6.30

[a] [PNPDPP] = 1.0 x 10^{-5} M, [TAPS] = 0.0050 M, pH 8.0, 25.0 °C.

Table XII. Dependence of k_{obsd} on [IBA] in Polyelectrolytes[a]

[IBA] x 10^5 (M)	k_{obsd} x 10^2 (s^{-1})	
	50N+PE	44P+PE
0.00	0.028	0.014
0.40	-	0.897
0.60	-	1.310
1.00	0.88	2.040
2.00	1.73	4.290
3.00	2.64	-
4.00	3.39	8.200
k_{IBA} ($M^{-1}s^{-1}$)	848	2050

[a] Polyelectrolyte concentration was 0.4 mg/mL.

Another comparison has been done using polyelectrolyte 44P+PE, which is poly(styrene-co-VBC) in which the chloromethyl groups were modified by tri(*n*-butyl) phosphine (44% ring substitution). The activities of the hydrolysis were measured at 0.4 mg/mL 44P+PE and are listed in Table XII with 50N+PE. The plot of the k_{obsd} versus IBA concentration is in Figure 11. The 44P+PE with k_{IBA} of 2.05 x 10^3 $M^{-1}s^{-1}$ is even more active than the 50N+ latex.

Effect of NaCl Concentration on Kinetic Activity. The pseudo first-order rate constants of PNPDPP hydrolysis at six different NaCl concentrations with 0.2 mg/mL of the 50N+ latex, 75N+ latex, 50N+PE, and 75N+PE were measured. The k_{obsd} of the 75N+ latex decreases more rapidly with increasing NaCl concentration than that of the corresponding polyelectrolyte except in 0.005 M NaCl as shown in Figure 12 for the latex and the polyelectrolyte. In 0.10 M NaCl, the activity of the 75N+PE is the same as that of 75N+ latex but only one fourth of the activity of the latex without NaCl. However, the activities of the 50N+ latex and 50N+PE decrease about the same magnitude with

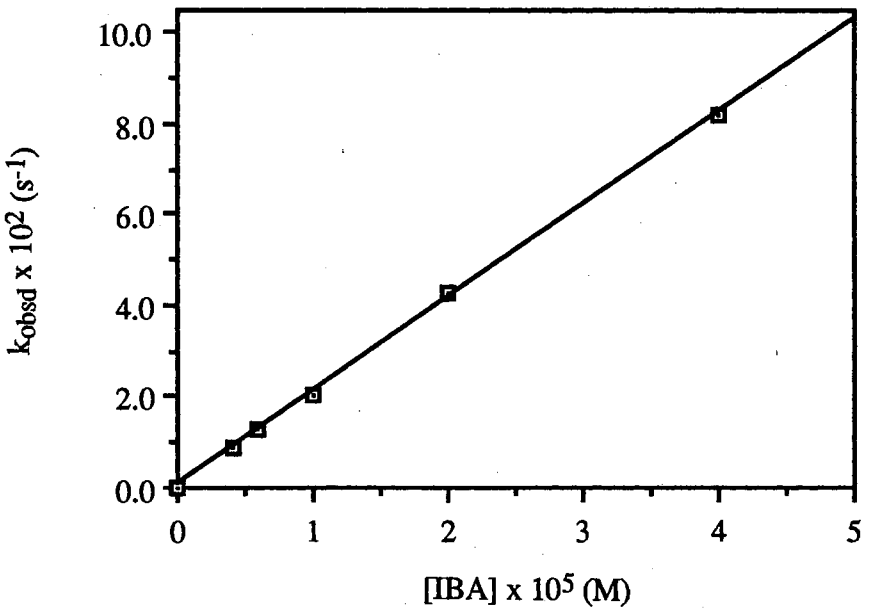

Figure 11. Dependence of k_{obsd} on IBA concentration in 0.4 mg/mL 44P+PE.

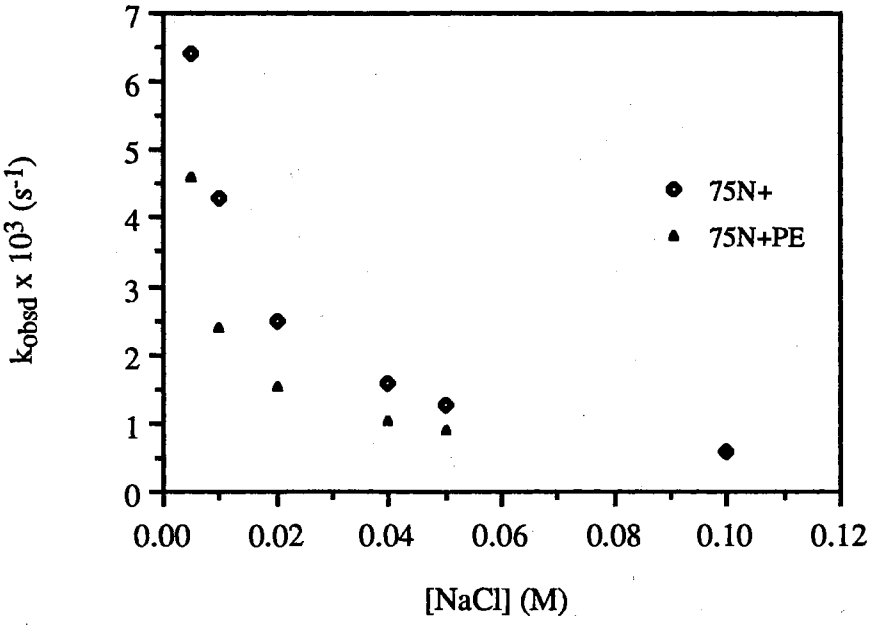

Figure 12. Dependence of k_{obsd} on NaCl concentration in 0.2 mg/mL $75N^+$ latex and $75N^+PE$ with 4.0 x 10^{-5} M IBA.

increasing NaCl concentration as shown in Figure 13. The k_{obsd} values of the hydrolysis in the 50N$^+$ latex, 75N$^+$ latex, 50N$^+$PE, and 75N$^+$PE with different concentrations of NaCl are listed in Table XIII.

Table XIII. Dependence of k_{obsd} on [NaCl] in Latexes and Polyelectrolytes[a]

sample	k_{obsd} x 10^3 (s^{-1}) added NaCl (M)					
	0[b]	0.005	0.010	0.020	0.050	0.100
50N$^+$	53.8	11.30	7.70	4.12	2.31	1.33
50N$^+$PE	–	5.40	3.32	2.07	0.97	0.55
75N$^+$	23.1	6.40	4.30	2.47	1.25	0.59
75N$^+$PE	5.3	4.60	2.40	1.53	0.90	0.58

[a] Solid content of the latexes and polyelectrolytes: 0.2 mg/mL and [IBA] = 4.0 x 10^{-5} M.

[b] Chloride concentrations in 50N$^+$ latex or 50N$^+$PE and in 75N$^+$ latex or 75N$^+$PE are 4.8 x 10^{-5} M and 7.0 x 10^{-5} M respectively.

Effect of Buffers on the Kinetic Activity. The pseudo first-order rate constants were measured in three buffers, 3-[N-morpholino]propanesulfonic acid (MOPS), 3-[N-tris(hydroxymethyl)methylamino]-2-hydroxypropanesulfonic acid (TAPSO), and

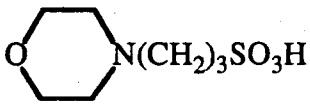

$N(CH_2)_3SO_3H$

MOPS

$(HOCH_2)_3CNHCH_2CH(OH)CH_2SO_3H$

TAPSO

$(HOCH_2)_3CNH(CH_2)_3SO_3H$

TAPS

N-tris(hydroxymethyl)methyl-3-aminopropanesulfonic acid (TAPS) at 0.0050 M in the pH range from 7.0 to 9.0. The pK_a values of three buffers are 7.2, 7.6, and 8.4, respectively

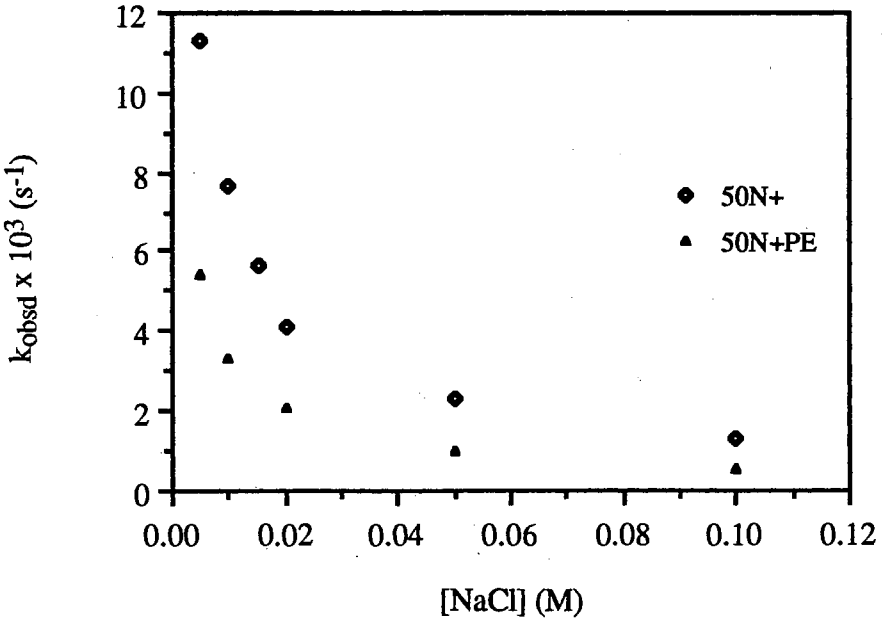

Figure 13. Dependence of k_{obsd} on NaCl concentration in 0.2 mg/mL 50N$^+$ latex and 50N$^+$PE with 4.0 x 10^{-5} M IBA.

in water at 25 °C. In Figure 14, the k_{obsd} values of the hydrolyses increase with increasing pH of MOPS and TAPSO. The activities are much different in MOPS, TAPSO, and TAPS in their common pH range: At the same pH the highest k_{obsd} is in TAPS buffer which has highest pK_a, and the lowest k_{obsd} value is in MOPS which has the lowest pK_a. However, in the presence of 0.02 M NaCl, the k_{obsd} values are 10 fold lower than those with no added NaCl, and the differences of k_{obsd} values among these three buffers with NaCl are much smaller as shown in Figure 15. The data are listed in Table XIV.

Table XIV. Kinetic Activity[a] in Three Buffers with and without NaCl

	$k_{obsd} \times 10^3$ (s^{-1})					
pH	MOPS	TAPSO	TAPS	MOPS[b]	TAPSO[b]	TAPS[b]
7.0	12.3	-	-	1.49	-	-
7.2	17.2	27.6	-	1.88	2.12	-
7.4	16.6	23.5	-	2.02	2.38	-
7.6	18.5	28.7	-	2.64	2.81	-
7.8	21.6	32.5	46.0	3.30	3.31	3.50
8.0	-	34.0	48.0	-	3.66	4.12
8.5	-	-	42.3	-	-	-
9.0	-	-	38.3	-	-	-

[a] In 0.2 mg/mL 50N+ latex, [IBA] = 4.0×10^{-5} M. [b] Added 0.020 M NaCl.

Two other buffers, taurine (pK_a 9.06) and glycylglycine (pK_a 8.4) were tested for the IBA-catalyzed PNPDPP hydrolysis at pH 9.0 and pH 8.0 respectively and

$H_2NCH_2CH_2SO_3H$ — taurine

$H_2NCH_2CONHCH_2CO_2H$ — glycylglycine

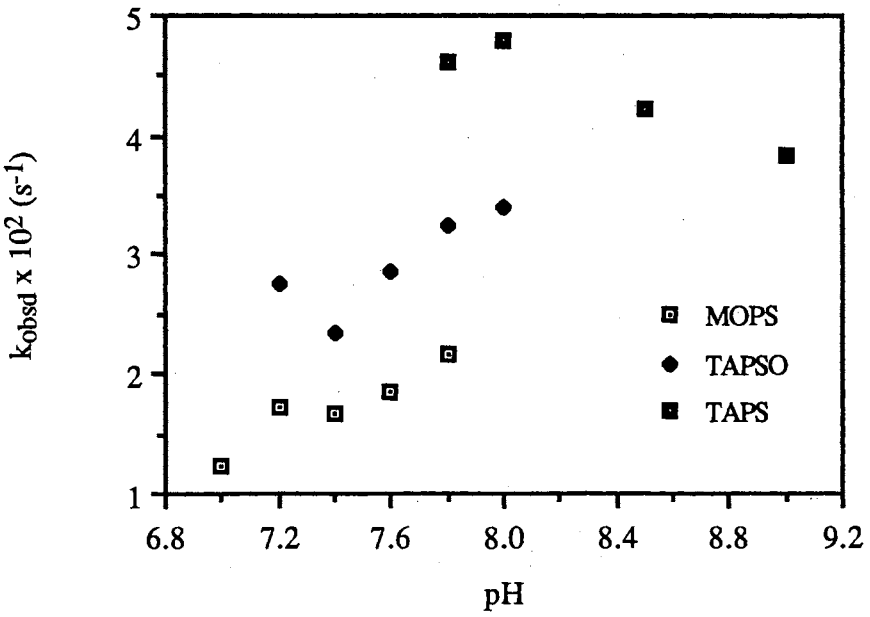

Figure 14. Dependence of k_{obsd} on pH in three buffers with 0.2 mg/mL 50N+ latex and 4.0 x 10^{-5} M IBA.

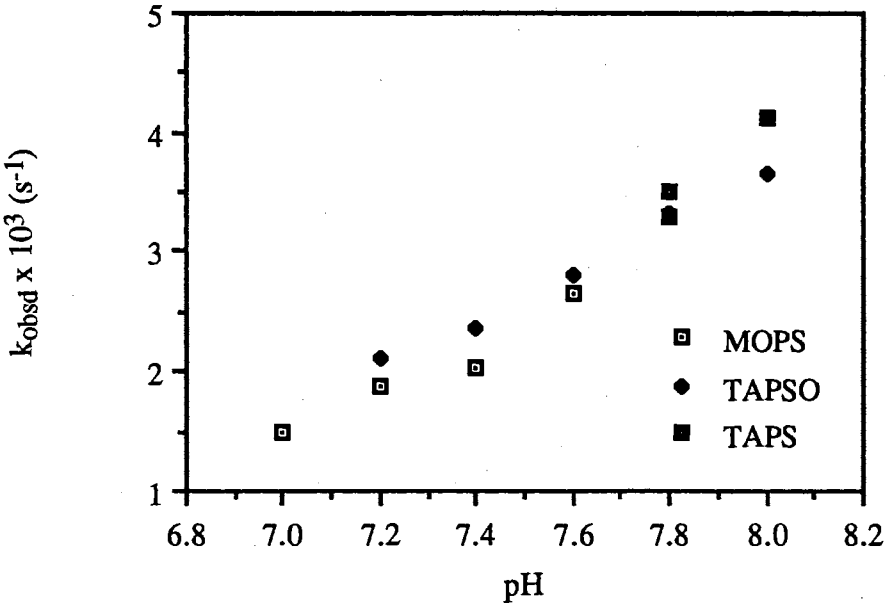

Figure 15. Dependence of k_{obsd} on pH in three buffers with 0.2 mg/mL 50N$^+$ latex and 0.20 M NaCl and 4.0 x 10^{-5} M IBA.

the values of k_{obsd} and k_{IBA} are listed in Table XV. The rates of hydrolysis in these two buffers were almost the same as in TAPS buffer. These results indicated that univalent buffers are good for the stability of the latexes and have the same activities for the hydrolysis.

Table XV. Activities for PNPDPP Hydrolysis in Different Buffers[a]

pH	[IBA] x 10^5 (M)	k_{obsd} x 10^2 (M)	pH	[IBA] x 10^5 (M)	k_{obsd} x 10^2 (M)
taurine			glycylglycine		
9.0	0.0	0.11	8.0	0.0	0.03
	1.0	0.67		1.0	1.46
	2.0	2.65		2.0	2.68
	3.0	3.62		3.0	3.84
	4.0	4.88		4.0	5.35
k_{IBA} ($M^{-1}s^{-1}$)		1,250			1,288

[a] In 0.2 mg/mL $50N^+$ latex.

Effect of TAPS pH on the Kinetic Activity. The second-order rate constants k_{IBA} of the hydrolysis in the $50N^+$ latex were measured also at pH 8.5 and 9.0 of TAPS. The results are listed in Table XVI. In the range of pH 8.0 to 9.0, the activity of the hydrolysis decreases with increase of the buffer pH.

Table XVI. Activities of PNPDPP Hydrolysis in TAPS at Different pH[a]

pH	[IBA] x 10^5 (M)	k_{obsd} x 10^2 (M)	pH	[IBA] x 10^5 (M)	k_{obsd} x 10^2 (M)
9.0	0.0	0.07	8.5	0.0	0.07
	1.0	1.33		1.0	1.30
	2.0	2.25		2.0	2.56
	3.0	3.11		3.0	3.80
	4.0	3.83		4.0	4.23
k_{IBA} ($M^{-1}s^{-1}$)		929			1,078

[a] In 0.2 mg/mL 50N+ latex.

Activity of PNPEPP Hydrolysis in the 50N+ Latex. The substrate PNPEPP was tested for the IBA-catalyzed hydrolysis with different amounts of the 50N+ latex. PNPEPP hydrolyzes faster than PNPDPP. The activity of the hydrolysis increases with increasing amount of the latex even at 0.8 mg/mL. Higher solid content was not tried due to excessive scattering by the latex in the UV measurement. The kinetic data of PNPEPP hydrolysis catalyzed by IBA are listed in Table XVII. The plot of k_{IBA} versus the solid content of the 50N+ latex is in Figure 16.

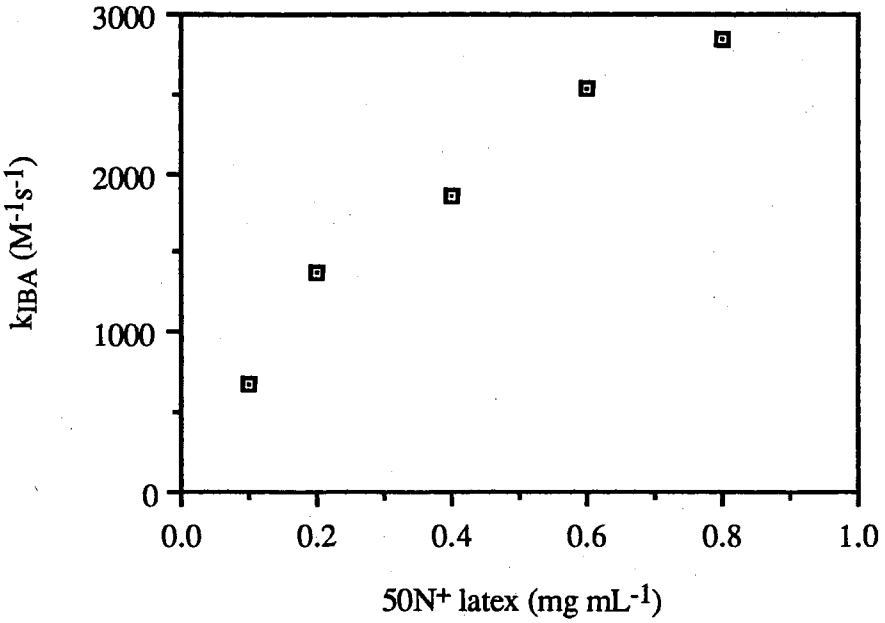

Figure 16. Dependence of k_{IBA} on solid content of the 50N+ latex for PNPEPP hydrolysis.

Table XVII. Dependence of Activity on [IBA] and Amount of PNPEPP

[IBA] x 10^5 (M)	k_{obsd} x 10^2 (s^{-1}) solid content (mg mL^{-1})				
	0.1	0.2	0.4	0.6	0.8
0.00	0.03	0.062	0.083	0.104	0.09
0.40	–	–	0.93	0.997	1.26
0.60	–	–	1.23	1.69	1.79
1.00	0.873	1.69	2.15	2.4	2.74
2.00	1.35	3.08	3.45	5.05	5.18
3.00	1.99	4.07	5.64	–	–
4.00	2.86	5.73	7.73	10.2	11.6
$k_{IBA}(M^{-1}s^{-1})$	678	1372	1864	2530	2844

Discussion

Nature of the Reaction. The catalyzed hydrolysis is a complex second-order reaction which involves both catalyst anions and hydroxide ions. The hydroxide ions are consumed during the hydrolysis, and catalyst ion concentration will be constant if it is a true turnover catalyst. If the first step in Scheme 2 is rate limiting, the overall reaction follows pesudo first-order kinetics. If the second step is rate limiting in a buffer solution, there will be fast reaction of an amount of PNPDPP equal to the amount of the IBA in the dispersion followed by slower zero-order reaction of the rest of the PNPDPP. The latter case is called "burst kinetics".[21] In this work, as shown in Figure 3, a plot of $\ln(A_\infty - A_t)$ versus time using 1.0 x 10^{-5} M PNPDPP and 0.4 x 10^{-5} M IBA is linear for more than four or five half lives (more than 94 or 97% conversion). All other kinetic runs using less IBA

Scheme 2

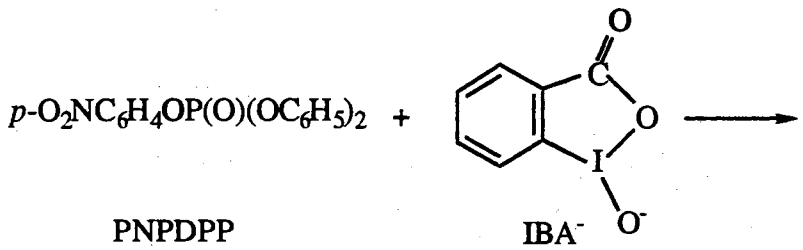

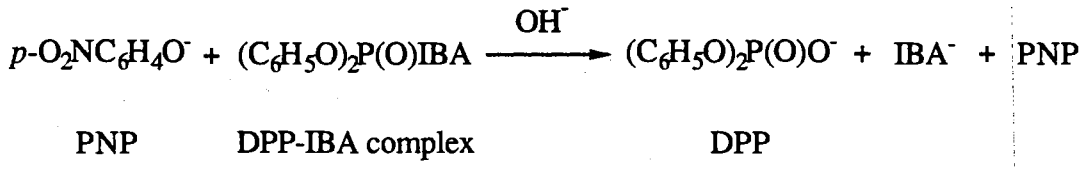

than PNPDPP also showed good pseudo-first order kinetics. This proves that the first step is rate limiting and the IBA is an efficient catalyst. There are no "burst kinetics" in the latexes.

In the latex dispersion, the rate of the reaction will be affected by the intrinsic activity of the latex. The intrinsic activities include the intrinsic rate constant, which is the intraparticle second-order rate constant, the binding constants of catalyst anions and hydroxide ions to the active sites of the latexes, and the binding constant of the substrate to the latex phase, i.e. the intraparticle concentrations of catalyst, nucleophile, and substrate. We have studied the effects of the concentrations of catalyst and substrate on the activity by variation of the concentration of the latexes. Determination of the intrinsic rate constants in the latexes and the binding constants of catalyst and substrate would require evaluation of these data along with the ionization constants of the IBA and the buffer and the ion exchange equilibria involving buffer anion, IBA anion, product anion, and chloride ion. Such evaluation will not be possible until a computational method for fitting all of these parameters is developed.

Dependence of k_{obsd} and k_{IBA} on Solid Contents of the Latexes and Polyelectrolytes. The k_{obsd} and k_{IBA} with the 50N$^+$ latex increase with increasing of the latex solid content until about 0.2 mg/mL and then decrease with further increase of the amount of the latex (Figure 5). The CTACl micelle system shows the same effect by increasing the amount of the surfactant.[2] Considering the ion content of the latex and its volume, the increasing activity is due to increasing fraction of IBA anion bound to the latexes. The decreasing activity at higher amount of the latex occurs when a large fraction of the IBA is bound already, and more latex decreases the concentrations of IBA anion and of PNPDPP in the particle phase. The same tendency is shown also with the 75N$^+$ latex and with the 75N$^+$PE which are in Figures 7 and 10.

Dependence of k_{IBA} on Ion Concentration of the Latexes. The volume of the latexes plays an important role in catalysis since the larger the volume of the dispersed phase, the less concentrated the substrate and the catalyst in that phase. Figure 9 shows that the activity of the latexes depends on the concentrations of ion exchange sites in the particle phase. The two latexes with lowest ion concentration do not swell much in the buffer. The 75N$^+$ latex with the highest percent of ionic repeat units shows lower activity because it is swollen more in the buffer and has a lower concentration of binding sites and of PNPDPP in the particle phase. Among the five latexes, the 25N$^+$ latex has the highest ion concentration. All of the results are consistent with the conclusion that the higher the binding site concentration in the latex, the more active the latex for the hydrolysis.

Effect of NaCl on Activity of the Latexes and Polyelectrolytes. The rates of the hydrolysis in the 75N$^+$ and 50N$^+$ latexes are higher than in the 75N$^+$PE and 50N$^+$PE. This can be understood as the same binding site concentration effect as with latexes. A linear polyelectrolyte in water normally has a highly expanded random coil conformation due to intrachain coulombic repulsion. The latexes swell in water as ion exchange resins, but the extent of swelling depends on their degree of cross-linking. If we

consider the volume occupied by polyelectrolyte coils to be a pseudo-phase, the latexes have smaller particle phase volume than the polyelectrolytes. If the two polymers have the same ion content in dry form, the larger the volume of the dispersed phase, the less the concentration of binding sites, the lower the concentrations of PNPDPP and IBA in that phase, and the less active the polymer catalyst.

The 44P$^+$PE possesses 2.06 mmol/g of P$^+$, more binding sites than the 25N$^+$ latex but less than the 50N$^+$ latex. However, it is more active than either latex for the hydrolysis. This may be because the tri-*n*-butylphosphonium groups are softer and have more affinity for the softer catalyst anions than for hard chloride anions. The higher the binding constant of IBA catalyst to the dispersed phase, the faster the hydrolysis.

At different NaCl concentrations, the activities of the 75N$^+$ latex and 75N$^+$PE change differently. To understand this difference we consider two factors: (1) The fraction of IBA bound decreases when NaCl concentration increases because of mass-action of the chloride anions from NaCl. This may also affect the intraparticle second-order rate constant for the hydrolysis. (2) The volume of the dispersed phase decreases with increasing amounts of NaCl. These two factors are opposite: the first factor will decrease the overall rate, but the second factor will increase the overall rate.

Comparing the 75N$^+$ latex and 75N$^+$PE, by mass action NaCl decreases the amount of IBA bound to both. However, the intrinsic rate constants in the latexes and the polyelectrolytes may be affected differently. On the other hand, the intraparticle concentrations of catalyst and substrate will change differently because the swollen volumes of the latexes and the expanded coil volumes of the polyelectrolytes will change differently after adding NaCl.

The decrease in hydrodynamic volume of a polyelectrolyte with added salt can be proved by measuring the viscosity of the solutions. These have been studied intensively.[22] The viscosities of polyelectrolytes change with their conformations in solutions. The conformation is affected by the nature of the fixed ions and counterions, the concentration

of the polyelectrolytes and the nature and the concentration of low molecular weight salts in solution. These factors all affect the degree of the dissociation of the counterions, and the intrachain coulombic repulsion. Like uncharged polymers in solutions, the more expanded the polymer chain, the more viscous the solution is. When NaCl is added to the polyelectrolyte solution, the hydrodynamic volumes of the polymer chains decrease because the intrachain electrostatic repulsions are reduced. The viscosity of the polymer decreases due to decreasing of the hydrodynamic volume.

The activity of the 75N$^+$ latex is higher than that of the 75N$^+$PE due to its smaller particle volume and higher concentration of catalyst and substrate in the dispersed phase. After adding NaCl the volume of the 75N$^+$PE decreased so that the concentration of substrate increased. However, the volume of the 75N$^+$ latex was not affected as much as that of the 75N$^+$PE because it was not expanded much in the first place due to its cross-linking. The increase of the concentration of substrate in the dispersed phase of the 75N$^+$PE increased the activity of the polyelectrolyte for the hydrolysis. This opposite factor causes the activity of the polyelectrolyte to decrease more slowly than that of the latexes, as shown in Figure 12. In 0.010 M NaCl they showed almost same activity.

For the 50N$^+$ latex and 50N$^+$PE, the activities decrease about the same amount with increasing NaCl concentration. This may be because the 50N$^+$PE has lower ion content and its chain extension is less than the 75N$^+$PE, and so there is less change of the substrate concentration in the dispersed phase than in the 75N$^+$PE case.

Effect of Buffers with and without NaCl. In the buffers TAPSO, MOPS, and TAPS the k_{obsd} increases with increasing of pH from 7.0 to 8.0 due to increasing amounts of IBA anions bound to particles. The k_{obsd} decreases after TAPS pH is higher than 8.0 due to competition of more TAPS anions with IBA anions for binding sites. Comparing the three buffers, the highest k_{obsd} is in TAPS which has the highest pK_a, and the lowest k_{obsd} is in MOPS which has the lowest pK_a. The concentrations of the buffer

anions and IBA anions in the aqueous phase at different pH were calculated and are listed in Table XVIII.

Table XVIII. Anion Concentrations of Buffers and IBA at Different pH

	anion concentration in aqueous solution (M)			
pH	$[MOPS^-] \times 10^3$	$[TAPSO^-] \times 10^3$	$[TAPS^-] \times 10^3$	$[IBA^-] \times 10^{5a}$
7.0	1.93	-	-	1.95
7.2	2.50	1.42	-	2.40
7.4	3.07	1.93	-	2.82
7.6	3.58	2.50	-	3.17
7.8	4.00	3.06	1.01	3.43
8.0	-	3.58	1.42	3.62
8.5	-	-	2.79	3.87
9.0	-	-	4.00	3.96

[a] The pK_a of IBA, 7.02, was measured by titrimetry in aqueous solution.[4]

The relationship of the k_{obsd} with the pK_a values of the buffers can be explained: The concentration of buffer anions at any given pH is higher in MOPS than in TAPS. The more buffer anions, the less catalyst anions can bind to the particles and the less the activity. The intrinsic binding constants of the different buffer anions may be different, but there is no experimental evidence available to test this possibility. In 0.02 M NaCl, the differences of k_{obsd} are much smaller than in pure buffers. This can be due to much smaller amounts of buffer anions bound in the presence of high $[Cl^-]$, which minimizes the differences in the amounts of IBA^- bound.

TAPS Buffer at Three pH Conditions. Kinetic activities in 0.0050 M TAPS buffer at pH 8.0, 8.5, and 9.0 were measured. The k_{IBA} decreases with increasing pH

because the amount of TAPS buffer anions increases with pH, and more TAPS anions bind to active sites of particles as discussed above. The lower kinetic activity is due to less binding of the catalyst anion.

Comparison of the Latexes with Other Systems. Many other heterogeneous systems have been used to promote the hydrolysis of PNPDPP catalyzed by IBA. Table XX shows the best results among them.

Four systems in the table remarkably improve the activity of the IBA-catalyzed hydrolysis. The latexes and CTACl micelles have by far the highest activities with the least amounts of added surfactant or polymer. Micelles and microemulsions are small molecular association colloids. The dispersed phase, which is formed by molecular association and called a "pseudophase", solubilizes substrate with its oil core and attracts catalyst with charge on the surface. The differences between them are that microemulsions dissolve more substrate but show lower activity. Probably most of the substrate stays in the oil core of a microemulsion, where it can not react with catalyst or nucleophile which is bound at the oil-water interface. Polymer latexes and ion exchange resins are stable particles which consist of cross-linked hydrophilic polymer chains. Both catalyst and organic substrate dissolve into the polymer gel phase and the reaction proceeds both on surface and inside the dispersed phase. However, ion exchange resins with 1000 μm size have mass transport and intraparticle diffusion limits to the reaction rates compared with the polymer latexes with < 1 μm size, and are less active than the latexes.

The above comparisons explain the higher activities of CTACl micelles and the latexes than of microemulsions and ion exchange resins. These two more active systems show the same initial increase and then decrease of activity as the amount of the dispersed phase increases. Comparing the best cases among them, the $50N^+$ latex with less solid content has k_{IBA} three times as high as that of the micelles. Moreover, the $50N^+$ latex with 5.0×10^{-5} M IBA has the same shortest half life as the micelles with 1.0×10^{-4} M IBA.

Thus the latex system is the best heterogeneous medium on a weight basis for the IBA-catalyzed phosphate hydrolysis. This may be due to its higher intrinsic activity than CTACl micelles. In this work we haven't been able to determine the intrinsic activity of the latexes.

Table XX. Rate of PNPDPP Hydrolysis Catalyzed by IBA at 25 °C

medium	[IBA] x 10^4, M	best $t_{1/2}$, sec	$k_{IBA\ max}$, $M^{-1}s^{-1}$	ref.
0.4 mg latex $25N^+$ mL^{-1}	0.40	9.5	1,722	17
0.2 mg latex $50N^+$ mL^{-1}	0.50	10.7	1,350	16
0.32 mg CTACl micelles mL^{-1}	1.00	10.7	645	2
25% CTACl, 5% Adogen 464, 1.4% hexadecane microemulsion[a]	2.49	386.5	7.2	5
3.33 mg IRA-35 ion exchange resin mL^{-1}[b]	30.67	10.0	22	15

[a] In 0.03 M borate buffer at pH 9.08. [b] In 0.02 M phosphate buffer at pH 8.0

The solubility pof PNPDPP is much more in microemulsions, which can be assumed to dissolve a weight of phosphate equal to that of the dispersed phase in the best case, than in any other systems. We found that the 0.01 mg/mL latex could dissolve 10 μM PNPDPP, which is 0.37 g PNPDPP/g particles, and is more than can be dissolved in micelles and ion exchange resins.

In practical use for decontamination of toxic phosphates in battlefield, latex powders and dry ion exchange resins have advantages of ease of transportation and storage over micelles and microemulsions. The latex powders and ion exchange resins can be used either as physical absorbents in dry form for liquid toxicants, or as dispersions and suspensions in water with catalyst for chemical decomposition. For common laboratories

and chemical transportation, microemulsions can be used to quickly dissolve large amounts of sprayed liquid toxicants and prevent evaporation before the further decomposing treatment. In farm fields or any emergency, "soap solution" (micellar solution) is the easiest and quickest way to clean the contamination on the surface of skin or equipment.

Conclusions

Ion exchange latexes and CTACl micelles have the highest activities of any colloidal or polymeric media for the IBA-catalyzed hydrolysis of PNPDPP and PNPEPP. The activity of the latexes depends on the concentration of the binding sites in the particle phase, which in turn depends on degree of substitution of the polymer with ion exchange groups and the swelling of the particles in buffer and electrolyte solutions. The higher the concentration of ionic sites in the latex, the more active the latex for the catalyzed hydrolysis. Polyelectrolytes with the same compositions as the latexes show the same effects on the hydrolysis. The polyelectrolytes with larger hydrodynamic volumes are less active than the latexes. Added electrolyte, NaCl, screens the charges of the latexes and the polyelectrolytes and reduces their volumes. It also reduces the activity as chloride ion competes with catalyst anion for latex and polyelectrolyte binding sites. The tri-*n*-butylphosphonium ion polyelectrolyte 44P$^+$ is very active for the hydrolysis because its binding sites may be more selective for catalyst anions than buffer anions and chloride ions.

Experimental Section

Materials. Preparation and characterization of the latexes are reported in Chapter II. N-Tris(hydroxymethyl)methyl-3-aminopropanesulfonic acid (TAPS), 3-[N-tris(hydroxymethyl)methylamino]-2-hydroxypropane sulfonic acid (TAPSO), 3-[N-morpholino]propanesulfonic acid (MOPS), and *o*-iodosobenzoic acid (IBA) from Sigma,

taurine, glycylglycine, and *p*-nitrophenol from Aldrich, and *p*-nitrophenyl diphenyl phosphate (PNPDPP) and *p*-nitrophenyl ethylphenylphosphinate (PNPEPP) from the U.S. Army CRDEC were used as received. ^{1}H and ^{13}C NMR spectra of PNPDPP and PNPEPP are in appendices. Deionized water with resistivity of 1.4×10^{6} ohm cm was used for all experiments.

Instruments. A Varian DMS 200 UV-visible spectrophotometer was equipped with a thermostated block for 10 mm cells, a circulating bath controlled to 25.0 ± 0.1 °C and an EPSON LX 800 printer.

Extinction Coefficient of *p*-Nitrophenoxide Anion in Basic Solution. Six solutions of sodium *p*-nitrophenoxide at pH 10 in the range of 0.8-4.8 $\times 10^{-5}$ M gave a linear plot of absorbance at 402 nm versus concentration, and the molar extinction coefficient from the slope of the plot is 19,000 $M^{-1}cm^{-1}$.

Preparation of IBA Stock Solutions. IBA stock solutions (5.0×10^{-4} M) were prepared by dissolving 66.0 mg of IBA in each of three small beakers with 10 drops 0.05 M NaOH with the help of a spatula. Each solution was diluted to about 5 mL, and mixed respectively with 60.8 mg of TAPS, 52.3 mg of MOPS and 64.8 mg of TAPSO each in 5 mL of water under stirring. The mixtures were adjusted to pH 8.0 with 0.05 M NaOH by pH meter and transferred to 50 mL volumetric flasks. The pH electrode and the beakers were washed several times with water, and the washing water was collected in the flasks. The solutions were diluted to mark with water. IBA stock solutions in pH 8.5 and 9.0 TAPS buffer were prepared by the same procedure as above. The IBA solution was made fresh before use.

The activities of IBA solutions stored for two months were experimentally tested, and the results are listed in Table XXI. The activity of the IBA solution kept at room temperature decreased, but it was almost the same when kept in a refrigerator. However,

the activity of IBA in a latex dispersion decreased even when it was kept in the refrigerator. The decrease of the activity was also observed in our experiments when the samples stood at room temperature after 2 or 3 h. This may be caused by the instability of IBA anions in the latex dispersions. The kinetic data in this work were always obtained using fresh IBA solution, and the first run was used to avoid the instability of IBA in the latex dispersions.

Table XXI. IBA Activity vs. Time[a]

[IBA] x 10^5 (M)	k_{obsd} x 10^2 (s^{-1}) RM[b]	RF[c]	RFmix[d]
latex conc.(mg mL^{-1})	0.102	0.154	0.154
0.00[e]	0.03	0.04	0.04
1.00	0.58	1.82	1.18
2.00	1.01	3.23	1.94
3.00	1.26	4.89	3.61
4.00	1.71	5.88	3.88
k_{IBA} ($M^{-1}s^{-1}$)	404	1475	783

[a] Experiments were done in the 50N+ latex two months after preparation of the IBA stock solution and samples. [b] The IBA stock solution was kept in room temperature. [c] The IBA stock solution was kept at 5 °C. [d] The mixture of IBA and latex dispersion was kept at 5 °C. [e] The control experimental data were taken from Table IV.

Preparation of Latex Stock Dispersions. The latex stock dispersions were prepared by mixing a certain amount of a latex dispersion of known solid content and 6.25 mL of 0.020 M TAPS buffer (pH 8.0) in a 25 mL volumetric flask and diluting with water. For example 2.14 mL of the 50N+ latex with 5.98% (w/v) solid content was used for stock dispersion with 0.00512 mg/mL.

Preparation of Hydrolysis Media. Hydrolysis media for kinetic study were prepared by diluting various amounts of the latex stock dispersions and the IBA stock

solution with 0.0050 M TAPS buffer (pH 8.0) to the mark in 25 mL volumetric flasks. For instance, 1.0 mL of 50N$^+$ stock latex dispersion and 1.0 mL of IBA stock solution will result in 25 mL of dispersion containing 0.204 mg/mL latex solid and 2.0 x 10^{-5} M IBA.

The kinetic media for study of NaCl effects were prepared by mixing various amounts of NaCl stock solution (0.50 M in 0.0050 M buffer at certain pH), with IBA stock solution and latex stock dispersion in buffer in 25 mL volumetric flasks, and diluting with buffer. For example, if 2.0 mL of IBA stock solution in pH 8.0 (0.0050 M) TAPS, 1.0 mL of 50N$^+$ latex stock dispersion in the same buffer, and 1.0 mL of NaCl stock solution in the same buffer are mixed in a 25 mL volumetric flask, after diluting with same pH and concentration TAPS the dispersion will contain 4.0 x 10^{-5} M IBA, 0.204 mg/mL latex solid, and 0.020 M NaCl.

Binding of PNPDPP to the Latex. Binding of substrate PNPDPP at the latex was tested at solid contents 0.02 and 0.4 mg/mL 50N$^+$ latex in 0.0050 mM TAPS at pH 8.0 without IBA. In 10 mL volumetric flasks, 0.02 and 0.4 mg/mL 50N$^+$ latex dispersions were prepared, and 20 μL of PNPDPP stock solution was injected and mixed thoroughly right before ultrafiltration (the concentration of PNPDPP in the latex dispersion was the same as that for kinetic studies). The latex was washed with 10 mL portions of water, and the filtrate was collected in a 25 mL volumetric flask. The latex was washed again with portions of 8 mL of acetonitrile to dissolve PNPDPP from the latex, and the filtrate was collected in a 10 mL volumetric flask. The solutions were diluted to the mark, and the filtrates were measured by UV for PNPDPP in water and acetonitrile solution. Two repeated experiments for 0.02 mg/mL 50N$^+$ latex showed that 80 and 83 % of PNPDPP were in acetonitrile solutions which were bound to the latex. In the water filtrate there was no PNPDPP absorbance but 5 % of the *p*-nitrophenoxide absorbance at about 400 nm expected after complete hydrolysis. The residual latex had a light yellow color after ultrafiltration. The experiments could not be done in 0.4 mg/mL latex. The latex

dispersion had a concentrated yellow color before ultrafiltration because PNPDPP was hydrolyzed faster in this concentrated latex.

Hydrolysis of Phosphate Esters. Kinetics were followed by UV absorbance at 402 nm for *p*-nitrophenoxide anion in latex and polyelectrolyte. The sample and reference cells were filled each with 2.5 mL of the hydrolysis medium. The substrate, 5 μL of *p*-nitrophenyl diphenyl phosphate stock solution in acetonitrile, was injected to start the experiment. In order to reduce acetonitrile and concentration effects on absorbance and scattering in the dispersions, 5 μL of acetonitrile was injected into the reference cell before injection of the substrate. The hydrolysis was done in UV cells with lids and magnetic stirring at 25.0 ± 0.1 °C.

For each latex solid content, k_{obsd} values were obtained as the least squares slopes of plots of $\ln(A_\infty - A_t)$ versus time for at least five half lives. The k_{IBA} value for each latex solid was the least squares slope of a plot of at least four values of k_{obsd} versus the concentration of IBA. The coefficients R for k_{obsd} and k_{IBA} are larger than 0.995.

In the kinetic studies, almost half of the experiments were repeated right after the first runs. The rate constant of the first run in the repeated experiments was usually chosen since the time of preparing samples would be the same for each kinetic run and error due toinstability of IBA in the dispersions wuold be minimized. In one or two cases the second run data were taken because they gave a better linear fit with the data of different IBA concentrations than the first run data. If the rate constants of two repeated runs varied by more than 5 %, a new sample was prepared and the kinetic experiment was redone until they agreed.

References

(1) Moss, R. A.; Alwis, K. W.; Bizzigotti, G. O. *J. Am. Chem. Soc.* **1983**, *105*, 681.

(2) Moss, R. A.; Alwis, K. W.; Shin, J.-S. *J. Am. Chem. Soc.* **1984**, *106*, 2651.

(3) Moss, R. A.; Kim, K. Y.; Swarup, S. *J. Am. Chem. Soc.* **1986**, *108*, 788.

(4) Mackay, R. A.; Longo, F. R.; Knier, B. L.; Durst, H. D. *J. Phys. Chem.* **1987**, *91*, 861.

(5) Burnside, B. A.; Knier, B. L.; Mackay, R. A.; Durst, H. D.; Longo, F. R. *J. Phys. Chem.* **1988**, *92*, 4505.

(6) Knier, B. L.; Durst, H. D.; Burnside, B. A.; Mackay, R. A.; Longo, F. R. *J. Solution. Chem.* **1988**, *17*, 77.

(7) Ramesh, V.; Labes, M. M. *J. Chem. Soc., Chem. Commun.* **1988**, 891.

(8) Hammond, P. S.; Forster, J. S.; Lieske, C. N.; Durst, H. D. *J. Am. Chem. Soc.* **1989**, *111*, 7860.

(9) Moss, R. A.; Chatterjee, S.; Wilk, B. *J. Org. Chem.* **1986**, *51*, 4303.

(10) Panatta, C. A.; Garlick, S. M.; Durst, H. D.; Longo, F. R.; Ward, J. R. *J. Org. Chem.* **1990**, *55*, 5202.

(11) Katritzky, A. R.; Duell, B. L.; Durst, H. D.; Knier, B. L. *J. Org. Chem.* **1988**, *53*, 3972.

(12) Katritzky, A. R.; Duell, B. L.; Durst, H. D.; Knier, B. L. *Tetrahedon Lett.* **1987**, *28(34)*, 3899.

(13) Moss, R. A.; Chung, Y.-C.; Durst, H. D.; Hovanec, J. W. *J. Chem. Soc. Perkin Trans.* I **1989**, 1350.

(14) Moss, R. A.; Chung, Y.-C. *J. Org. Chem.* **1990**, *55*, 2064.

(15) Moss, R. A.; Chung, Y.-C. *Langmuir* **1990**, *6*, 1614.

(16) Ford, W. T.; Yu, H. *Langmuir* **1991**, 7, 615

(17) Chapter II, Synthesis and characterization of cationic latexes.

(18) Beaudry, W. L.; Ward, J. R., U. S. Army CRDEC, personal communication.

(19) Moss, R. A.; Scrimin, P.; Rosen, R. T. *Tetrahedron Lett.* **1987**, *28*, 251.

(20) Ford, W. T.; Yu, H.; Lee, J. J.; El-Hamshary, H. submitted to *Langmuir.*

(21) Bender, M. L.; Kezdy, F. J.; Wedler, F. C. *J. Chem. Educ.* **1967**, *44*, 84.

(22) Noda, I.; Tsuge, J.; Nagasawa, M. *J. Phys. Chem.* **1976**, *74*, 710.

APPENDIX

FTIR AND NMR SPECTRA

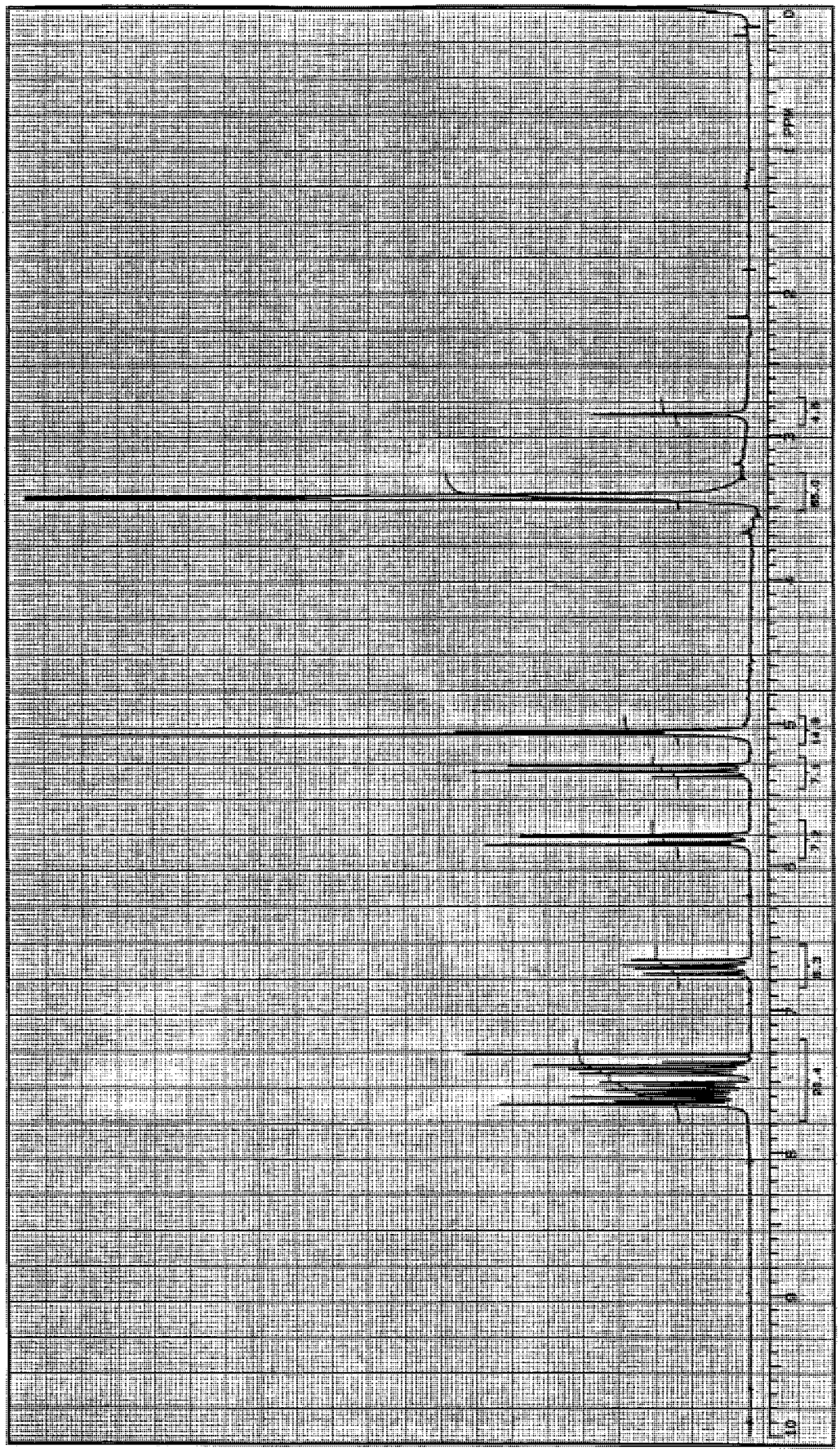

Figure 1. ^1H NMR Spectrum of vinylbenzyl(trimethyl)ammonium chloride.

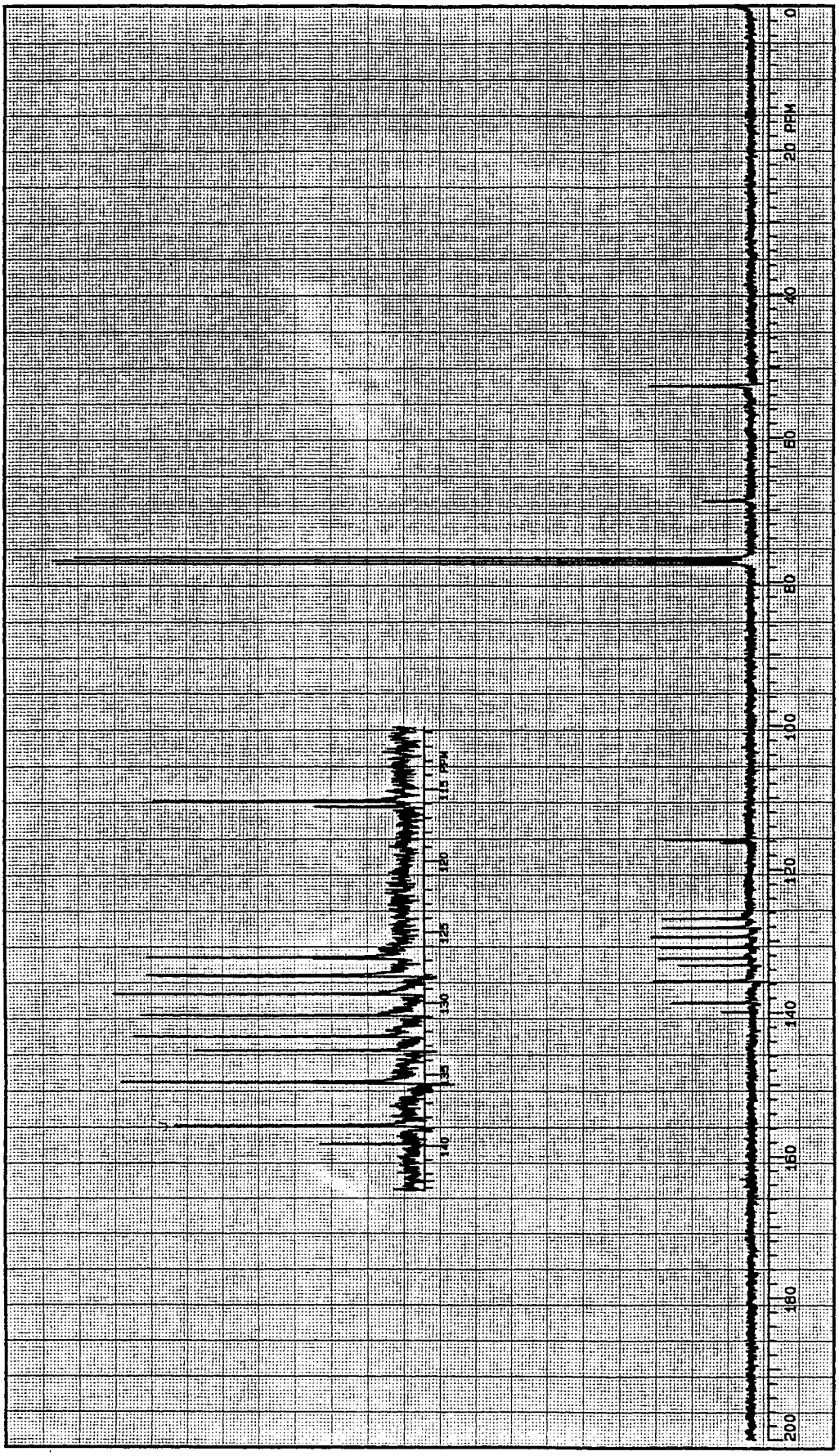

Figure 2. ^{13}C NMR Spectrum of vinylbenzyl(trimethyl)ammonium chloride.

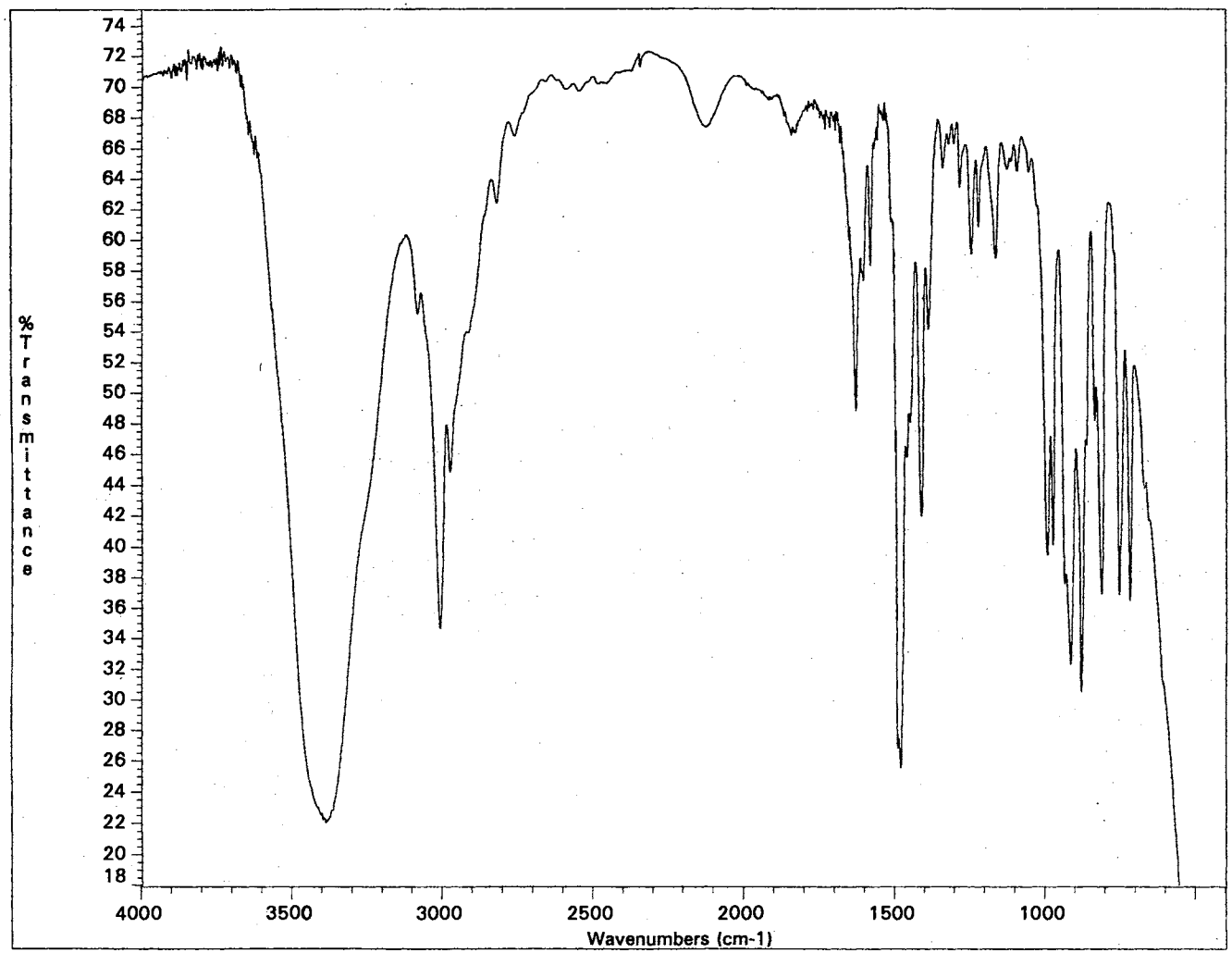

Figure 3. FTIR Spectrum of vinylbenzyl(trimethyl)ammonium chloride.

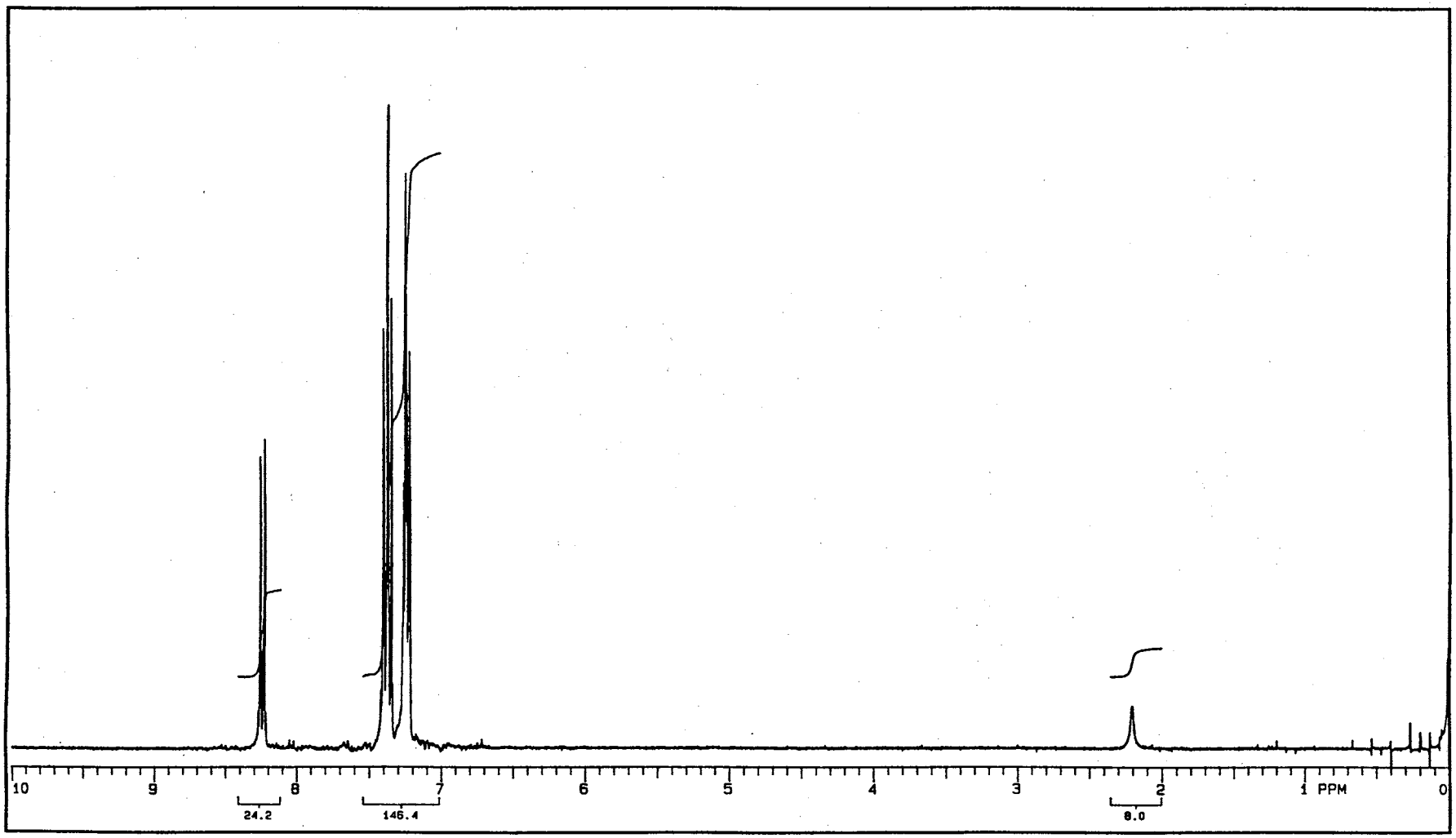

Figure 4. ^{1}H NMR Spectrum of *p*-nitrophenyl diphenyl phosphate.

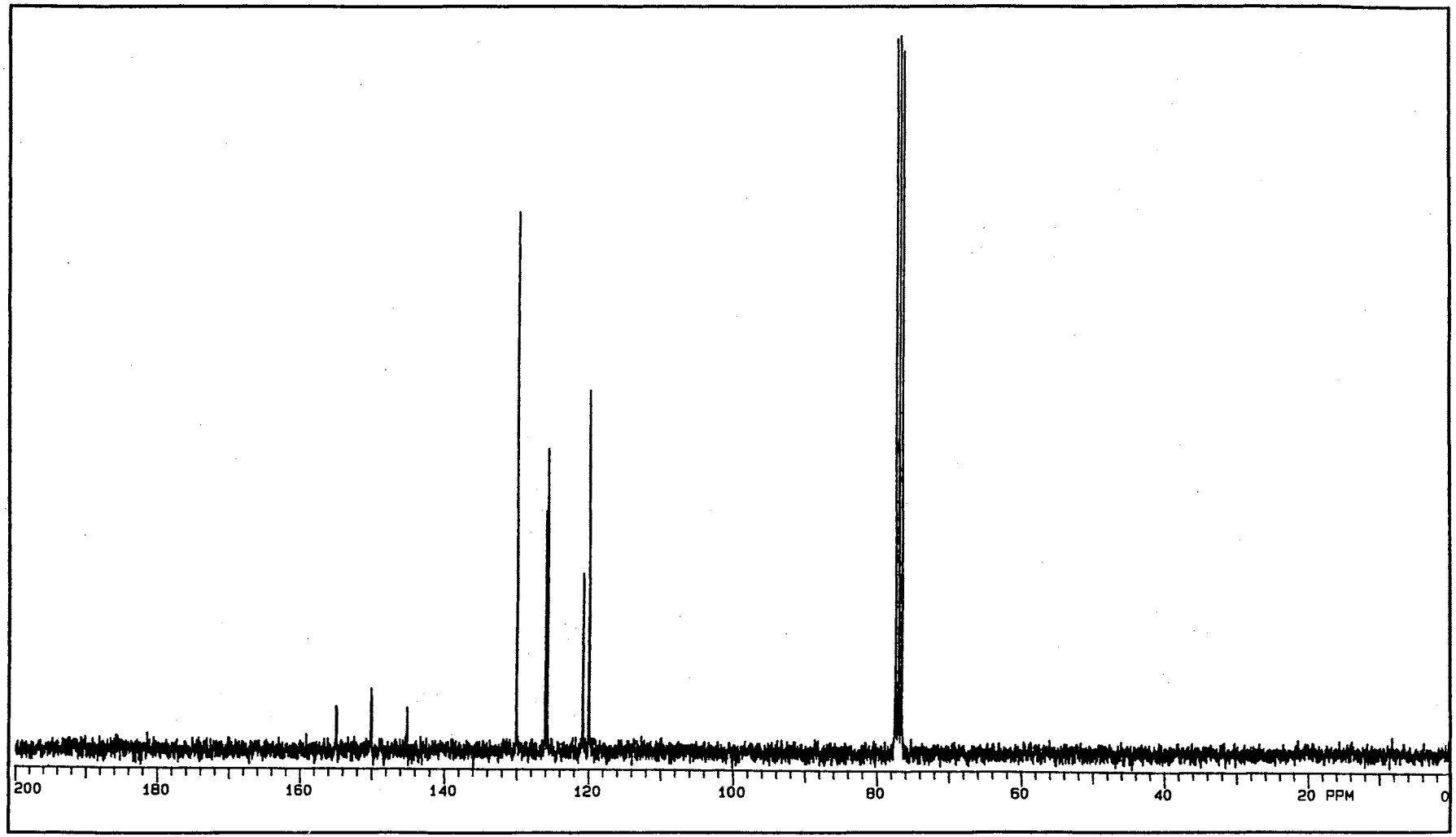

Figure 5. ^{13}C NMR Spectrum of *p*-nitrophenyl diphenyl phosphate.

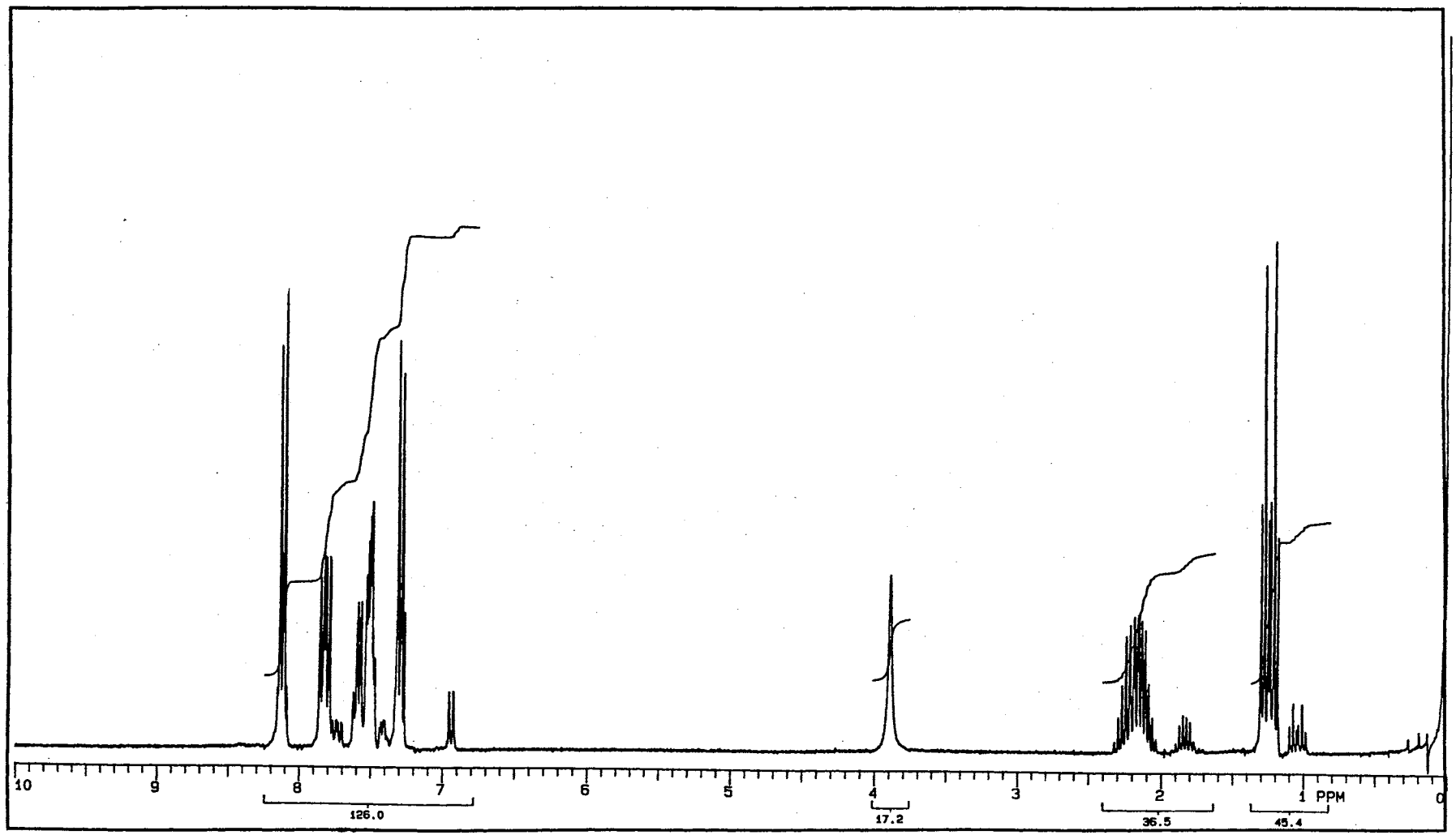

Figure 6. ^{1}H NMR Spectrum of *p*-nitrophenyl ethylphenylphosphinate.

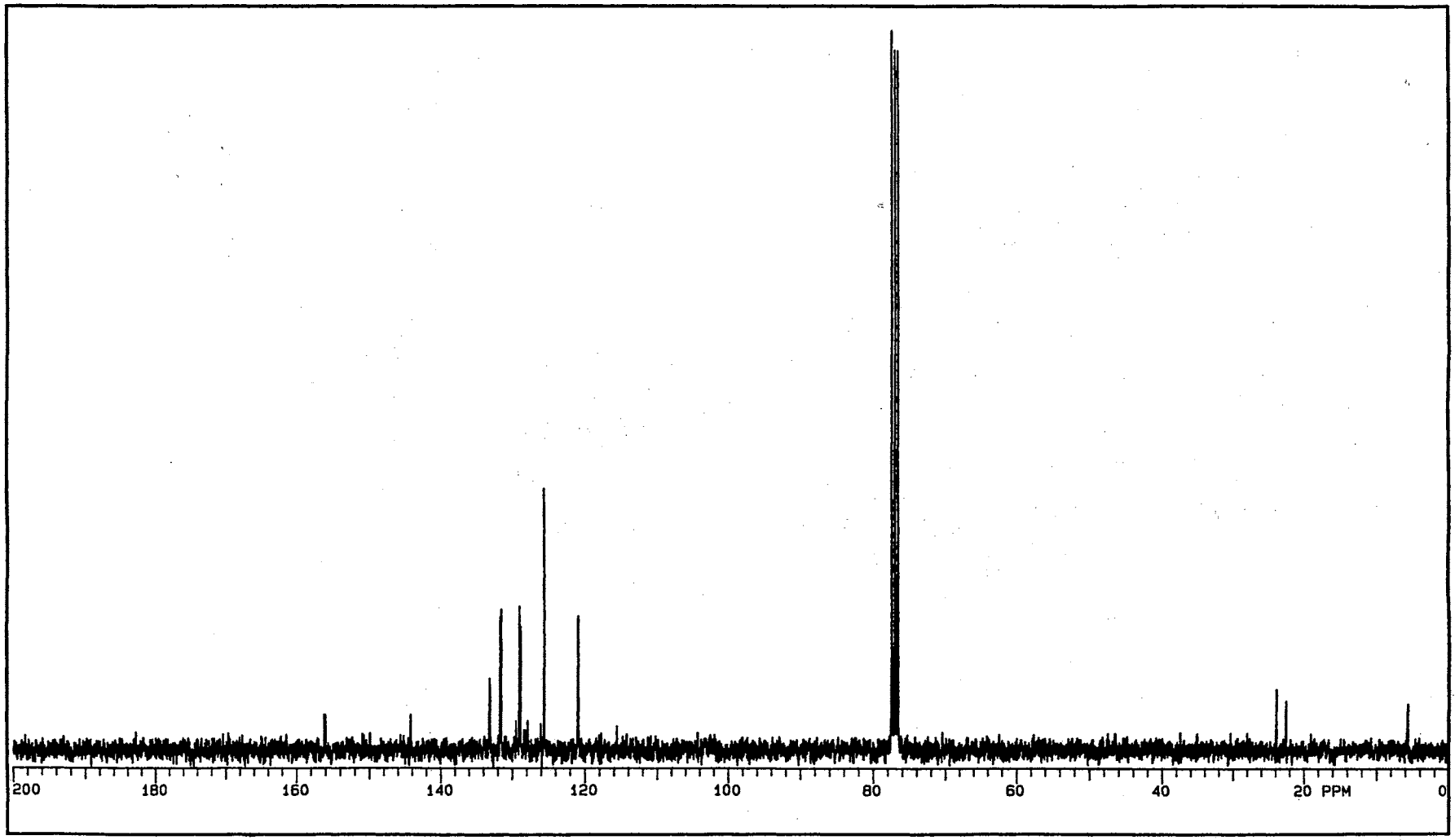

Figure 7. ^{13}C NMR Spectrum of *p*-nitrophenyl ethylphenylphosphinate.

VITA

Hui Yu

Candidate for the Degree of

Doctor of Philosophy

Thesis: CATIONIC LATEXES FOR *o*-IODOSOBENZOATE CATALYZED ORGANOPHOSPHATE HYDROLYSIS

Major Field: Chemistry

Biographical:

Personal Data: Born in Beijing, China, June 22, 1960, the daughter of Da Yu and Yuenfang Tu

Education: Graduated from Jiangong Middle School, Wuhan, China, in July 1978; received Bachelor of Science Degree in Chemistry from Wuhan University, China in July 1982; received Master of Science Degree in Polymer Chemistry from Wuhan University, China in December 1985; completed requirements for the Doctor of Philosophy Degree at Oklahoma State University in May 1993.

Professional Experience: Chemical Engineer, Beijing Industry Chemical Institute, Beijing, China October 1985 to December 1987; Teaching and Research Assistant, Department of Chemistry, Oklahoma State University in January 1989 to May 1993.